Theses - Daytona Beach

Dissertations and Theses

Summer 2008

Modeling, Analysis and Testing of a Semi-Active Control System for Landing Gear Applications

David James Majko
Embry-Riddle Aeronautical University - Daytona Beach

Follow this and additional works at: https://commons.erau.edu/db-theses

Part of the Aerospace Engineering Commons

Modeling, Analysis and Testing of a Semi-Active Control System for Landing Gear Applications

By

David James Majko

A Thesis Submitted to the

Graduate Studies Office

In Partial Fulfillment of the Requirements for the Degree of

Master of Science in Aerospace Engineering

Embry Riddle Aeronautical University

Daytona Beach, Florida

Summer 2008

UMI Number: EP32018

INFORMATION TO USERS

The quality of this reproduction is dependent upon the quality of the copy submitted. Broken or indistinct print, colored or poor quality illustrations and photographs, print bleed-through, substandard margins, and improper alignment can adversely affect reproduction.
In the unlikely event that the author did not send a complete manuscript and there are missing pages, these will be noted. Also, if unauthorized copyright material had to be removed, a note will indicate the deletion.
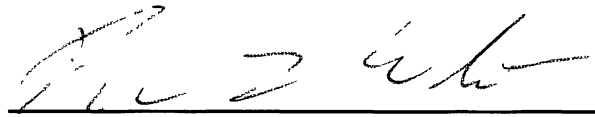
UMI®

MODELING, ANALYSIS AND TESTING OF A SEMI-ACTIVE CONTROL SYSTEM FOR LANDING GEAR APPLICATIONS
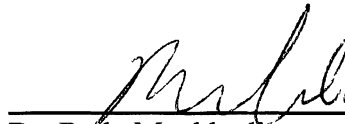
By

David James Majko

This thesis was prepared under the direction of the candidate's thesis committee chairman, Dr. Darris White, Department of Mechanical Engineering, and has been approved by the members of this thesis committee. It was submitted to the Aerospace Engineering Department and was accepted in partial fulfillment of the requirements of the degree of Master of Aerospace Engineering.

THESIS COMMITTEE:

_____
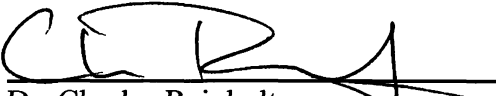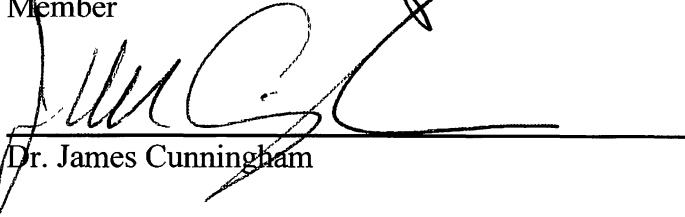Dr. Darris White
Chairman

_____
Dr. Reda Mankbadi
Co-Chair Member

_____
Dr. Charles Reinholtz
Member

_____
Dr. James Cunningham

_____   12/02/08
Dr. Habib Eslami Department Chair, Aerospace Engineering   Date

ACKNOWLEDGEMENTS

ABSTRACT

Author: David James Majko

Title: Modeling, Analysis and Testing of a Semi-Active Control System for

Landing Gear Applications

Institution: Embry Riddle Aeronautical University

Degree: Master of Aerospace Engineering

Year: 2008

There have been several recent studies on the potential benefits of controllable dampers. Controllable dampers can use a fluid with controllable properties, such as Magneto – Rheological fluid (MR fluid), or control the damping force by changing orifice size. For this project, controllable dampers were created using MR fluid. When exposed to a magnetic fluid, the viscosity of MR fluid can change significantly. By replacing the standard damper oil in an aircraft landing gear and exposing the system to an appropriate magnetic field, the damping coefficients of the system can be changed almost instantaneously to accommodate nearly any situation. This trait allows a real time controller to monitor the system and adjust damping characteristics to match current conditions. Using the 'no-jerk' Skyhook control strategy, the control system attempts to minimize the acceleration, force and displacement transmitted to the fuselage from the ground. This reduction in applied load can translate into reduced aircraft weight, and longer fatigue life for some components. Unlike previous studies, the controllable damper configuration for this project used an externally mounted electromagnet located between the damper and remote reservoir, as opposed to an electromagnet located internal to the damper body. This design allows landing gear to use semi-active MR dampers with few modifications to existing designs. A set of dampers were tested in the standard and controllable configurations on a shock dynamometer. A SimMechanics model, which was calibrated using the dynamometer data and from limited 2-DOF experimental test data, was used to predict the improvement in transmissibility resulting from these modifications. The results indicate that controllable dampers using a 'no jerk' skyhook control policy can reduce transmissibility of ground input to the fuselage.

TABLE OF CONTENTS

LIST OF TABLES

TABLE OF FIGURES

CHAPTER 1 INTRODUCTION

Controllable dampers can use non-traditional oil known as Magneto – Rheological fluid, which will be referred to as MR fluid throughout this paper. MR fluid is composed of small magnetic particles mixed with some type of carrier fluid, which in this case, is synthetic oil. When exposed to a magnetic field, these particles align along the magnetic flux lines and change the viscosity of the fluid almost instantaneously. With this property, the damping coefficients of a damper using this fluid can also be changed instantaneously as needed. This feature allows a control system to monitor conditions and make any adjustments. With real time monitoring, the damping rate can be continuously adjusted to minimize the acceleration, force and displacement of the body connected to the suspension. The purpose of this paper is to determine the feasibility of using the proposed controllable damper configuration for aircraft landing gear suspensions. The purpose of this design is to reduce the force applied to the main landing gear supports upon landing and take-off, impact, allowing the landing gear to be designed to withstand a smaller force i.e. smaller and lighter landing gear. Also with lighter loads the fatigue life of this part can be improved allowing for longer part life and possibly longer service intervals equating to a cheaper maintenance cost.

Landing gear History

The landing gear is a critical component in aircraft design. Since the beginning of flight there has been a need to safely land the aircraft. Landing gear may be viewed as a suspension system similar to that of a vehicle. All the basic components such as a wheel or tire, damper and some connecting links are incorporated into the design of a landing gear. Basic arrangements of typical landing gear are shown in figure 1. According to Raymer[36], in his book <u>Aircraft Design: A Conceptual Approach</u>   the most commonly used

Single main	Taildragger	Quadricycle
Bicycle	Tricycle	Multi-bogey
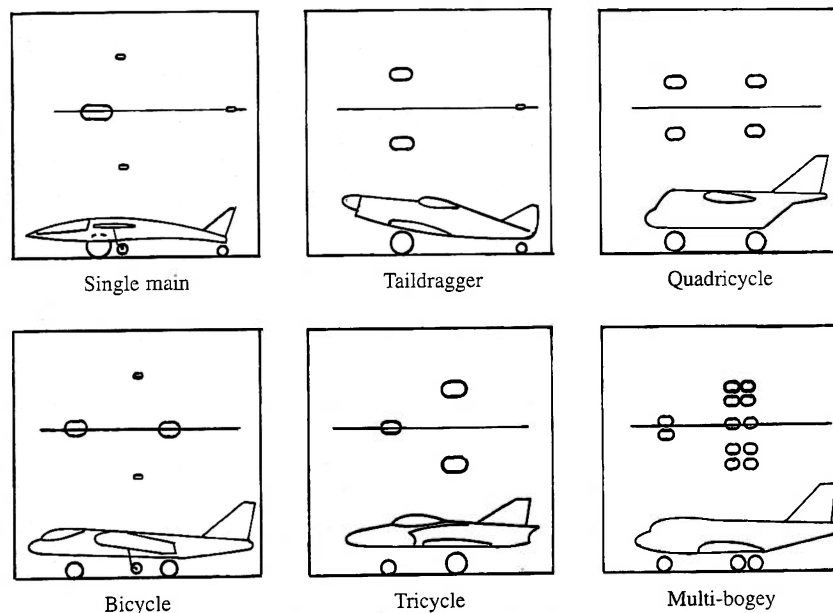
Figure 1. Landing Gear Arrangements[36].

arrangement used today is the "tricycle" gear. This landing gear arrangement consists of a two main wheels aft of the CG away from the centerline and one nose wheel forward of

the CG on the centerline of the plane[36]. Typical design considerations include aircraft weight, payload, tire size, gear arrangement, and landing surface. In instances where a single wheel is unsatisfactory figure 3, a large a multi-wheel landing gear is used figure 2.
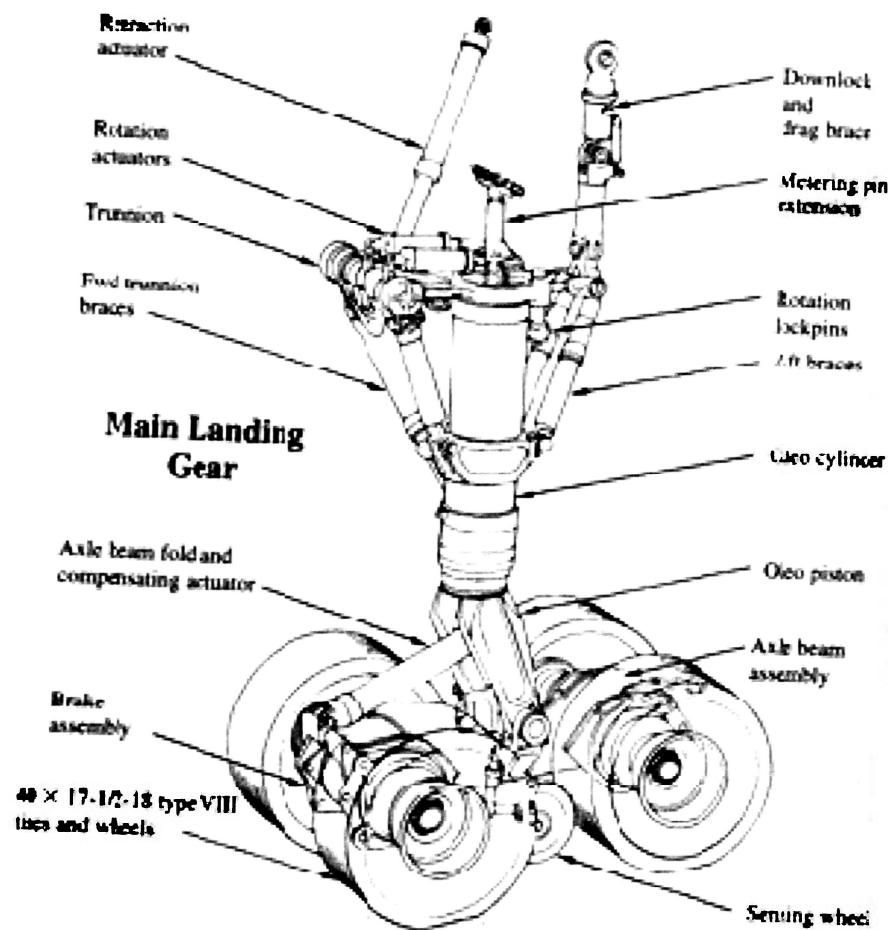
Figure 2. Multi-Wheel Landing Gear Arrangement[36].

SUSPENSION TYPES

SUSPENSION TYPES

Suspension Definition

Suspension is a term used to describe a system of components that usually consists of springs, dampers, and linkage arms connecting a body to the ground through a wheel. Examples are the connection of a motor vehicle frame to the ground through the wheel, and an airplane fuselage to the ground through the wheel. An example of a simple car suspension known as a MacPherson strut is shown in figure 3 and a typical aircraft landing gear known as a strut suspension in figure 3. Both consist of similar general components that make up a suspension system.
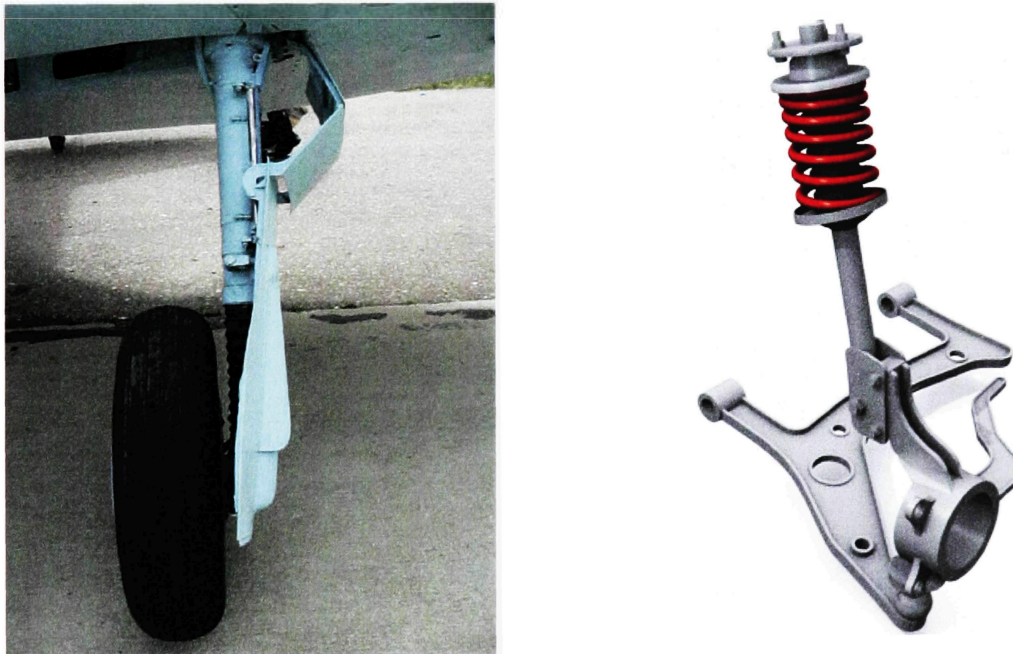
Figure 3. MacPherson Strut of a Vehicle[23] and Aircraft[32].

Shock Absorber/Damper Designs

The design of a shock absorber or damper in landing gear is crucial to passenger comfort and airframe longevity. The shock absorber is designed to smooth out the ride while taxiing and absorb impacts during bad landings[36]. The most common types of shock absorber designs are shown in figure 4. Of all these designs the oleo pneumatic
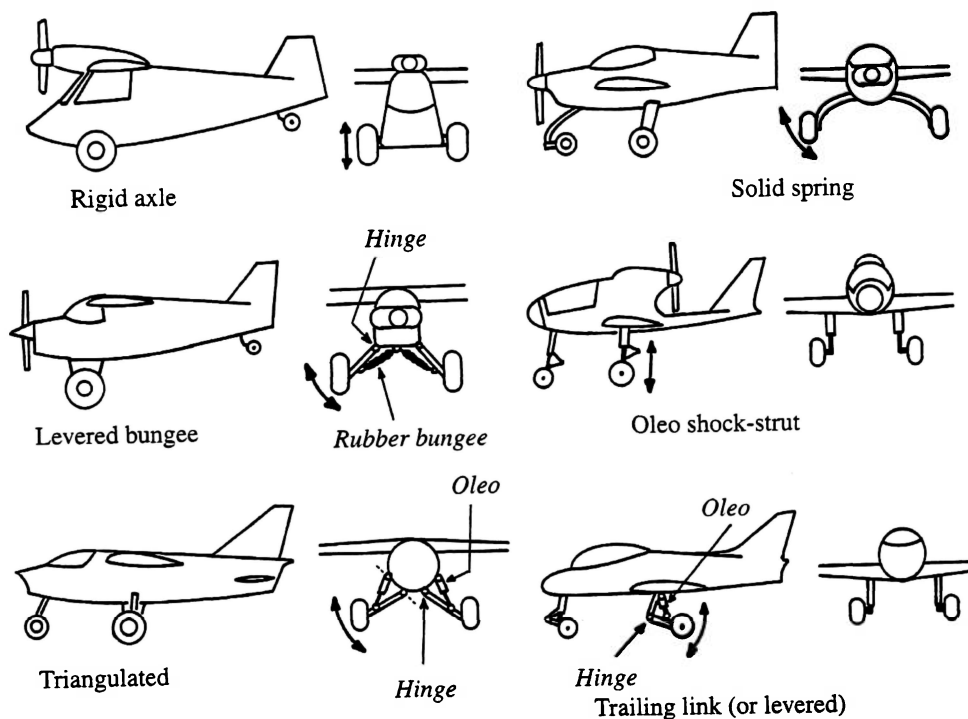
Figure 4. Shock Absorber Designs[36].

shock strut is the most common according to Raymer. This oleo pneumatic or "oleo" shock absorber was "patented in 1915 as a recoil device for large cannons"[36]. A typical ole damper is shown in figure 5. This system uses a type of oil and compressed air or other inert gas to act as a damper and spring respectively. From figure 5, a piston that is connected to the wheel of the aircraft pushes a into the shock absorber tube. This piston

pushes oil through a small orifice creating a damping effect while the movement of oil from one chamber to the other will compress the gas in the upper chamber acting as a spring. This design is used in aircraft landing gear, as well as vehicle suspension systems
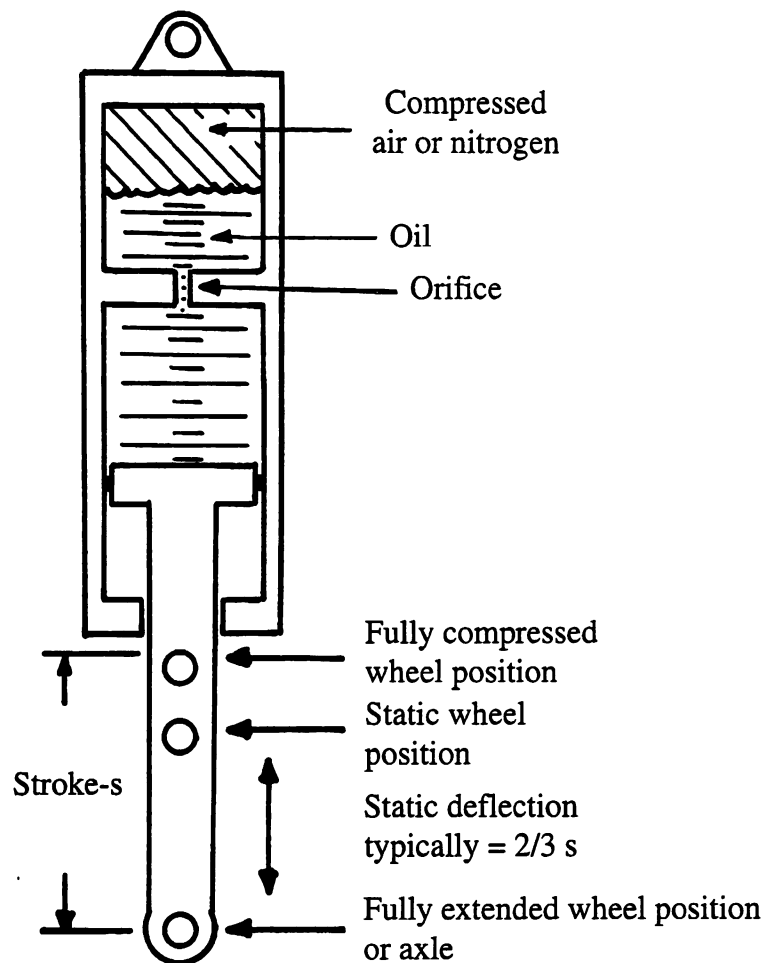
Figure 5. Common Oleo Damper[36].

Passive Suspension

A passive suspension system is one in which the spring rate and damping rate are not adjustable over a period of time. A basic setup is shown in figure 7. They are more

RIDE QUALITY vs. DAMPING

DAMPING LOW TO HIGH
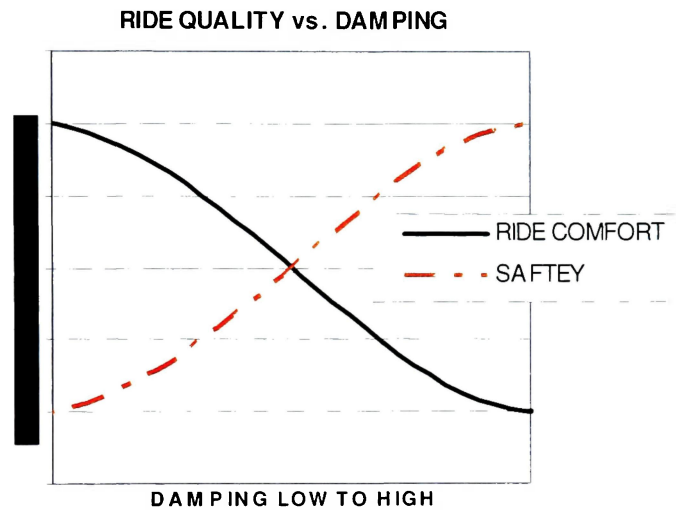
Figure 6. Ride Comfort VS. Ride Safety.

or less fixed and chosen either by initial conditions or experimentation to achieve optimal settings for a particular condition. According to a study by Simon[38] passive systems there is a tradeoff between ride handling and ride comfort. For example if the suspension is designed with high damping rate the body of the vehicle will react harshly to vibrations by the road and transmit most of the input excitation to the body equating to a poor ride comfort. However this high damping level yields a stable vehicle. To achieve a better ride comfort a low damping rate is ideal but the vehicles suspension becomes more unstable. This type of suspension can only be optimized to a certain extent. As seen from figure 6 there is a compromise between ride comfort and stability.
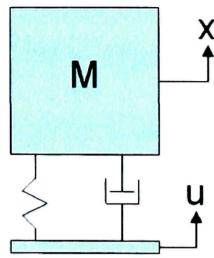
Figure 7. SDOF Passive Mass Spring Damper.

Active Suspension

Active suspensions eliminate a passive damper and sometimes a spring on a suspension system. Instead of a damper, a force actuator is used to add and dissipate energy into a system, similar to figure 8. Unlike the force actuator, a traditional damper can only dissipate energy. Some examples of force actuators are solenoid, hydraulic or electromagnetic recuperative[1]. This type of suspension can bridge the gap between ride quality and stability. Although this suspension has major benefits over a passive one, there are
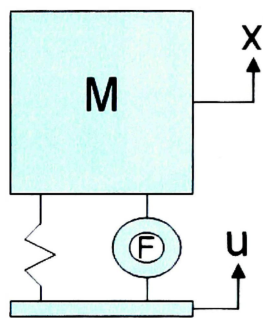
Figure 8. SDOF Active Suspension.

still some major disadvantages. These disadvantages include power requirements, cost, and no fail-safe design. In addition force actuators typically require large amounts of power and can be bulky in design. At present active suspension systems are available on luxury cars as a result of their high price[1]. Also most force actuators do not have a failsafe design. If something breaks or malfunctions with the actuator you can be left with no damping at all, which could be extremely dangerous. This reason along with others is why active suspensions have not been very marketable.

Semi-Active Suspension

Semi-active suspensions bridge the gap between passive and active suspensions. This type of system uses a spring and damper just like the passive system except that the damper is controllable, see figure 9, meaning the damping rate can be adjusted almost instantly. These types of controllable dampers require smaller amounts of power than typical active dampers. Power is required to adjust the current damping level, but unlike force actuators, no power is required to energize the system.
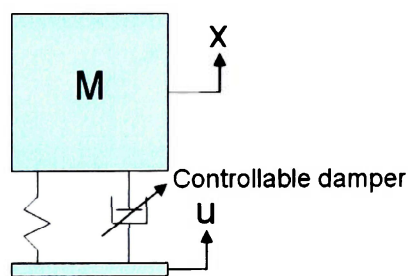
Figure 9. Semi-Active Suspension.

The damping level adjustment can be managed by numerous control systems. Additionally semi-active dampers can include a fail-safe mechanism which offers a minimal amount of damping, if power is lost.

Adaptive Control Suspension

Adaptive control suspension systems use a type of servo mechanism to adjust compression and rebound settings on a damper. See figure 10 for diagram. These adjustments are made based on static weight of vehicle or perhaps intended driving conditions. Therefore this system is adjustable but not over a period of dynamic operation. An example of adaptive control is the suspension system which monitors the position between the vehicles chassis and axle at start up[17]. These air control systems let the driver pick different levels of vehicle handling from soft to firm. These initial adjustments are performed by the onboard CPU, meaning it is not a real time adjustment.
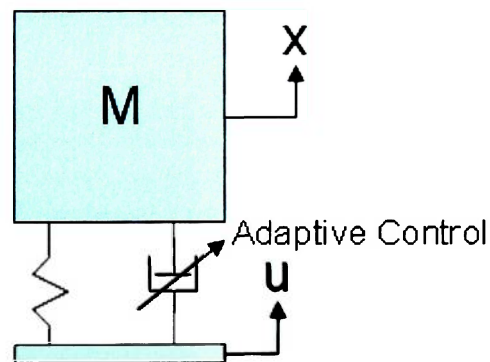
Figure 10. Adaptive Control.

MR FLUID

Description

MR fluid or smart fluid consists of "20-40 percent by volume relatively pure, 3-10 micron diameter iron particles, suspended in a carrier liquid such as mineral oil, synthetic oil, water or glycol."[27] In a damper case synthetic oil is the carrier liquid. "Proprietary additives, similar to those found in commercial lubricants to discourage gravitational setting and promote particle suspension, are commonly added to LORD Corporation's state-of-the-art MR fluids to enhance lubricity, modify viscosity and inhibit wear"[24]. When no magnetic field is present the fluid behaves as a pure Newtonian fluid showing a linear relationship between shear stress and shear rate. This can be seen in figure 13. With an applied magnetic field the viscosity of MR fluid changes allowing the fluid to be used in numerous applications. With the use of electromagnets that can vary magnetic field intensity, the fluid has controllable yield strength, making it ideal for

Figure 11. MR Fluid Without a Magnetic field (left) and With a Magnetic field (right)[15].

damper control. Figure 11 depicts the fluids change of state in the presence of a magnetic field. MR fluids can be controlled in two different modes, allowing for a wide range of applications. These two modes are known as "Valve Mode" and "Direct Shear Mode". The two modes can be seen in figure 12. Valve mode, used for dampers, is the most common. Direct Shear Modes are used for rotational braking such as clutches and brakes.
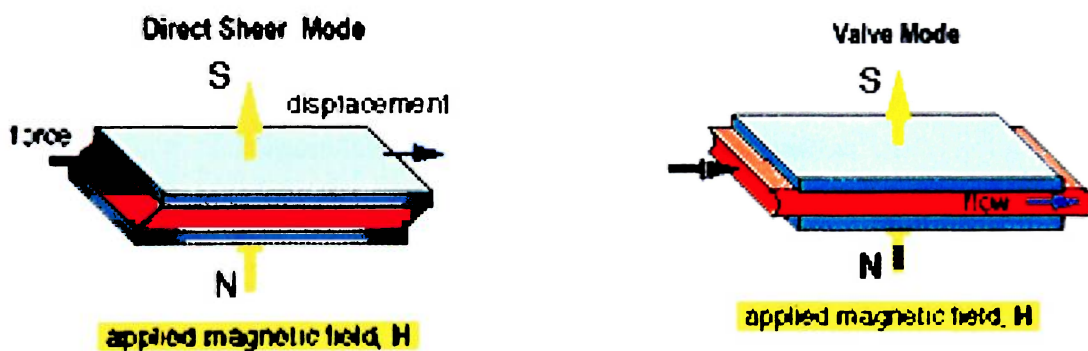
Figure 12. MR Fluid Operating Modes Valve and Shear[27].

Shear Stress as a function of Shear Rate with
no Magentic Field applied at 40°C (104°F)
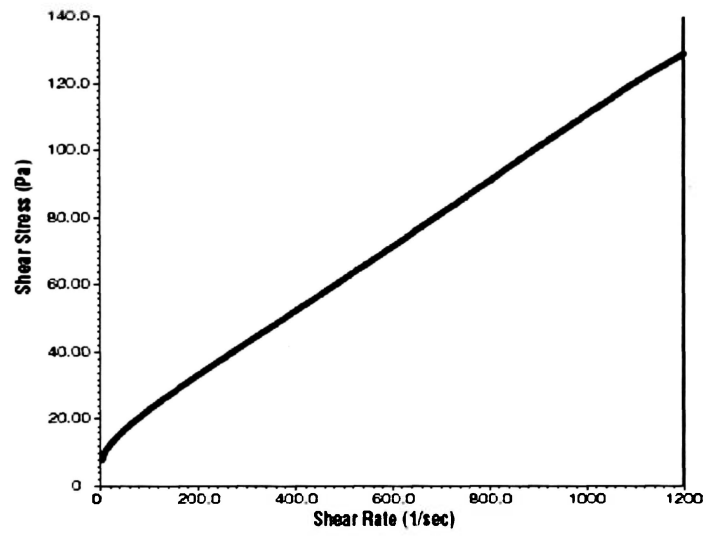
Figure 13. Newtonian Fluid Characteristics[30].

REVIEW OF LITERATURE

Keyword: MR Fluid

MR fluid was first discovered in 1940 by Jacob Rabinow[6]. He was issued the first patent on a new technology which in the late 80's offered little use. The advent of computer technology and digital processors offered a means to control the fluid in an effective manner. Now one of the leading manufacturers of MR fluid is the Lord Corporation. In the past 10 years the Lord Corporation has accrued extensive patent portfolio making them the leader in MR fluid technology[24]. Applications for MR fluid devices have increased over the years. Areas where MR devices are used include; mechanical engineering, civil engineering, military, defense, optics, automotive, aerospace, and medical devices[27]. Additional examples of MR technology can be found on the Lord website. In the automotive industry the main MR device is the primary suspension. Delphi's MagneRide™ damper uses MR fluid technology to provide real time damping adjustments to give exceptional ride quality and handling. Many vehicles use these dampers as standard equipment on their vehicles. These vehicles[27] include but are not limited to: Figure 14 depicts Delphi's MR damper and current production vehicles with MR damper technology.

- Acura MDX

- Audi TT

- Audi R8

- Buick Lucerne

- Cadillac DTS

- Cadillac SLR

- Cadillac SRX

- Cadillac STS

- Chevrolet Corvette

- Ferrari 599GTB

- Holden HSV Commodore

Figure 14. Vehicles (Left) with Delphi's MR Dampers[12] (Right).

Other automotive devices include truck cab and seat suspensions, and clutches used on everything from military to agricultural vehicles. A military application for MR technology is body armor[25]. The military is experimenting with MR fluid as a means to enhance body armor[44]. Another application for civil and structural engineers is seismic vibration protection.
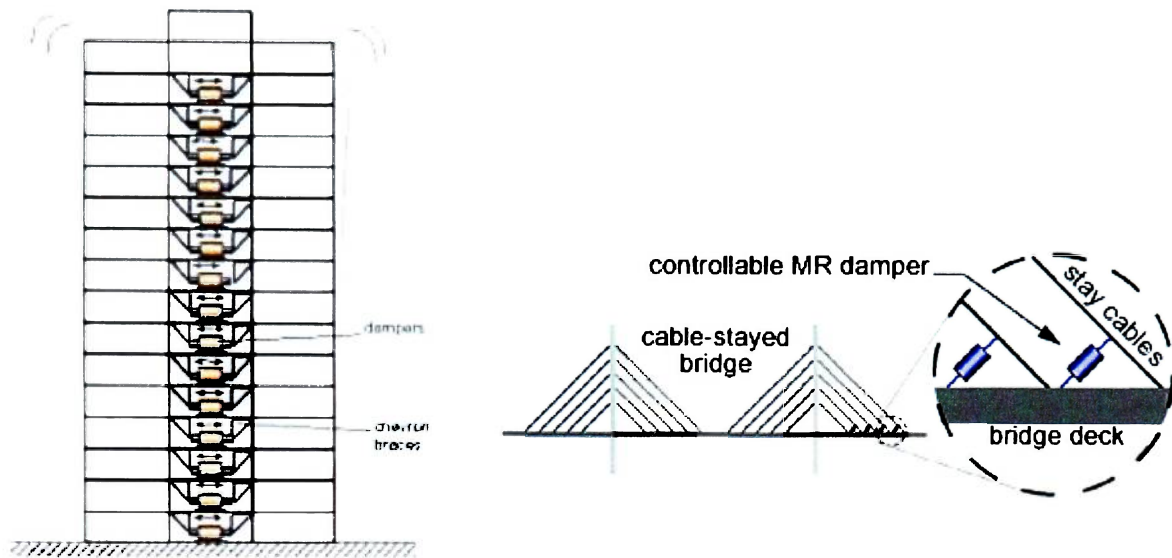
Figure 15. MR Dampers for Buildings and Bridges[6].

"LORD MR fluid devices enlarge the control envelope of base-isolation and distributed damping systems that protect against initial shocks and aftershocks"[24]. A diagram is shown in figure 15. Another civil engineering application is "LORD MR fluid dampers attached to cables provide a continuously controllable, cost-effective solution to wind-rain-induced cable gallop"[24] as seen in figure 15. Medical applications include the "Prolite™ Smart Magnetix™ Above-the-Knee Prosthetic to increase gait balance, stability and energy efficiency. It uses controllable MR technology adapted from LORD Motion Master™ Ride Management System truck seat damper"[24]. See figure 16 for details.

active motion
control element to
control knee
motion

- data processing
  to analyse gait

- software programs
  to calculate actions

sensors to
gather gait data
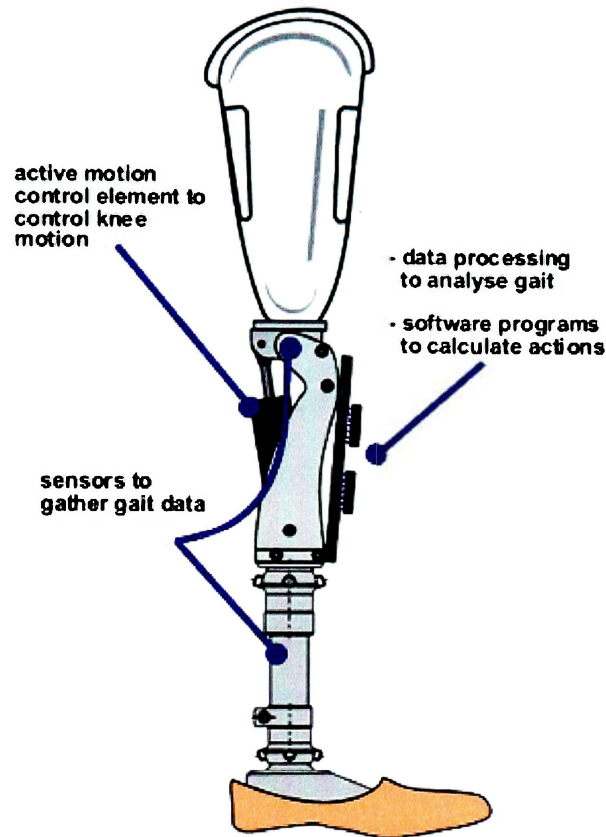
Figure 16. MR Medical Devices.

All of these devices have inherent benefits which include; continual optimization, inherent stability, failure safety, mechanical simplicity, small device/package size, fast response time, and low power consumption.

Keyword: Controllable Damper

There is extensive research comparing the advantages of an active or semi-active damper, to passive systems. Karnopp[10] concludes that similar performance gains can be made between active and semi-active systems over passive. Semi-active system are a more logical choice because they only require signal processing and low level power supplies making them a simpler and more cost effective alternative to active systems. In

an experimental test performed by Krasnicki[21], a semi-active damper system was retrofitted to an off road motorcycle to evaluate the performance of an "On-Off" semi-active system. This self contained system showed significant results by minimizing the acceleration of the motorcycle frame. Another significant study by Hiemenz[18] on a crew seat out of a SH-60 Seahawk helicopter showed that an MR semi-active damper can reduce the vertical vibration that is transmitted thought the seat to the crew member by 76%. In addition a single degree of freedom, SDOF, model was used to emulate the complex vehicle seat. It concluded to be a significant tool in modeling and performance predictions of the MR damper design. A study by Choi and Wereley[7] showed that by using ER/MR fluids in shock struts of helicopter tail landing gear, a reduction in dynamic load and vibration were achieved. This study was performed both analytically and experimentally. Finally, in a full scale study conducted by Wray and Jimenez[20] in 2005, a Stryker vehicle was tested on the Yuma Proving Grounds over varying terrain types. The overall results were significant. The addition of MR dampers to the vehicle saw an increase in speeds up to 72% along with reductions in vehicle vibrations and vehicle pitch motion. These reductions would increase battlefield effectiveness, safety levels for both operator and crew, and reduce the potential for vehicle damage and maintenance.

Keyword: Control Policies

The purpose of control policies is to absorb as much of the input energy as possible, by governing the control of a semi-active system. On such control policy developed by Karnopp, Crosby, and Harwood[10] called "Skyhook dampening" simulates a damper connected from the body to an inertial reference frame to damp out body motion.

This idea is impractical for experimental testing. In contrast this is where a MR or controllable damper can be used to simulate the skyhook configuration. This study concluded that with the use of a skyhook control policy, results could be attained similar to those of an active system. A similar type of system used experimentally by Krasnicki[21] used and "On-Off" skyhook control policy. They type of controller is extremely simple and does not require a complicated micro processor. In this system either the damper is at its maximum damping when it is energized or at its lowest when it is not energized. Another version of the Skyhook control policy is called the Continuously Variable Damper or "CVD" as stated by Motta, Pereira, and Zampieri[29]. In this study both systems were modeled in MATLAB and with the given results the CVD system showed some performance gains over the simpler On-Off system. According to Simon[38] both the On-Off and skyhook control policies have similar performances with the CVD system having a slight advantage. Also in Simon's[38] research there are two ways to models a skyhook control system, one is velocity dependent and the other is displacement dependent. Either was deemed appropriate however the choice depended on the type of monitoring equipment used. The velocity skyhook system requires separate components to measure velocity than does the displacement control policy. A study conducted by Carl and Wang[43] in 1999 used a fuzzy logic controller. There basis for this design was that it is a natural methodology for solving problems with little or no information available. This control scheme worked exceptionally well and showed significant reduction in vertical loads seen by a landing impact. Finally in a study by Choi and Wereley[8] a sliding mode controller was developed for theoretical tests trying to

attenuate acceleration and displacement of the landing gear. This controller was used because it is robust against parameter variations and external stimuli.

Summary:

With today's advancements in fluid technology and computer controlled devices, optimal gains can be made over existing or traditional passive type suspension systems. MR fluid is not new but has recently received attention due to advancements in micro processor technology. MR fluid has been used in all fields from aerospace to medical with excellent results in controllable dampers. Researched literature focuses little on the relationship between theoretical modeling and experimental data, especially with regards to aircraft suspensions. Controllable suspensions are not new but the introduction of MR fluid adds new applications to active suspension dampers. Active suspension systems, the preferred improvement over passive systems, are heavy, require extensive modifications, increased input power and are expensive. Semi-active suspensions systems can be an alternative. The benefits include: little or no modification time, low input power, inherent fail-safe designs, can be packaged in small spaces, and have comparable performance to that of active systems. There are numerous systems that can be used to control a damper. None however offer the simplicity and functionality of the skyhook policy. Which is the most commonly used damping policy used with controllable dampers.

Objective:

The author explores the use of semi-active MR dampers on aircraft landing gear to reduce the transmissibility of the landing impact to the body. This paper includes a theoretical model in SimMechanics, as well as experimental test data. Given the cost of a functional landing gear assembly, experimental data was collected from the suspension system of the SAE collegiate series Baja vehicle at the Daytona Beach campus. Both the aircraft and Baja vehicle suspensions can be modeled using the same approach, therefore validating the theoretical simulation. A new method for fluid control will be used where by a rudimentary fluid controlling device will be installed, eliminating internal control requirements. This will be discussed further in Ch 3 damper development.

Approach:

The three distinct approach phases are discussed below:

- Phase 1: In this phase a mathematical model was developed in the MATLAB program SimMechancis. Both passive and semi-active models were used to compare acceleration transmissibility. The 'no jerk'[2] skyhook control policy was used for the semi-active case.
- Phase 2: This phase includes the selection of suitable dampers for the Baja vehicles front suspension. A simplistic passage way to control the fluid was designed. This phase also researched and purchased data collection methods and monitoring systems for the vehicle.
- Phase 3: This phase involves actual testing on the Baja SAE vehicle with passive dampers. Data was collected with a simple track set-up utilizing two parking curbs for small inputs and a 1 foot ramp for impact landings. The data was used to tune and validated the passive SimMechanics model.

CHAPTER 2 HARDWARE

This chapter will discuss the hardware used to perform, collect and analyze all the data associated with a semi-active suspension damper design. First, damper selection and suitability will be addressed. Second, electromagnet design and relative location to the fluid will be addressed. For this study, MR fluid will be controlled externally unlike tradition systems that modify the internal components of the damper. Since this type of control mechanism is uncommon, a number of different variations were utilized.

DAMPER DEVELOPMENT

The selection of a stock damper to modify into an MR damper is critical. Of all the selection criteria a damper that can be retrofitted with MR fluid and semi-active control system are the most important. There are many different manufactures who design dampers. Some of the more well known automotive ones such as Penske, Monroe, Koni, Bilstein, and Carrera make quality high performance shocks. For this study Penske shocks were chosen due to their quality and reputation for making one of the best dampers on the market for automotive racing applications.

Twin Tube Shock Description

A twin tube shock simply has two tubes inside the shock body, with the body being the outer tube. The inner tube or what is known as the pressure tube is inside the
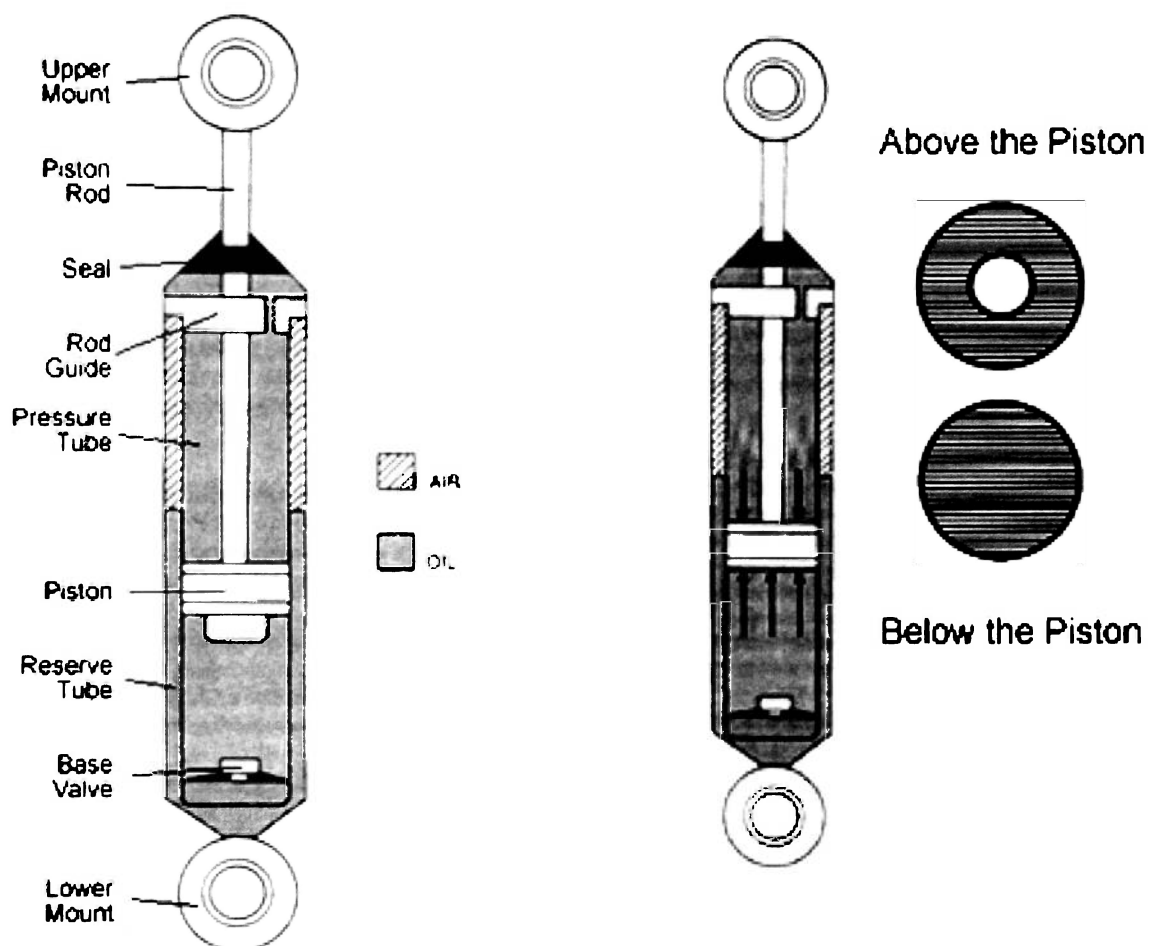
Figure 17. Typical Twin Tube Damper[40].

body. See figure 17 for reference. As you can see in the figure, the shaft and piston are inside the inner tube. Notice that the outer tube is partially filled with either pressurized air or nitrogen. The reason for this is that as the piston moves up and down in the inner tube the volume on each side of the piston is different. Since there is a change in volume

there must be some place for the fluid to go. Pressurized gas being a compressible medium allows the fluid to flow from the inner tube to the outer tube to compensate for the change in volume. This oil will flow out of the inner tube through a valve which is known as the base or "foot" valve. This base valve helps control the compression damping rate.

Mono-tube Shock Description

A mono-tube shock includes a single tube in which the shaft and piston move in and out of the tube. Since this tube is filled with oil only and to account for the volume change as the shaft is displaced into the body, there must be a reservoir filled with compressed air or nitrogen somewhere in the shock. In figure 18 you can see that there is a dividing piston that is allowed to float inside the tube sealing off the gas chamber from the oil in the rest of the shock body.
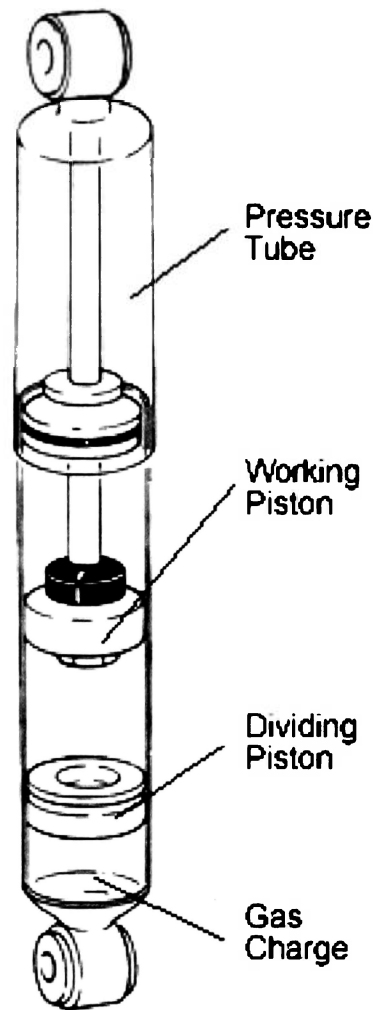
Figure 18. Mono-Tube Damper Design[40].

As the shaft enters the body this dividing piston is allowed to move, accommodating the displaced fluid. This design is fairly simple and has many advantages over a twin tube damper. They can be mounted in almost any orientation and have the ability to cool faster since the tube is directly exposed to air. This type of damper can come in two different configurations. One configuration shown in figure 18 houses the gas chamber inside the main body of the damper. This is one of Penske's 7600 series dampers. The other design has a remote reservoir which houses the gas chamber, figure 19. This is one of Penske's 8100 series dampers. One main advantage

of this type of configuration is that it comes with an adjustable orifice to change the damping rate in compression with the turn of a knob. Usually the remote reservoir is attached to the body tube with the use of high pressure Teflon lined stainless steel braided hose. This allows for flexible mounting locations for the reservoir. Remote reservoir dampers are quite popular with racers looking for an edge by having an adjustable damper. This allows the user to adjust shock setting for different situations. It however is not adjustable with time. Another style of remote reservoir is called the piggy back. In this case the remote reservoir is fixed to the body of the damper and is not movable.

The 8100 Series is a simple, high-quality, high-performance, double-adjustable damper that can be used for a variety applications. A single rebound bleed style adjuster is packaged in the shaft and a six setting drum style compression adjuster is found in the remote reservoir. The 8100 can accept both 2.25 and 2.50 I.D. spring hardware and is available in a wide array of lengths. As the most diversified Penske shock, the 8100 is currently used in all types of applications.

Hose Length Available in 1" increments from 4" to 36"

1.72" Bore for Maximum Performance

6 Setting Compression Adjuster *(see page 16)*

Unique Piston Designs for Greater Versatility

2.25" or 2.50" Spring Hardware Available

Low Friction Shaft Seal

Low Friction Reservoir Piston

Threaded Bearing for Ease of Servicing and Rebuilding

Nitrogen Chamber with Separator Piston

5/8" Chrome Plated Chrome-Moly Shaft

Sweep Adjuster *(see page 17)*

Figure 19. Penske Mono Tube Damper Courtesy of Penske

MR Shock Design

For this study an adjustable remote reservoir damper from Penske's Custom Axis division was selected. This specific damper was custom made to fit the Baja SAE's vehicle suspension parameters. The remote reservoir set up will allow a new alternative
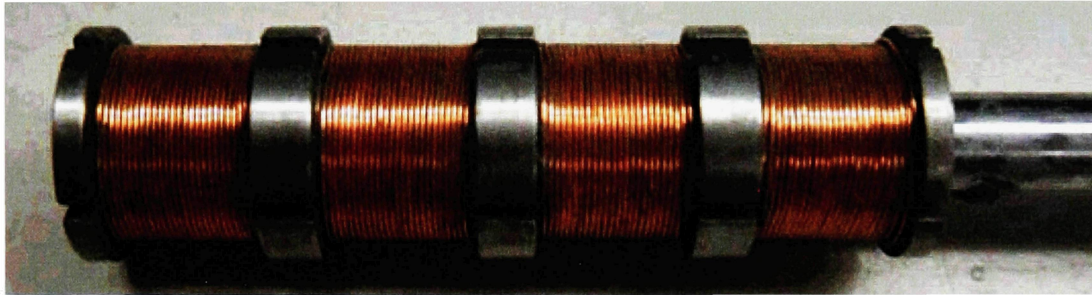
Figure 20. MR Coil Mounted Piston[14].

for controlling the MR fluid in the damper. Traditional MR dampers use a modified piston with coils of magnet wire wrapped around it. Figures 20 and 21 show the typical design of an electromagnet wound onto a piston. Figure 20 has four coils wrapped around the shaft of the piston. This design allows more surface area to be effected by the magnetic flux lines. This design controls the fluid in a relatively small area between the piston and the tube the piston rides in as seen in figure 21. In a study by Gavin, Hoagg, and Dobossy[14] the design of the electromagnet piston in figure 21 can increase damping within 50 milliseconds and can decrease it inside of 20 milliseconds.
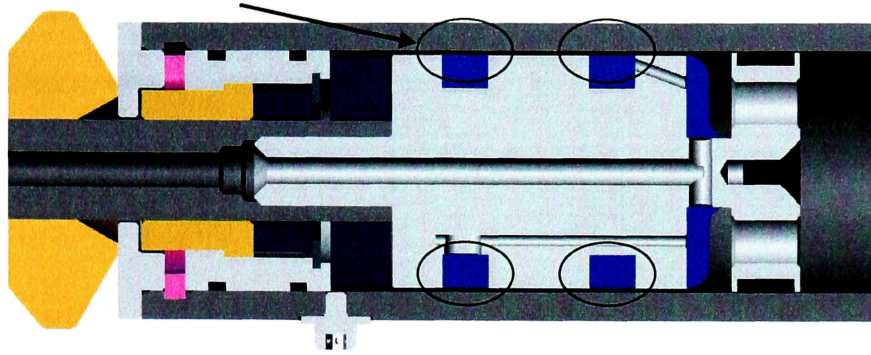
Figure 21. MR Piston Choking Points[33].

In Poynor's[33] research on innovative designs for Magneto-rheological dampers, multiple designs were considered including a double ended damper and a piloted hydraulic damper. However, the mono tube was a better choice over the twin tube design. For the purpose of this study, a new control method was used. Since the Penske shock ordered has a remote reservoir, the design goal for this project is to develop an easier method of manufacturing and control. The traditional method of making MR damper's as described above require wire to be run all the way up to the piston through the shaft. This requires the shaft to be hollow. Since the shaft is under extreme load this is a crucial design step. Retrofitting the damper would require a hole to be drilled the length of the shaft. This method would require extensive precision CNC machining. Instead the fluid will be controlled without modifying the internals of the damper. As shown in figure 22 the magnetic field will be applied to the fluid between the damper body and the remote reservoir. This coil housing will have the ability to control the fluid that is displaced by the piston shaft entering the body. The coil housing will be plumbed in between the body and reservoir. This device will allow little or no modification to the damper especially to the piston shaft. In the preceding pictures the process of changing

out the oil filled damper with MR fluid is shown. Penske Custom Axis[11] has a detailed

manual of damper service and adjustment.
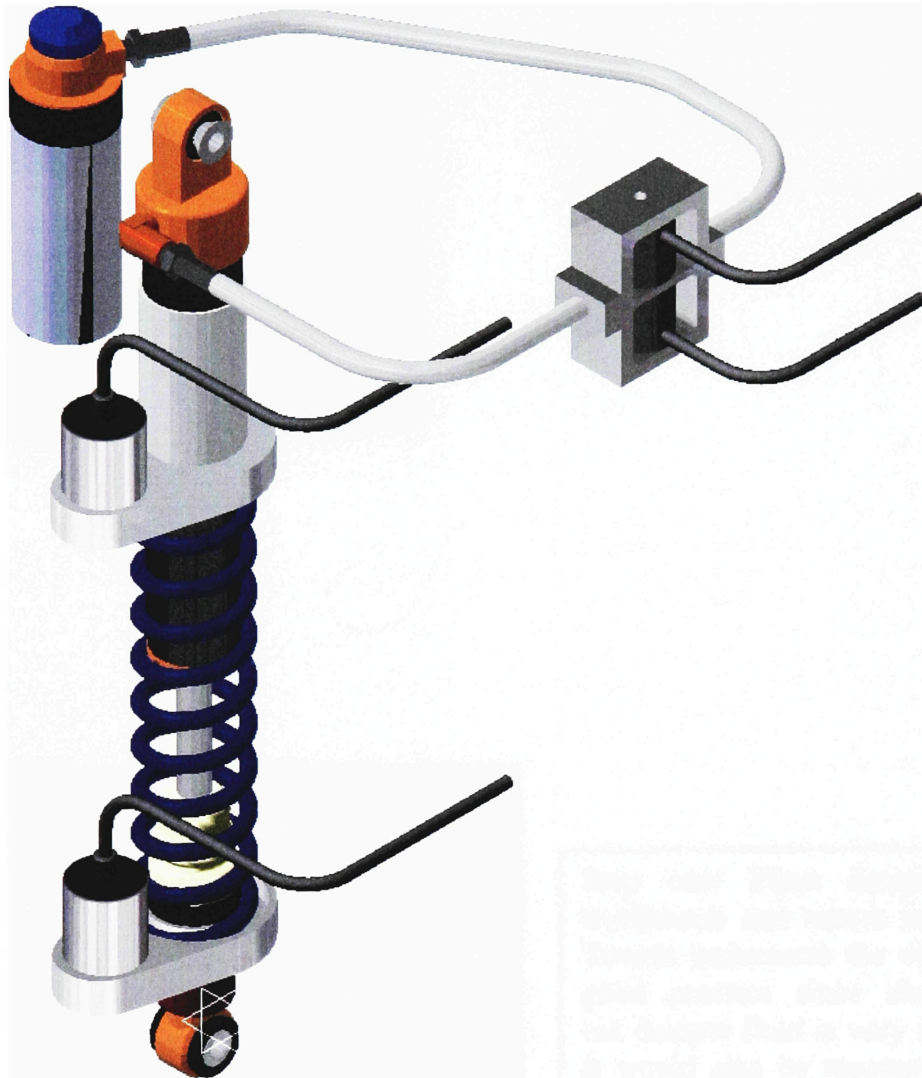
Figure 22. CAD Model of Prototype MR Damper

Typical equipment needed to change a damper's fluid includes a rubber mallet, gloves, pliers, damper wrench, Teflon tape, Q-tips, piston wrench, tongue depressors, and reservoir filler.

Step one: Place damper on workbench and secure in vice. Towels underneath the vice are good practice since changing out damper fluid is very messy. It would also be recommended to have numerous rags readily accessible.

Step two: Bleed out nitrogen in remote reservoir. Push down reservoir end cap and remove retaining ring. Carefully pull out reservoir end cap with pliers.

Step three: Use the damper wrench to unscrew the shaft bearing from the body.

Step four: Pull out entire piston shaft assembly. Set aside with a rag wrapped around it to limit the amount of fluid spill. Clean with a fast evaporating cleaner such as carburetor cleaner and set aside.
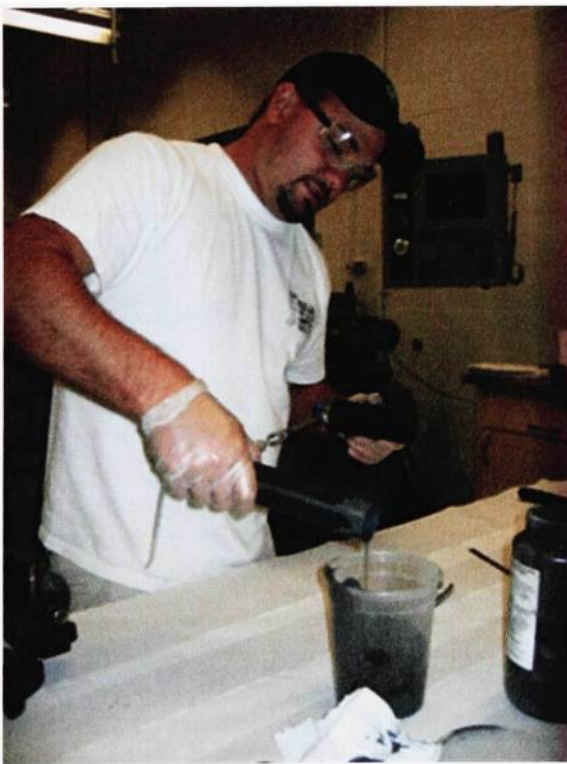
Step five: Pour fluid from damper body into a sealing plastic container.

Step six: Screw piston tool onto the floating piston in remote reservoir. Pull piston all the way to the top of the remote reservoir. Next carefully pull out floating piston being careful to not damage the seal on the piston. Lastly, drain fluid from reservoir and clean shock body and remote reservoir with cleaner.
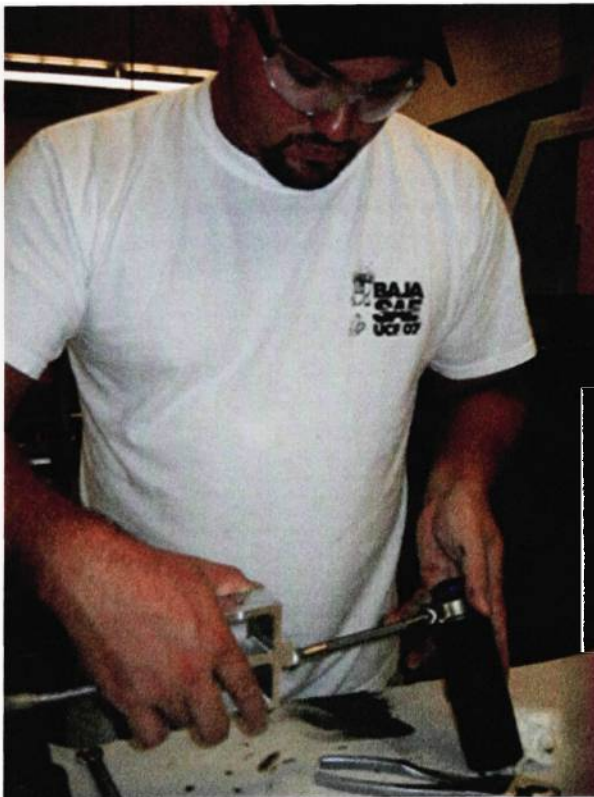
Step seven: Attach coil housing in-between reservoir and damper body. Make sure to use Teflon tape on all threads to obtain an air tight seal.

Step eight: With damper body clamped in vice, fill damper body with about an inch of MR fluid.
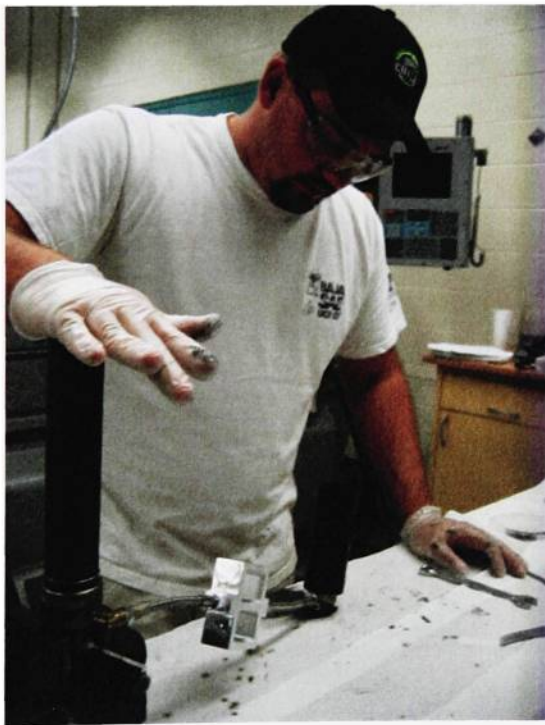
Step nine: Making sure the reservoir is below the damper body fitting, gently pat the top of the damper body to force fluid from body tube through the coil assembly and into the reservoir. This step bleeds any air out in-between the body and reservoir.

Step ten: Once MR fluid has seeped into the reservoir, fill reservoir with MR fluid up the retaining ring groove.

Step eleven: Insert floating piston into reservoir being VERY careful not to damage the seal. This is imperative. If it does not seal properly then the compressed nitrogen will bleed into the damper tube causing undesirable effects. Next turn the reservoir right side up and cycle the piston up and down in the bore to purge any air out of the reservoir.

Step twelve: Once there is no more air bubbling out of the damper body tube, press in the reservoir end cab and reinstall the retaining ring. At this point use compressed air of at least 100 psi to hold the floating piston in place while the piston shaft assembly is bled next.

Step thirteen: Fill the damper body tube with MR fluid about a half inch away from the bottom of the threads. Next insert the piston shaft assembly into the damper body tube being careful not to nick the piston sealing band. Now stoke the shaft in and out of the damper body to purge out any air trapped in the piston. Be careful not to pull it to far out and expose the piston to the air.

Step fourteen: Once all the air is out, pull shaft as far as you can without introducing air into the system. Then slowly screw down the shaft bearing making sure the shaft assembly does not move down into the body. Once it starts to get harder to screw in, let the compressed air out of the reservoir. Finish tightening.

Step fifteen: The last step is to use compressed nitrogen and fill the remote reservoir to approximately 175 psi. then your new MR damper is complete.

FLUID SELECTION

The Lord Corporation has three different types of hydrocarbon, or synthetic oil, based MR fluids. In choosing a fluid the only difference was its dynamic viscosity. Two ways of selecting the fluid were used. The first was to contact the Lord Corporation and have them recommend a type of fluid to use in our dampers. They recommended MRF-132DG for all damper applications. This was their middle weight fluid rated in viscosity. The second method was to compare their viscosities of both the standard damper oil and the MR fluid. The damper oil being compared was Silkolene, a well known synthetic oil manufacturer who makes damper oil for Penske Racing Shocks. Table 1 shows each type of fluid and its viscosity. For comparison, damper oil was used which measures kinematic viscosity instead of dynamic viscosity. For this reason the MR fluids dynamic viscosity was converted to kinematic using equation 1. Where υ is the kinematic viscosity, μ is the dynamic viscosity and ρ is the density of the fluid. The units of measure of the dynamic viscosity are centistokes.

$$v = \frac{\mu}{\rho}$$

Equation 1. Kinematic Viscosity

DAMPER OIL	VISCOSITY (Cst)
Silkolene 2.5 WT	13.60
Silkolene 7.5WT	37.00
Silkolene 15 WT	92.95
MRF-122EG	17.87
MRF-132DF	30.66
MRF-140CG	77.78

Table 1. Viscosity Comparison.

From the data in table 1, a middle range viscosity MR fluid would be the MRF-132DG, shown in figure 23, which verifies lord's recommendation. This will give the damper a mid range viscosity similar to that of mid range viscosity damper oil.
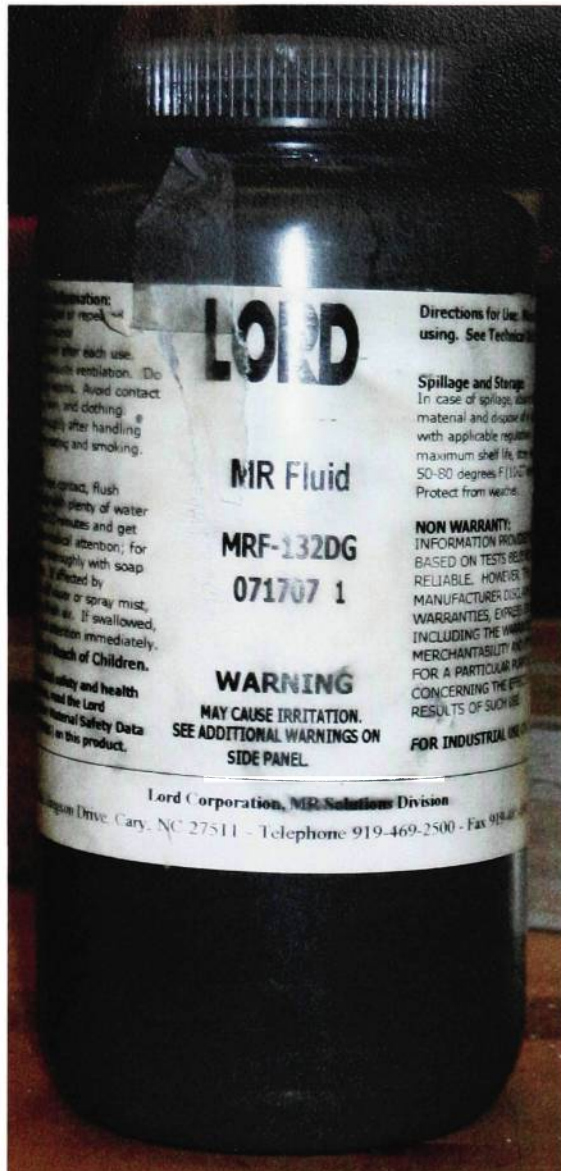
Figure 23. MR Fluid MRF-132DG.

ORIFICE SIZE DESIGN

Orifice size selection dictates magnetic field strength as was as introducing caivtation effects. If the orifice is too large the magnetic field strength required to change the MR fluids viscosity would be extremely large, making this an impractical design. A smaller orifice is better since the magnetic field strength required will be smaller, however cavitation becomes a concern. Cavitation is the formation of vapor bubbles in a high flowing fluid area that reduces the pressure to the vapor pressure of the fluid[31]. See figure 24 for a photograph. A direct relation can be made with the Bernoulli equation.
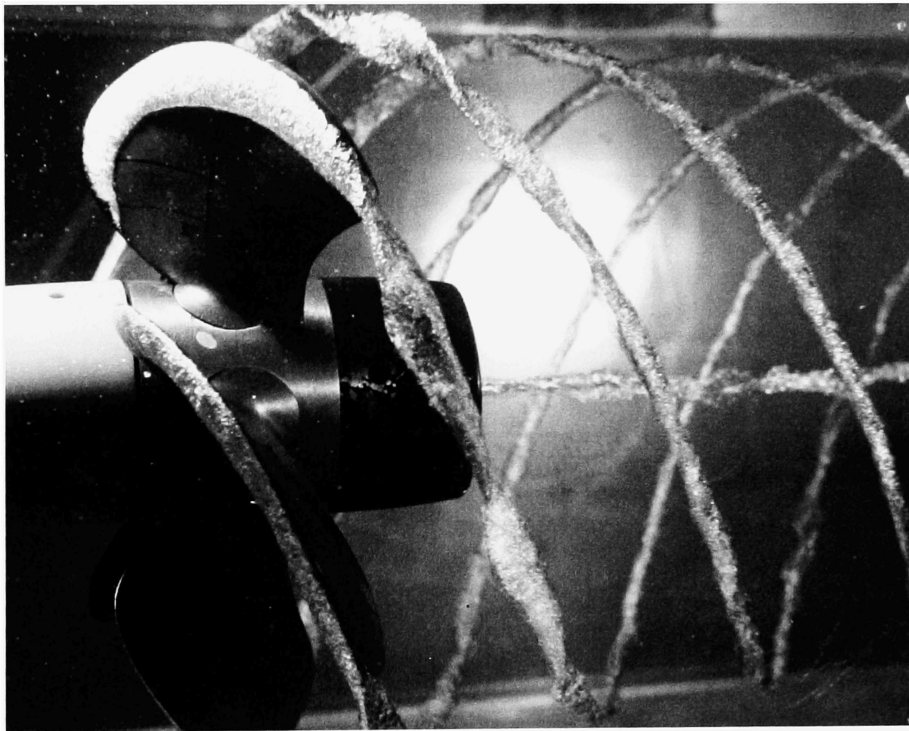
Figure 24: Cavitation in a Propeller[34].

In this equation p is the pressure, ρ is the density, V is the velocity, γ is the specific weight and z is the height change.

$$p_1 + \frac{1}{2}\rho V_1^2 + \gamma z_1 = p_2 + \frac{1}{2}\rho V_2^2 + \gamma z_2$$

Equation 2. Burnoulli's Equation.

As the velocity of a fluid increases i.e. going from a larger area to a smaller area the pressure drops to help accelerate the fluid through the smaller area. This velocity can be calculated with the continuity equation shown below. Here Q is the volume flow rate, A is the area of the object and V is its velocity.

$$Q = A_1 V_1 = A_2 V_2$$

Equation 3. Continuity Equation

All fluids have a vapor pressure; the vapor pressure for majority of damper oil is very near to 0 psi. Figure 25 depicts the problem being solved with the equations above. To set up the problem we need to find the pressure that will drop p_2 below the vapor pressure of damper oil. The data in table 2 was be used to solve this problem. The flow is considered incompressible, invisid and steady.
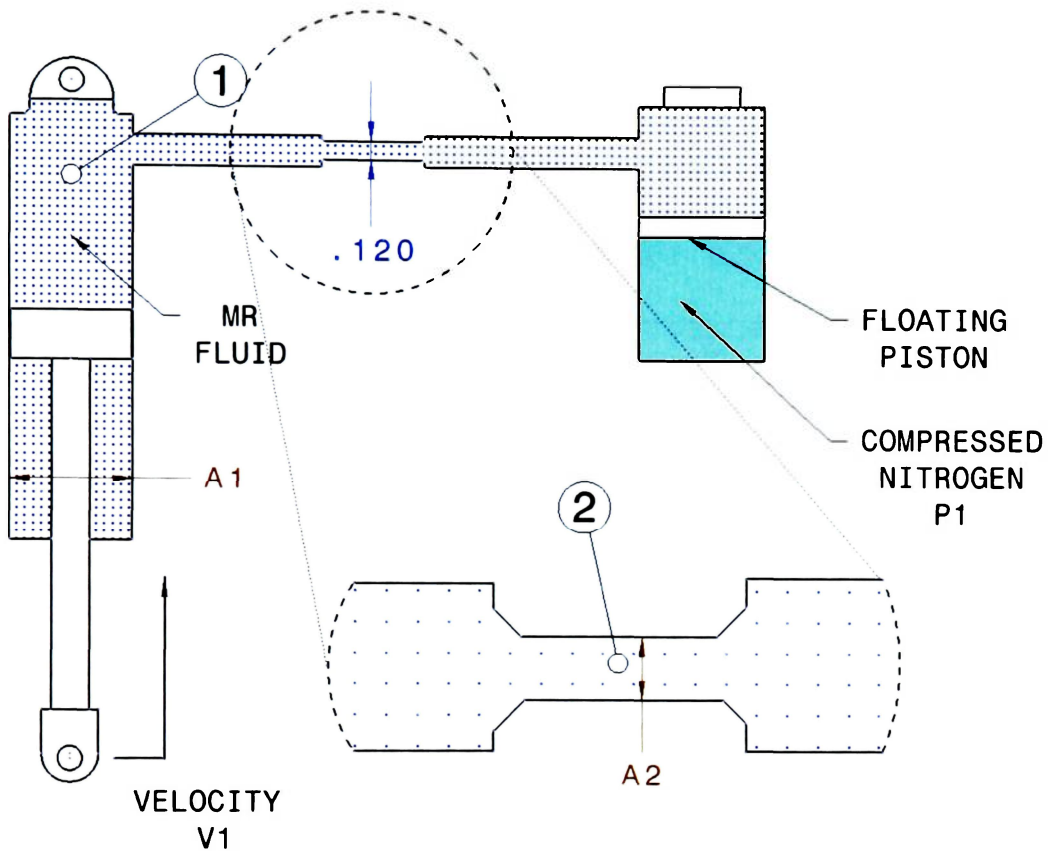
Figure 25. Cavitation Calculation Set-Up.

ITEM	QUANTITY	UNITS
V1	30	in/sec
P1	150	psi
A1	0.3068	in ^2
A2	0.0113	in^2
P2	Near Zero	psi
V2	Need to Find	in/sec
RHO	0.003368	slugs/in^3

Table 2. Initial Parameters for Cavitation Calculation.

Using the data in table 2 above, and equation 3, we find the velocity at V_2 is equal to 457.7 in/sec. Substituting this into equation 2, we can find P_2 which will verify if there is cavitation. The value of P_2 must be lower than the vapor pressure of around 0 psi. On a side note, the term P_1 is made up of two different components. One is the internal pressure charge in the reservoir and the other is the pressure generated by the force of the piston moving inside the damper body, which for our case is around 203 psi. This equates to a P_2 of 2.35 psi which is above 0 psi. This serves as verification that this size orifice will not cause cavitation.

MAGNETIC FIELD GENERATION

The magnetic field needed to change the viscosity of MR fluid can be very small depending upon the application. The field can be generated by one of two ways. The first being a permanent magnet such as a rare earth or neodymium, the second by an electrical current passing through wire. The most popular option is the electrical current passing through wire or electromagnet. This allows a controller to vary the current through the wire which has a direct relation to the magnetic field size and intensity. This change in magnetic field also has a direct relationship with the viscosity of the MR fluid, thus when applied to a damper it changes the damping rate almost instantly. For this study an electromagnet will be used.

Magnetic Field Requirements

The volume of MR fluid affected depends on the intensity of the magnetic field. The smaller the volume of fluid being controlled will require a smaller magnetic field. This is one of the most important design considerations. A well designed fluid control device requiring a small magnetic field is critical. If the magnetic field required is smaller, that means less current has to be put into the wire electromagnet. If less current is required then less power is consumed. This can be seen in the electrical power equation or Joule's Law. Here P = power, V = voltage, I = current or amps, and R = resistance in ohms.

$$P = V \times I$$

$$P = I^2 \times R$$

Equation 4. Power Law

Power consumption is curial in design. Making an electromagnet that requires little electrical power is an ideal since this system needs to be adapted to a vehicles or aircrafts electrical system with little or no modifications. The power supplied can either be DC or AC depending on particular applications. This study will use DC current as it is a readily available source on vehicles. Saturation is another consideration. At some point, the fluid will reach a state where more magnetic field strength will not change the yield stress. This can be shown in figure 26. As more magnetic field strength is applied the yield stress will converge to a steady value. This data is empirically determined by Lords[30] testing facilities. Another design consideration is determining the size or gauge wire to use. In previous studies wire gauges from 16 to 24 gauges have been used. Thicker gauge wire means fewer numbers of turns for a give size coil. However, more current can be supplied to the coil.
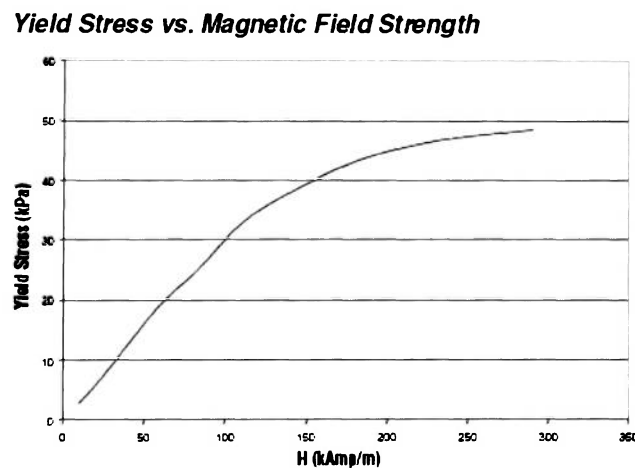
Figure 26. Yield Stress vs. Magnetic Field Strength[30].

Using smaller gauge wire allows more turns and thus increases the magnetic field generated, but results by Gavin, Hoagg, and Dobossy[14] showed 20 gauge to be an optimal choice for their experiment. This was determined to be the starting gauge for coil design. Another equally important design consideration was how the magnetic field flux lines pass through the fluid. It is imperative that the flux lines be perpendicular to the fluid flow. Flux lines that are not perpendicular do very little to change the fluid viscosity.

Initial Designs

Numerous initial designs were considered. The first consideration was flux line orientation and how to make them perpendicular to the fluid flow. Figure 27 shows the typical magnetic flux lines of a north south bar magnet.
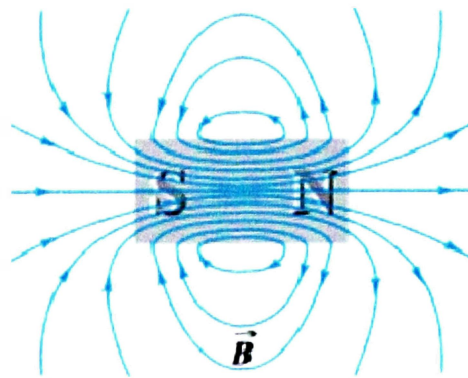
Figure 27. Magnetic Flux Lines of a Typical Magnet Courtesy of Addison Wesley Longman, Inc.

The flux lines extend straight out of each pole on the centerline. As the lines move away from the center the magnetic lines start to bend away from one pole and go into the other in a semi-circular shape. From physics[37] it is known that opposite poles attract. An example is displayed in figure 28. This attraction forms straight flux lines from the pole of one bar magnet to the opposite pole on the opposing bar magnet. It was decided that this would be a first approach to designing an electro magnet.
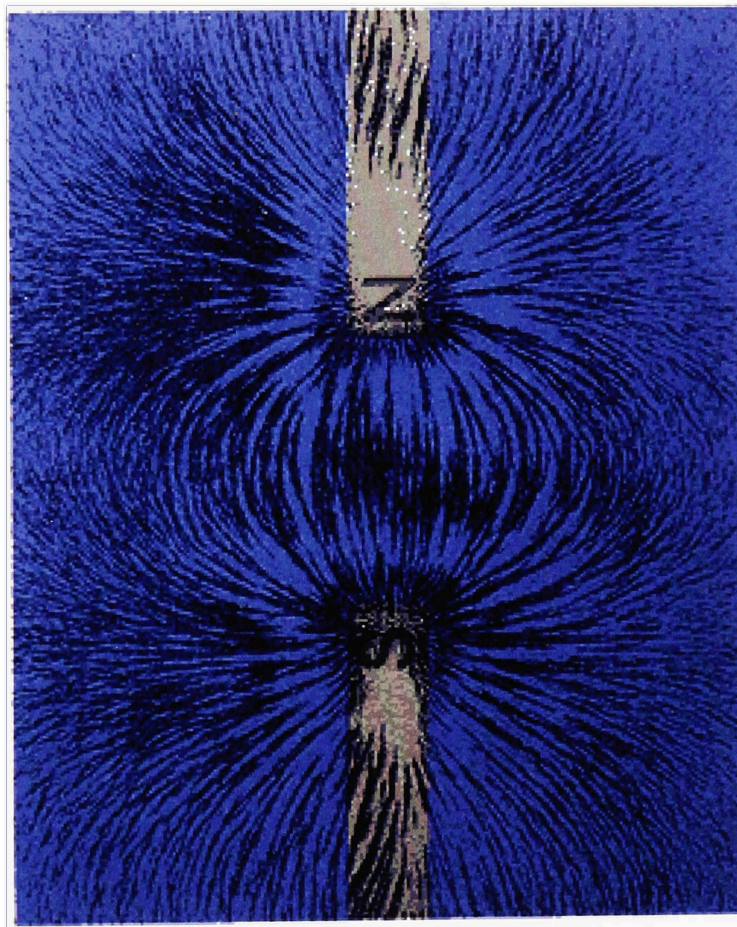
Figure 28. Magnetic Flux Lines of Two Opposite Pole Bar Magnets[37].

Designing an electromagnet is as simple as winding insulated copper wire around a ferrous core material such as steel. When electrical current is applied to the wire a magnetic field is formed. The magnetic field flux lines that are generated by the electrical current follows the right hand rule as figure 29 depicts.
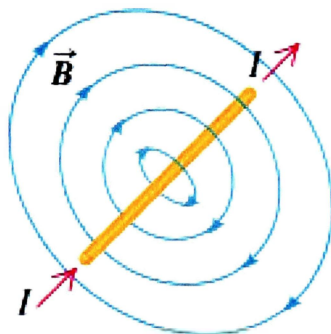
Figure 29. Magnetic Field Lines Generated by Current[37].

Now when this is applied to a coil of wires wrapped around a ferrous core. The magnetic flux lines flow out of the center of the coil similar to that of the bar magnet. Figure 30 shows a model of a coil of wire and the magnetic field lines that are generated.
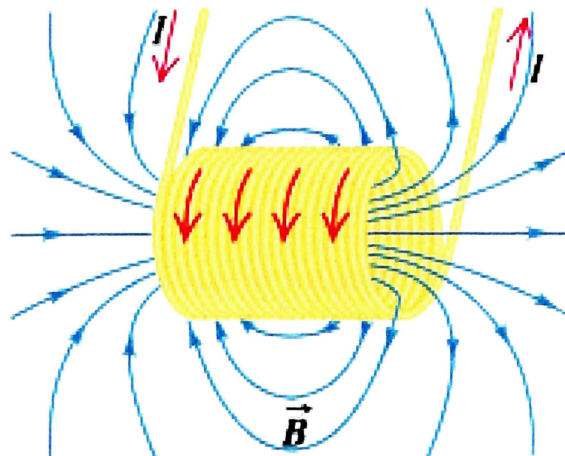
Figure 30. Magnetic Field Lines Generated by a Coil of Wire with Current Flow[37].

Applying the same knowledge as in figure 30 when two coils with opposite poles are facing one another the flux lines will attract each other and form parallel lines to the core centerline. It was decided to use a CNC lathe to wind electromagnetic coils. Another alternative to using two coils to generate straight flux lines was to use a toroidal coil with a break. In figure 31 a toroidal core is wound with magnetic wire. The flux lines follow the core and jump the gap forming straight lines. Here the fluid could be passed through the gap generating a magnetic field that is perpendicular to the fluid flow.
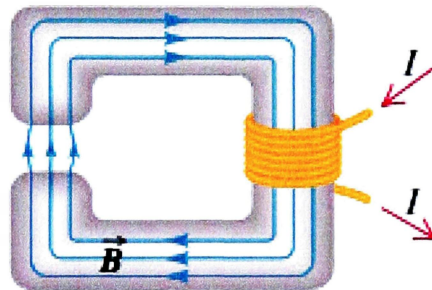
Figure 31: Magnetic Field Lines of a Square Electromagnet Coil With Gap

Courtesy of Addison Wesley Longman inc.

This design seems ideal however wrapping this type of coil with copper wire would have to be done by hand as compared to machine with the alternate design. To accelerate manufacturing, two cylinder type coils were made. Figure 32 shows a CAD drawing of this design. A soft ferrite core was used to increase the strength of the magnetic field and allow no residual magnetism when the current was turned off. The

current in each coil runs in opposing directions which creates a north and south pole near the fluid. This allowed the magnetic flux lines to jump through the orifice perpendicular to the fluid flow. See figure 33 for reference
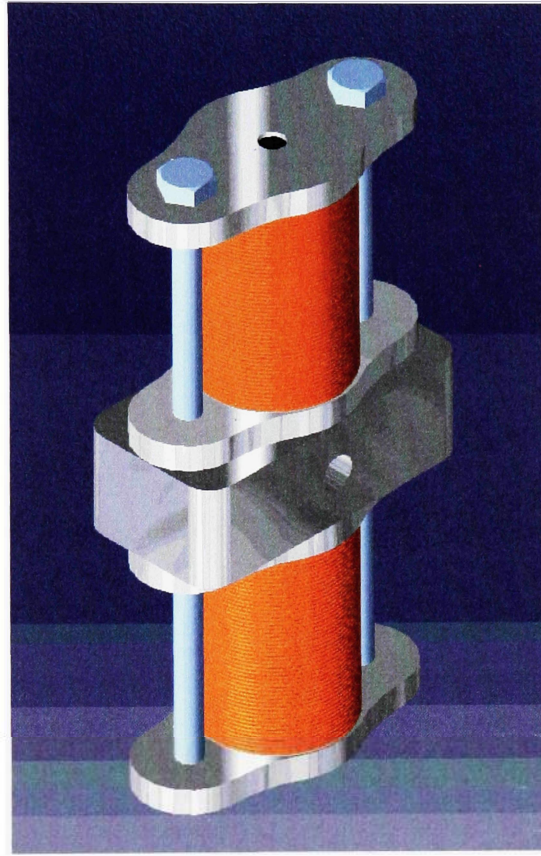
Figure 32. CAD Drawing of First Coil Housing.
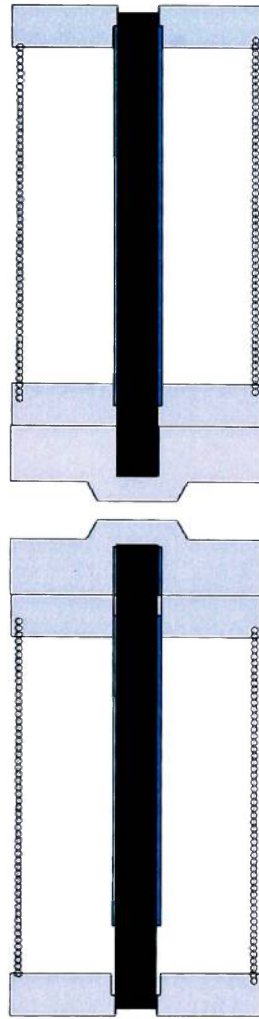
Figure 33. Cross Sectional view of Initial Coil Housing.

Each coil was hand wound using the university's CNC lathe. The process still required the user to move the wire back and forth, but was more efficient than winding exclusively by hand. See figures 34, 35, 36, and 37 to see the coil winding procedure. This design although extremely efficient for cost and manufacturability, had several flaws. Initial testing proved that these electromagnets were very poor at generating a magnetic field. Each coil had over 500 feet of enamel coated copper wire. With this size

electromagnet the field should have considerable strength, yet it would not hold a paperclip. The magnetic field was insufficient to have an effect on the MR fluid.
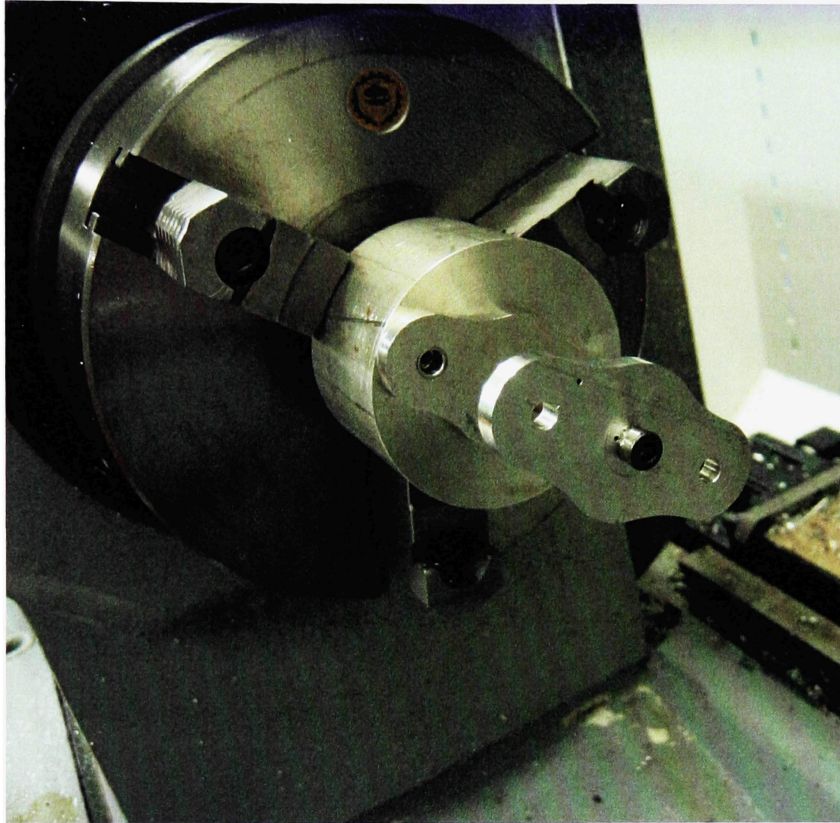
Figure 34. Coil Housing Mount on CNC Lathe.
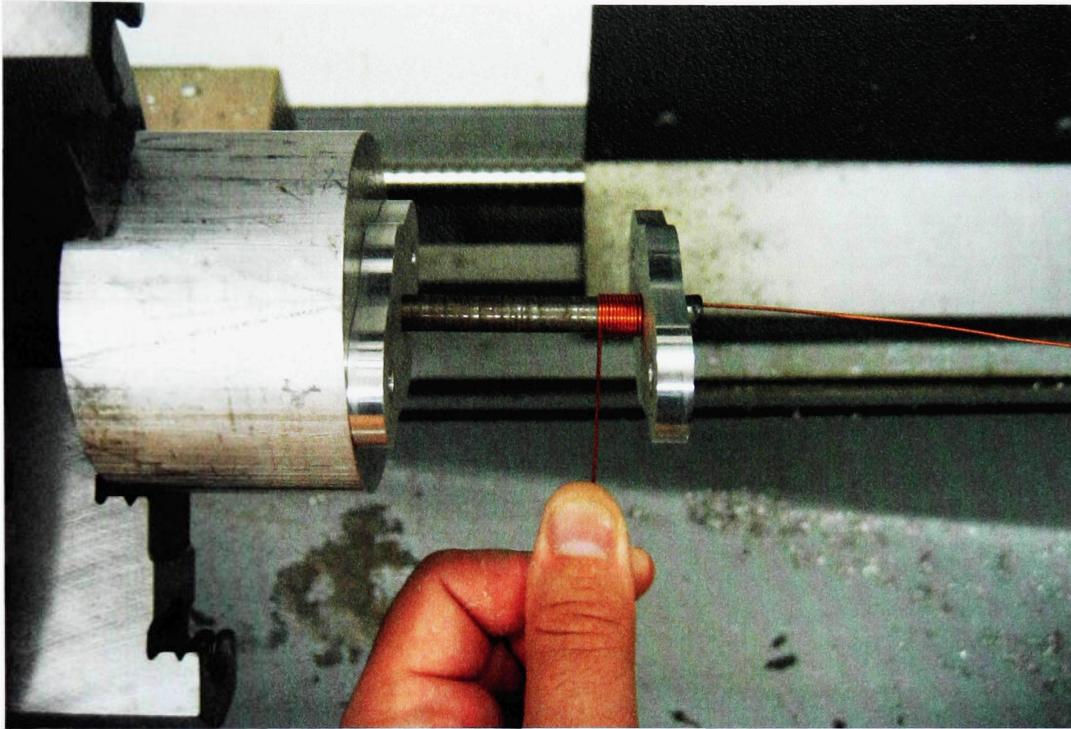
Figure 35. First Layer of Coil.
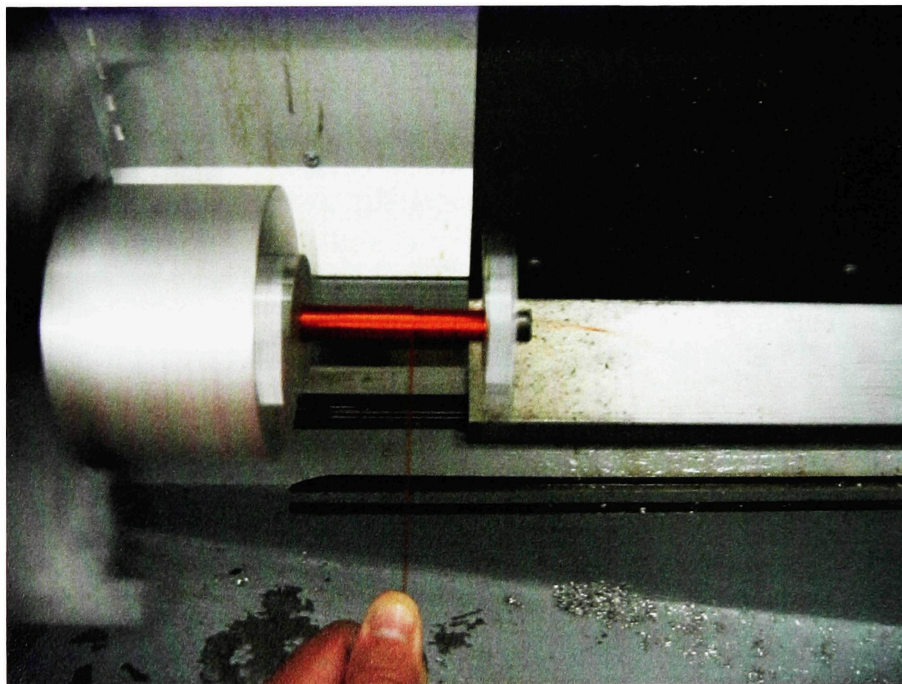
Figure 36. Second Layer of Wire.
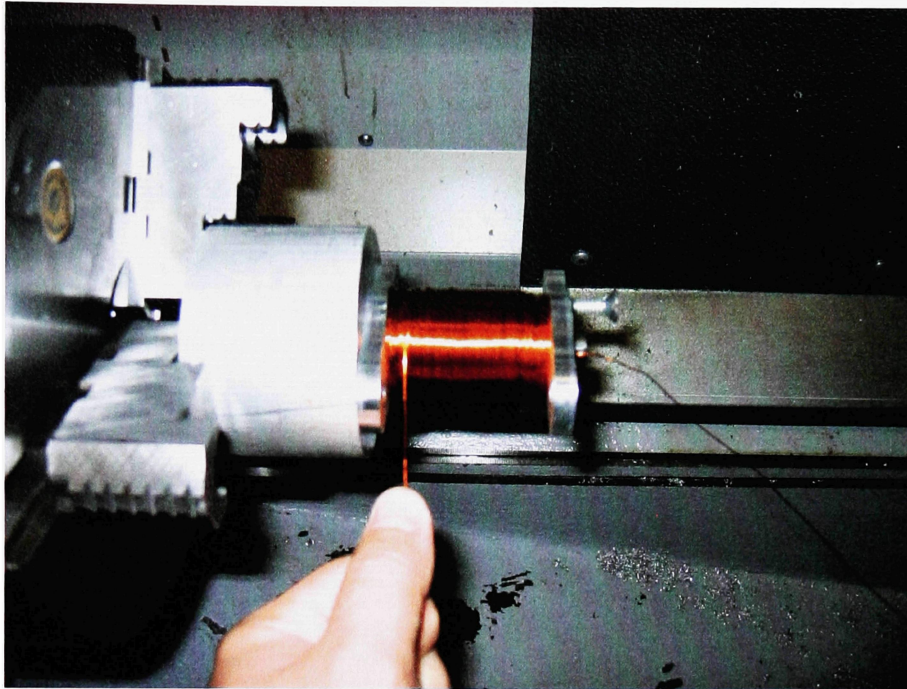
Figure 37: Finished Electromagnet.

The testing involved the comparison of a permanent rare earth magnet which had a significant effect on the fluid effecting damper performance. When compared to the electromagnet there was little or no difference in damper performance. Following failure different gauge wires were tested using very high current to increase the magnetic field strength. Increasing the current generated minimal effect but increased the temperature of the coils. Additional testing revealed the source of failure for the hand wound electromagnets. As seen in figure 38 the enamel coated copper wire was wound directly onto the steel core. In addition, also the wire made several sharp turns through the aluminum at each end, and the steel core was unpolished.
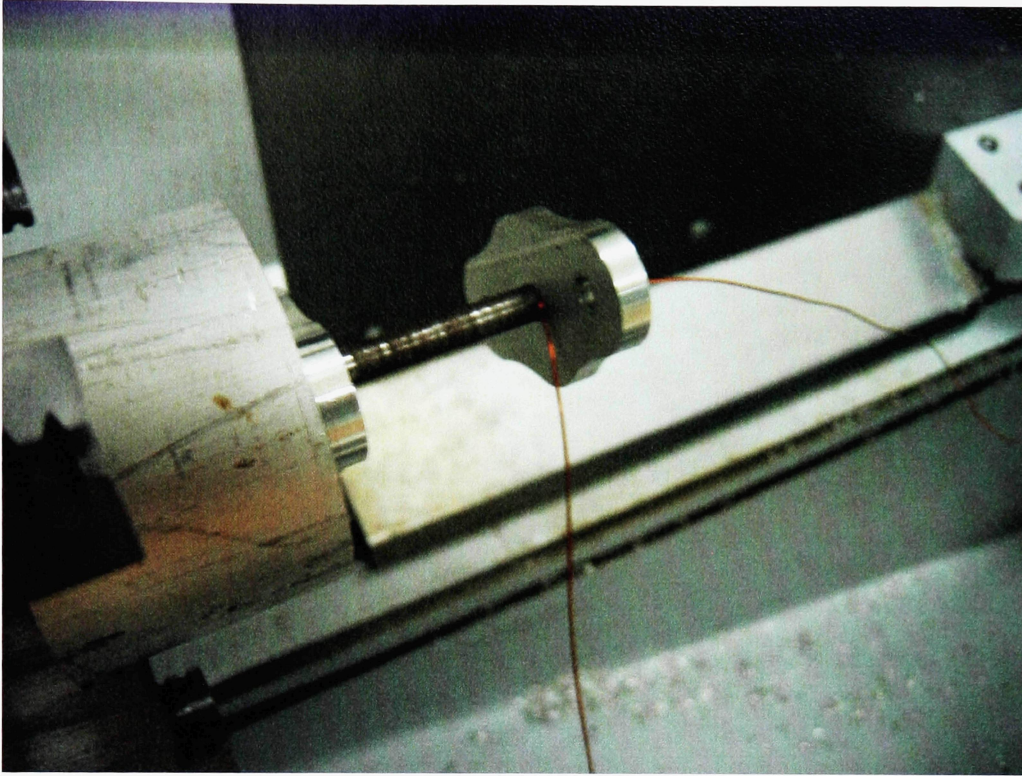
Figure 38: Sharp Bend in Copper Wire to Start Coil Wraps.

Using the CNC lathe the wire was tightly wrapped around the core. The rough surface may have penetrated the thin enamel coating causing a short. Secondly, the sharp bend at the start of the coil winding process may have worn down the coating causing a secondary short. Having a short in the coil dramatically affects its magnetic field strength and path of the flux lines. This may have contributed to the inefficiency of the hand wound coils.

Final Design

Following an extensive search, it was discovered that commercially produced electromagnets would fit to the existing design. The main difference being the addition of professionally wound electromagnets. These electromagnets from McMaster, seen in figure 39 had 50 lbs of pulling force, much stronger than the handmade ones. The size of the orifice remained the same at .120 inches. One new feature of this design included more surface area for the electromagnet to alter the MR fluids viscosity. A cut away view is shown in figure 40.
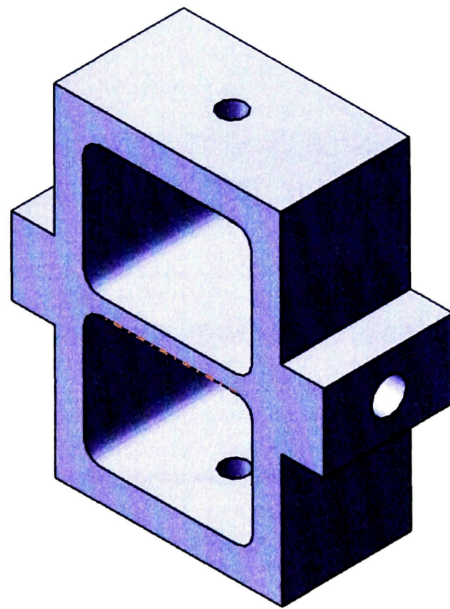
Figure 39. CAD Drawing of Final Coil Housing.
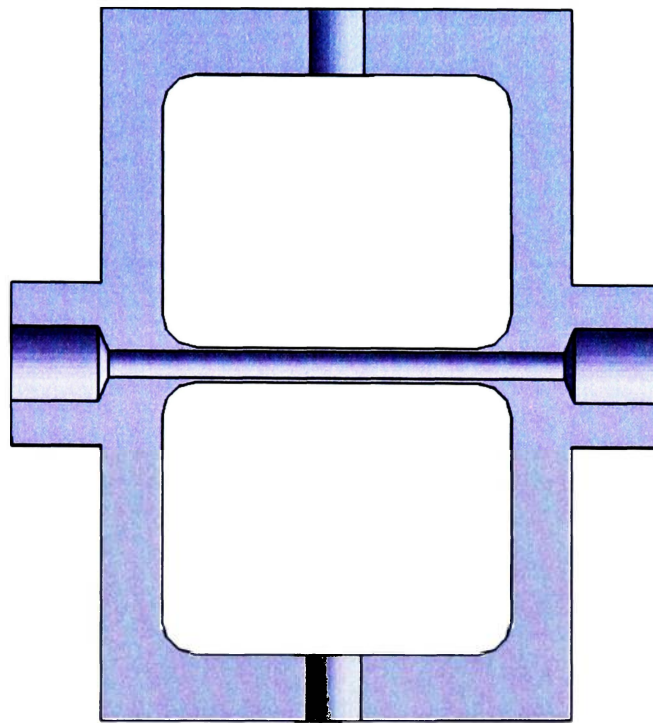
Figure 40. Cross Sectional view of final Coil Housing.

This coil housing was extremely simple to make compared to the previous design. The coil housing was made using the CNC machine in the university's manufacturing lab. The final design proved to be simpler and more economical. It required only 3 programs to manufacture while the previous design had more than 6. This reduced the manufacturing time by more than half. Part of the manufacturing process can be seen in figure 41.

Figure 41. CNC Machining of Coil Housing.

CHAPTER 3 SIMMECHANICS

SimMechanics, a tool box in MATLAB's Simulink program, is a block diagram modeling system that uses body and joint blocks that allow for change in coordinate systems, mass, and directions of motion. Instead of hard coding, block diagrams are made to represent mechanical systems and measure their response to stimuli. Examples of some basic systems easily modeled with SimMechanics include but are not limited too: a single pendulum, a double pendulum, a four bar mechanism, a suspension systems, and even robotic arms. In his paper, Unsal[42] validated SimMechanics and Simulink models by comparing single degree of freedom models and multi degree of freedom ones. Results revealed that both models were identical, validating it as an analysis tool.

Numerical Model

The suspension system of an aircraft is no different than that of an automobile. Because of this similarity the vehicle was simulated with a two mass quarter car model shown in figure 42. This modeling strategy for aircraft was used in studies by Wang and Carl[43]. In addition Choi, Wereley and Kruger, Kortum[22] used this modeling method to simulate vibration control of a landing gear suspension. These models were the basis for the study. The quarter car model has long been accepted as an acceptable model for vehicle suspensions. Simons[38] study along with Islam, Ahmed[19], Singla, Singhand[39] Motta, Zampieri, Pereira[29] all used the quarter car model to simulate vehicle suspension behavior to stimuli.
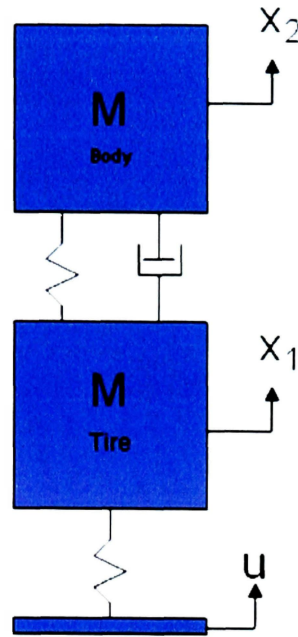
Figure 42. Quarter Car Model.

Using SimMechanics, a 2 body mass model was created similar to figure 42. The two bodies represented the tire mass including suspension components and the mass of the vehicle. Table 3 shows all the parameters of the model.

Parameter	Quantity	Units
M_1	25	lbm
M_2	187.5	lbm
K_{tire}	10000	lb/in
K_{spring}	125	lb/in

Table 3: SimMechanics Model Input

Passive SimMechanics Model

The first model shown in figure 44 was a typical passive linear model. Linear in that the force generated by the damper was directly proportional to the velocity. The equation below shows this relationship.

$$F = c \times v$$

Equation 5. Damper Force[9].

For each model the transmissibility was calculated. Transmissibility is the ratio of input amplitude to output amplitude. For this study a sine wave disturbance was used for input to the tire mass and compared with the output or amplitude or oscillation of the body mass. This ratio was calculated at numerous frequencies and plotted as amplitude vs. frequency. The Matlab code for each model can be found in appendix A. For each model a sampling frequency of 2000 Hz was used. Each frequency was tested until steady state was reached. Frequencies from 0 to 20 Hz were used for each test. 125 points were used to plot each line. For this linear case the damping coefficient 'C' in the spring & damper block was changed to a yield different damping ratio. The damping ratio ζ is defined according to Rao[35] as the damping constant divided by the critical damping constant.

$$\xi = \frac{c}{c_c}$$

Equation 6. Damping Ratio[35].

The input disturbance block shown in figure 43 was used to input initial position, velocity, and acceleration. The derivative of the sine wave was taken for velocity and taken again for acceleration. The variable of w was used in the constant block and for the sine wave frequency. This allowed programmed loops to change the frequency for each iteration.
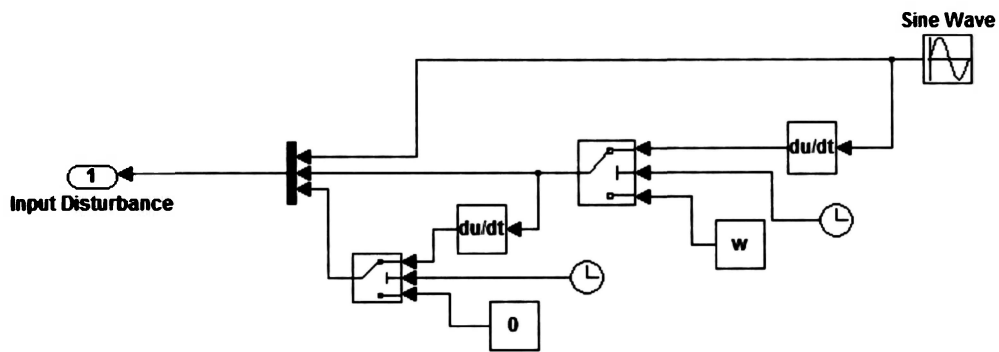
Figure 43. Input Disturbance Subsystem for Simulink.
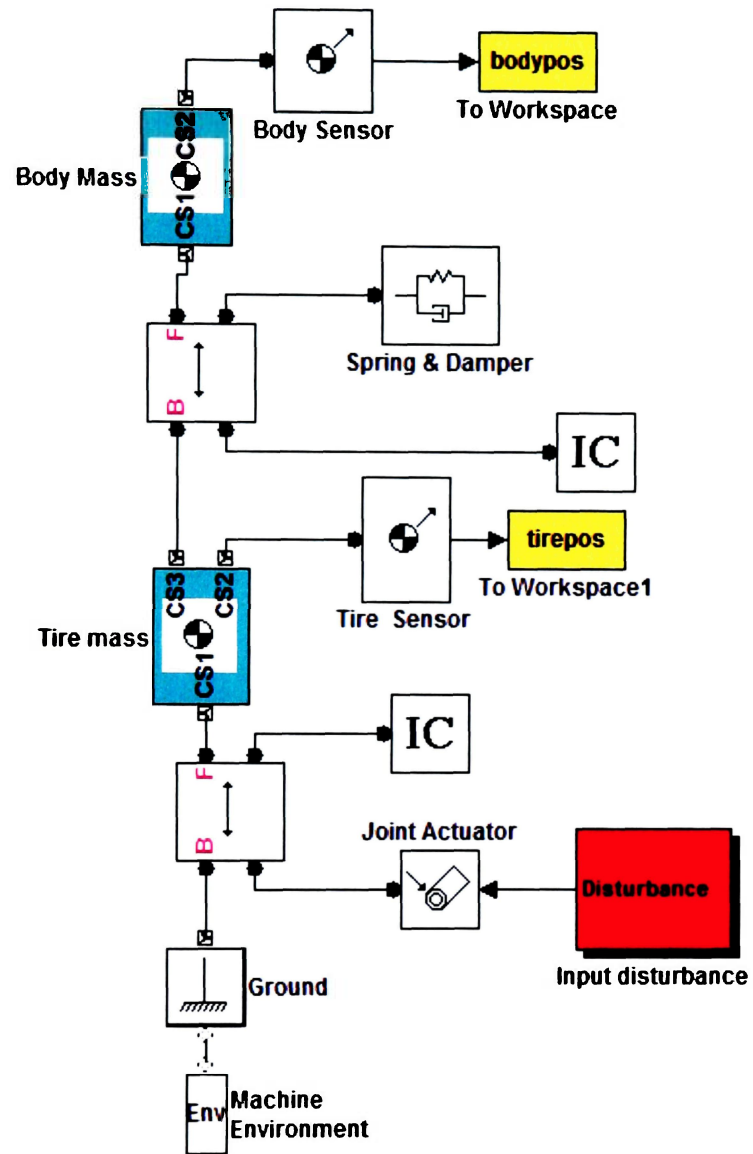
Figure 44. SDOF Base Excitation Model.
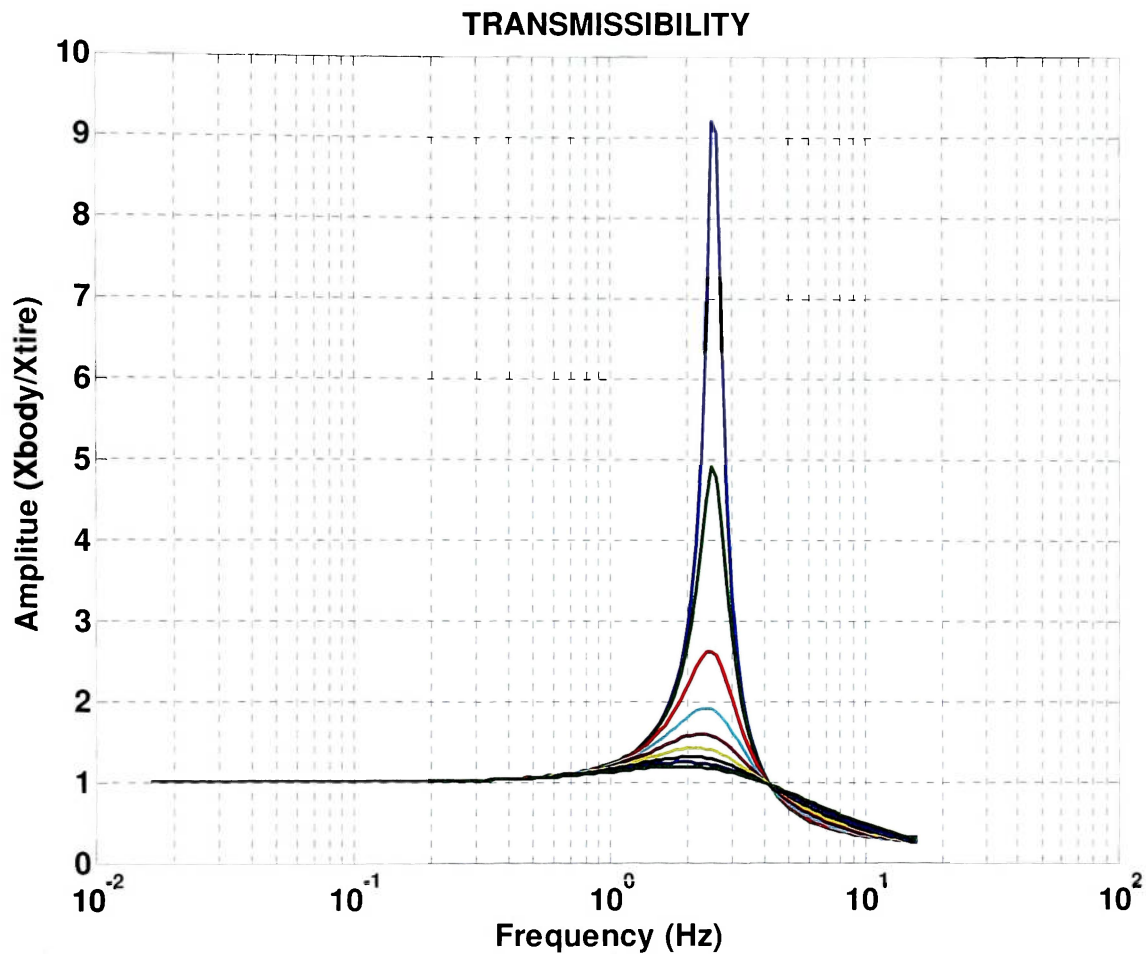
TRANSMISSIBILITY

Figure 45. Amplitude Transmissibility of a SDOF Model.

Figure 45 displays a plot of amplitude vs. frequency known as a transmissibility plot. Transmissibility is defined as "the motion imparted to a mass when the base to which its spring and dashpot supports are attaché is moving"[35]. The transmissibility plot is important tool in analyzing a vibration isolation system. This plot shows that as the damping ratio increases less motion is transmitted from the base to the body. This in turn leads to less motion, force and acceleration transmitted to the body. As shown in the plot there is not a single damping value that works for all conditions. At low frequencies a

high damping value is desirable. As the frequency increases more damping has an undesirable effect on the body mass by transmitting more of the base motion to the body. From the graph the point at which this transition takes place is called the frequency ratio. This specific point is where the acting frequency divided by the natural frequency of the system equals $\sqrt{2}$. This graph shows that there is a need for a damper to have the ability to change its damping ratio in real time. A controllable damper can be used to decrease this effect by changing the damping ratio as dictated by input conditions.
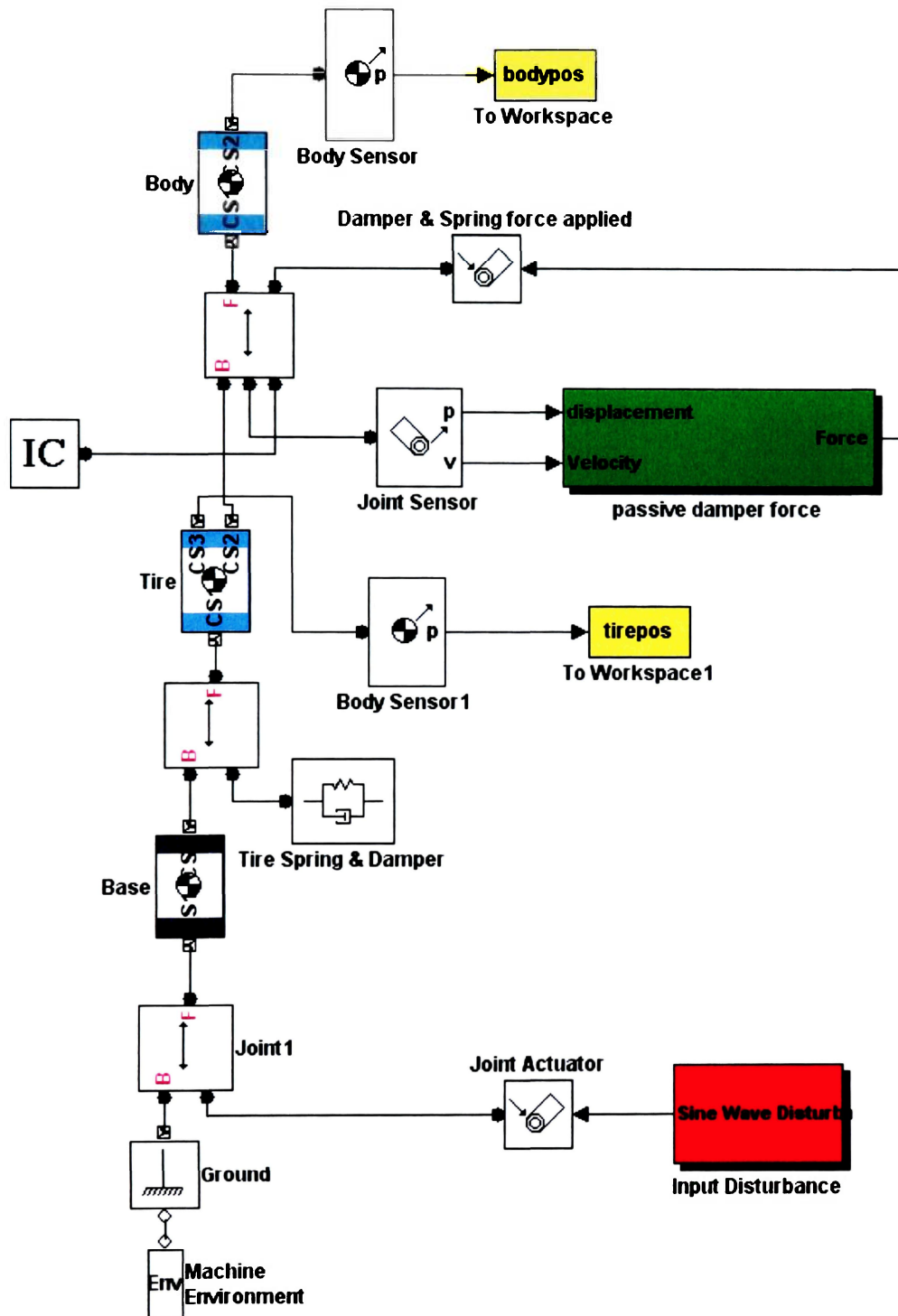
Figure 46. Passive 2DOF Base Excitation Model.

Figure 46 represents the next passive non-linear model test with purchased stock dampers. The purpose of this model was to analyze its transmissibility to that of the linear model and the non linear semi-active model to come. The main difference in this model was the green passive damper force block. This block is a subsystem used to calculate the non linear damper force shown in figure 47.
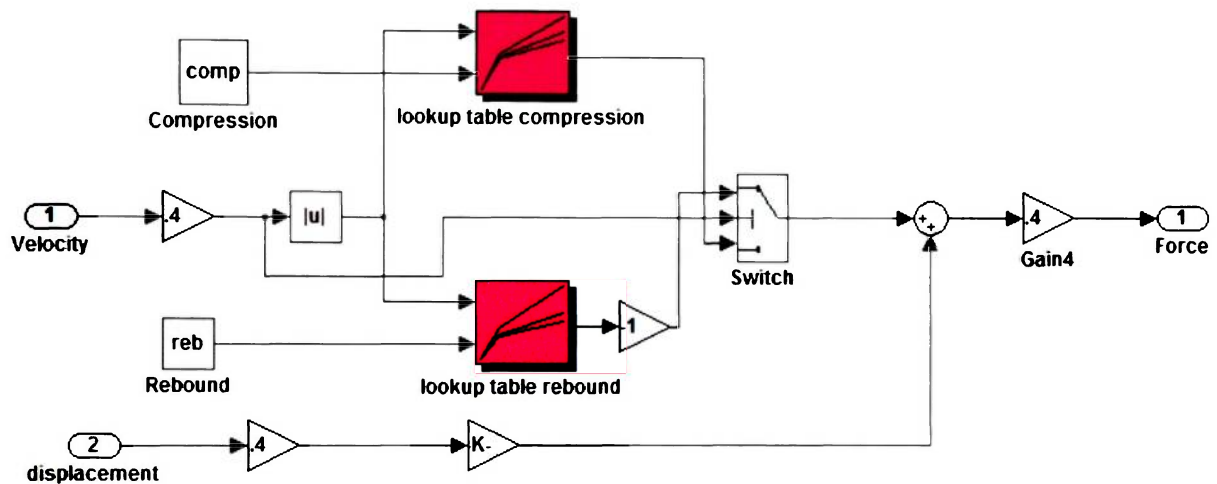
Figure 47. Passive Damper Force Calculation.

For this model the dyno graph for the damper was used as a look up table allowing it to simulate the actual damper. Since the actual damper dyno graph is non linear, the dyno graph was broken into two distinct linear lines to simplify the calculation and processing speed. Velocity and displacement were used to calculate both the damper force and the spring force. A gain of .4 was multiplied to the velocity and displacement and then again to the output force. This was done to account for the motion ratio of the suspension system. The motion ratio is defined by Haney[16] and Milliken[28] as the amount

of spring or damper displacement for a given wheel displacement. For the SAE Baja vehicle the wheel traveled a total of 10 inches to the dampers 4 inches giving it a motion ration of 4/10 or .4. Rebound and spring force calculation was multiplied by a gain of -1 to show that it was negative force acting against the input force of the wheel. Also for this block, compression and rebound settings were left as variables to allow for program manipulation. Since the damper is statically adjustable, min, max and intermediate settings were tested. This equated to 9 different combinations of compression and rebound. Figure 48 depicts the suspensions damped natural frequency at around 1 Hz. This corresponded to the calculated value of the undamped natural frequency of 1.03 Hz. Note that there is not direct determination for the damped natural frequency of a non linear system. They should however be close to one another with the damped natural frequency ω_d always less than the undamped natural frequency ω_n[9]

TRANSMISSILITY STOCK DAMPER
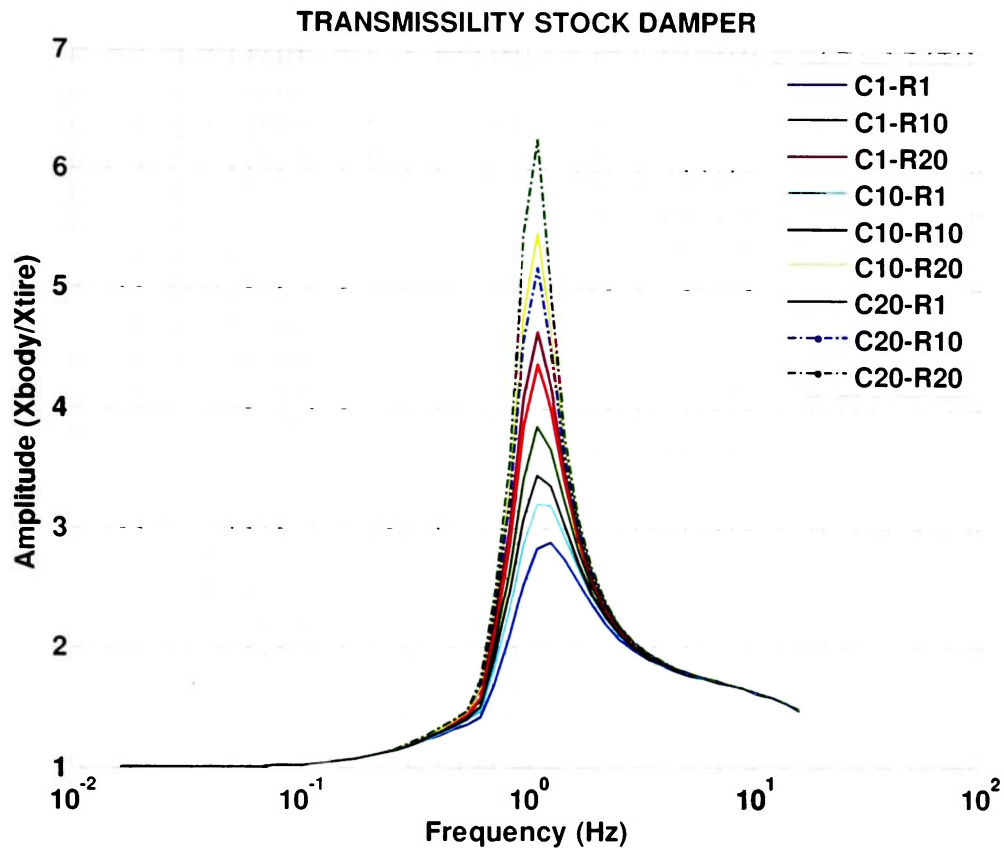
Figure 48. Passive 2DOF Transmissibility.

CONTROL POLICY

The skyhook policy developed by Karnoop[10] was used to control the MR damper. In previous studies the skyhook policy was one of the simplest and most efficient at reducing the transmissibility of the suspension. Two different methods of portraying skyhook exist. One is velocity based and the other is displacement based. For the purposes of this study, the velocity based model was used. In addition there are two different skyhook calculation methods. One is known as ON/OFF or max/min, while the other varies the damping force in a range from max to min.

Velocity Skyhook Control Policy

The velocity skyhook configuration is shown in figure 49. The principle of this system is that instead of being connected between the mass and the ground, the damper is connected to the sky. This allows the damper to function in a linear fashion depending on the mass velocity. This configuration is not achievable in real mechanical systems however; with the advent of MR fluid technology and sophisticated micro controllers a semi-active system can be designed.
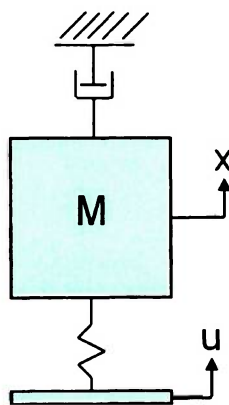
Figure 49. Skyhook Configuration.
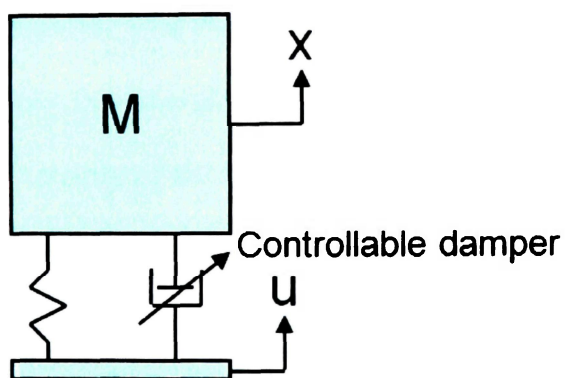
Figure 50. Actual Skyhook Model.

With an MR damper this system can be adapted into any typical suspension system by controlling the damper as if it were connected to the sky as shown in figure 50. There is one limitation that must be taken into account. That is the control policy of on/off calls for a maximum force and zero force. In a real damper this is not possible due to simple mechanical limitations. It is impossible to get zero force due to internal friction of the fluid; likewise the maximum force has a limit also due to pressure capabilities of individual dampers. For the MR damper to function properly there should be a significant difference between its minimum and maximum settings to take full advantage of this control policy.
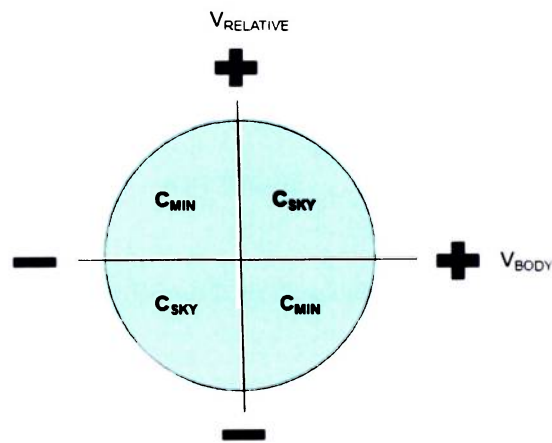
Figure 51. MR Damper Operating States.

This control policy has four operational states see figure 51. Based upon the relative velocity and the absolute velocity of the body, a damping coefficient can be determined. When both the relative and absolute velocities are the same sign the skyhook damping constant is applied. However when there are not the same sign the damper is set to a minimum damping constant. This control scheme was designed to dissipate energy without adding to the system. Figures 52 and 53 represent the dyno results of the stock

damper. These are simplified damper curves for input into the model. You will notice

two different slopes for each curve. The first slope with what is called low speed blow

by. This means at low shaft velocities the oil passes through the piston without activating

the shim stacks. Once a certain velocity is reached this blow by hole is choked off and

then the shim stacks are activated. For this reason the damping coefficient of a damper is

not linear.
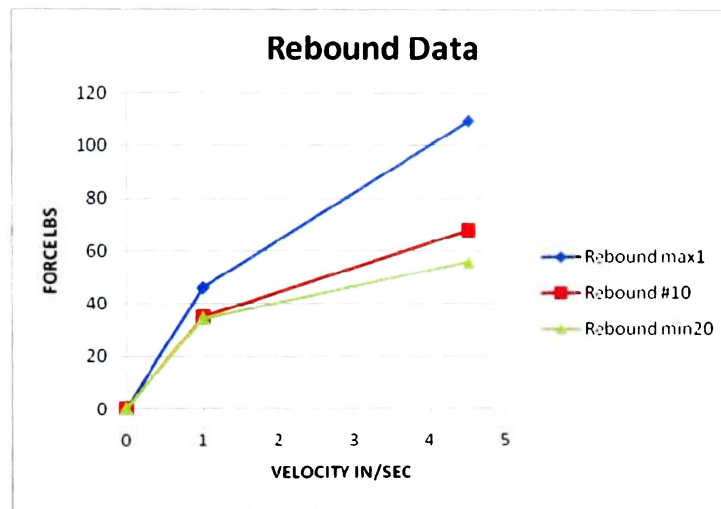
Figure 52. Simplified Rebound Data Used in Model.
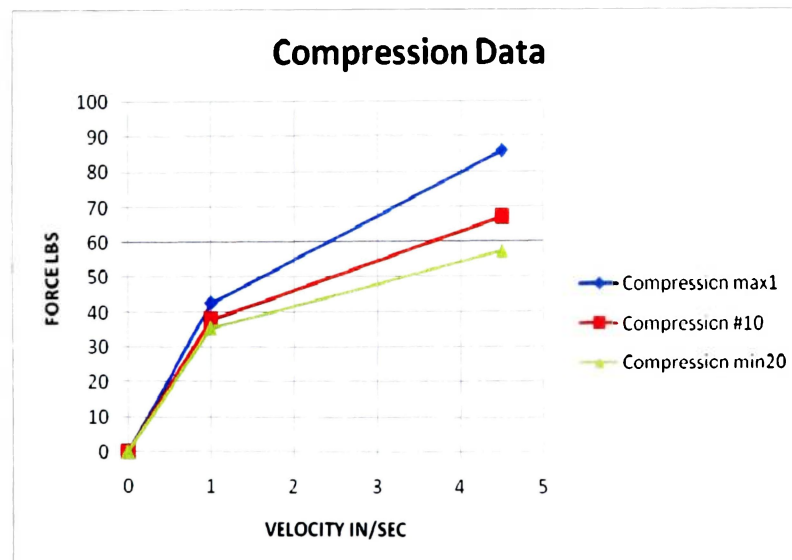
Figure 53. Simplified Compression Data in Model.

Semi-Active SimMechanics Model

The semi-active model is similar to the previous model with the addition of a

different control block diagram. This block diagram is the orange semi-active damper

force seen in figure 54.
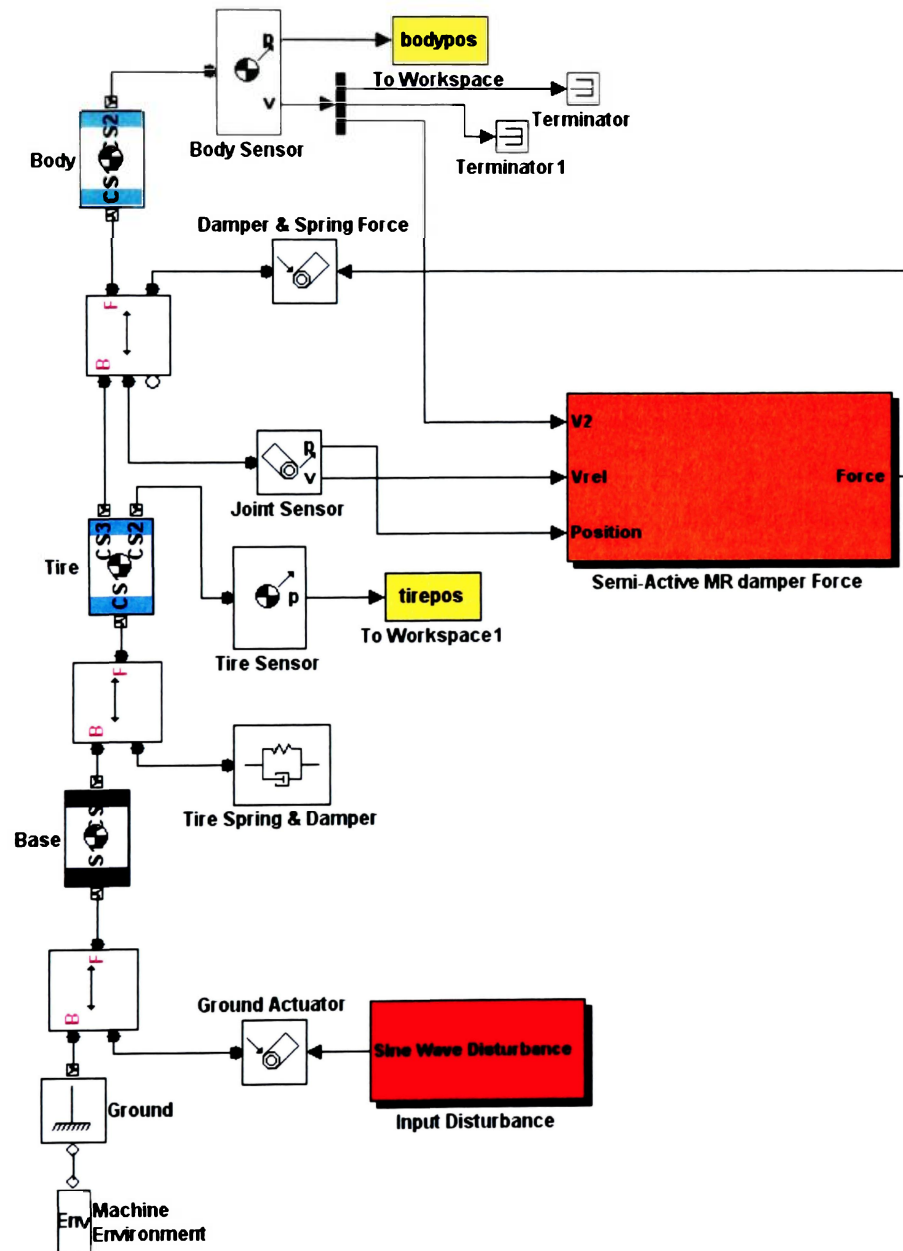
Figure 54. 2DOF Semi Active MR Damper Model.

Inside the semi-active MR damper force block is where the relative velocity, spring force and compression or rebound are calculated. See figure 55. Again the .4 here is due to the motion ratio previously stated. Two more subsystems were needed to implement the skyhook policy. These blocks were the skyhook force in green and the final check in grey. The skyhook force block contained two lookup tables, one for F_{min} and one for F_{max}. F_{sky} was calculated with a linear gain.
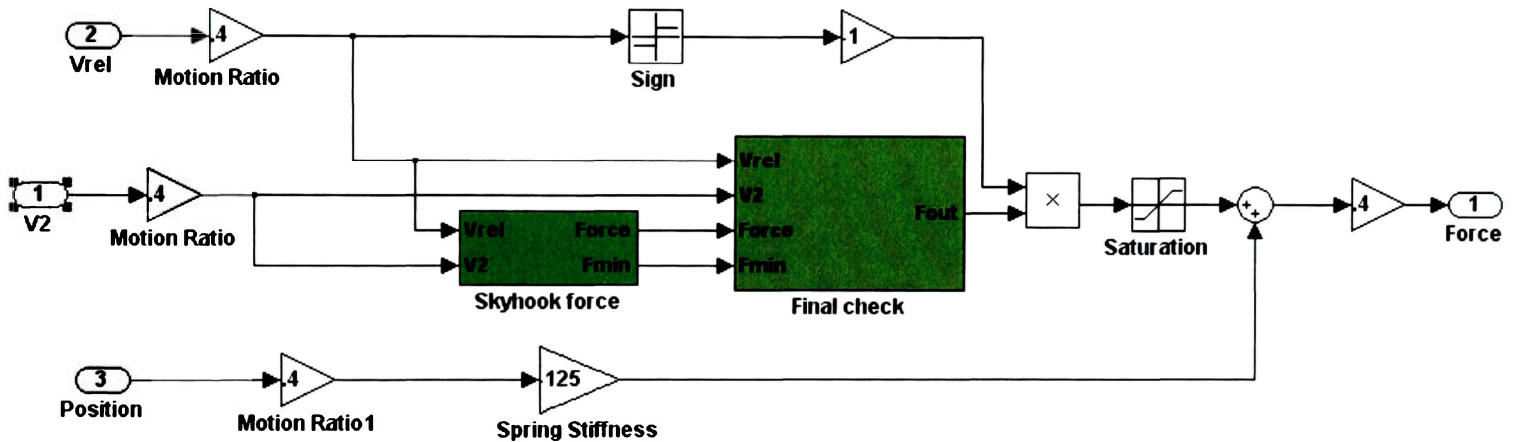
Figure 55. MR Damper Force Block.

All three values were simultaneously calculated and then compared to the desired F_{sky} term as seen in figure 56. This block diagram checked to ensure that F_{sky} was within the upper and lower limits of the damper, i.e. F_{min} and F_{max}. This force was then sent out to the next block for a final check based on the control policy discussed in figure 51.
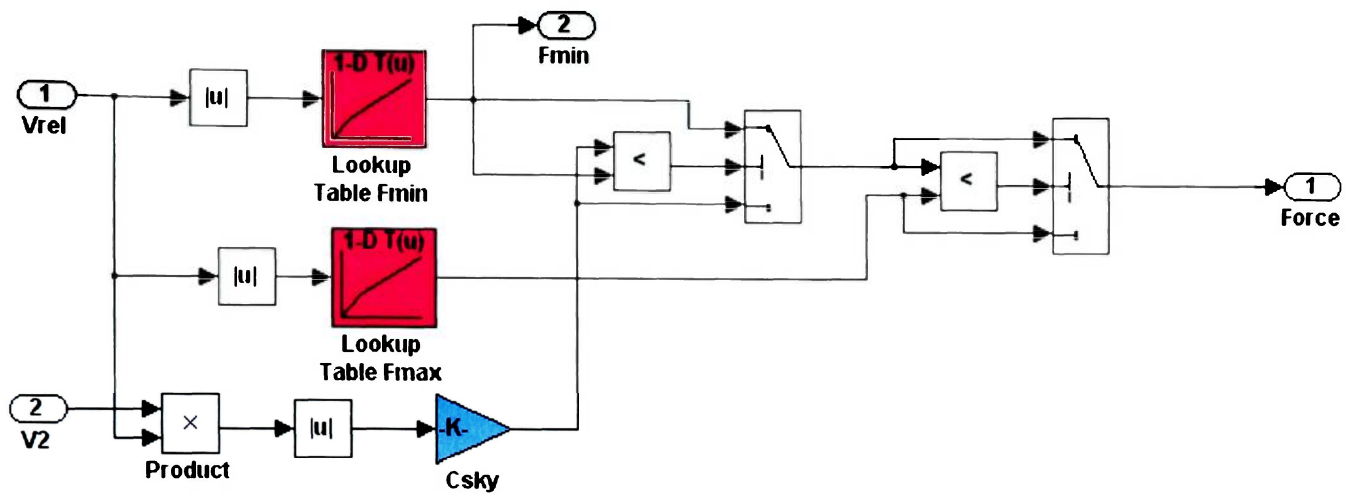
Figure 56. Skyhook Force Calculation.

This last block calculated the product of the relative velocity and absolute velocity. A same sign or positive sign passed the F_{sky} force. Otherwise the minimum damping constant was passed.
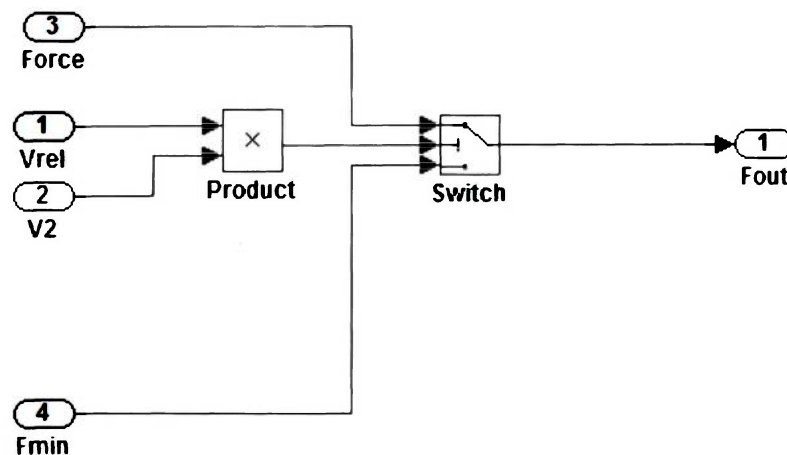
Figure 57. Check of Relative Velocity Time Absolute Velocity.

C_{sky} was chosen to be a range of values from 1 to 20. The transmissibility is shown in figure 58. From the plot you can see a dramatic difference in the amplitude near the natural frequency. The largest amplitude seen in the stock damper was 6.259 and the smallest was 2.88. The ideal MR setups largest value was 3.633.
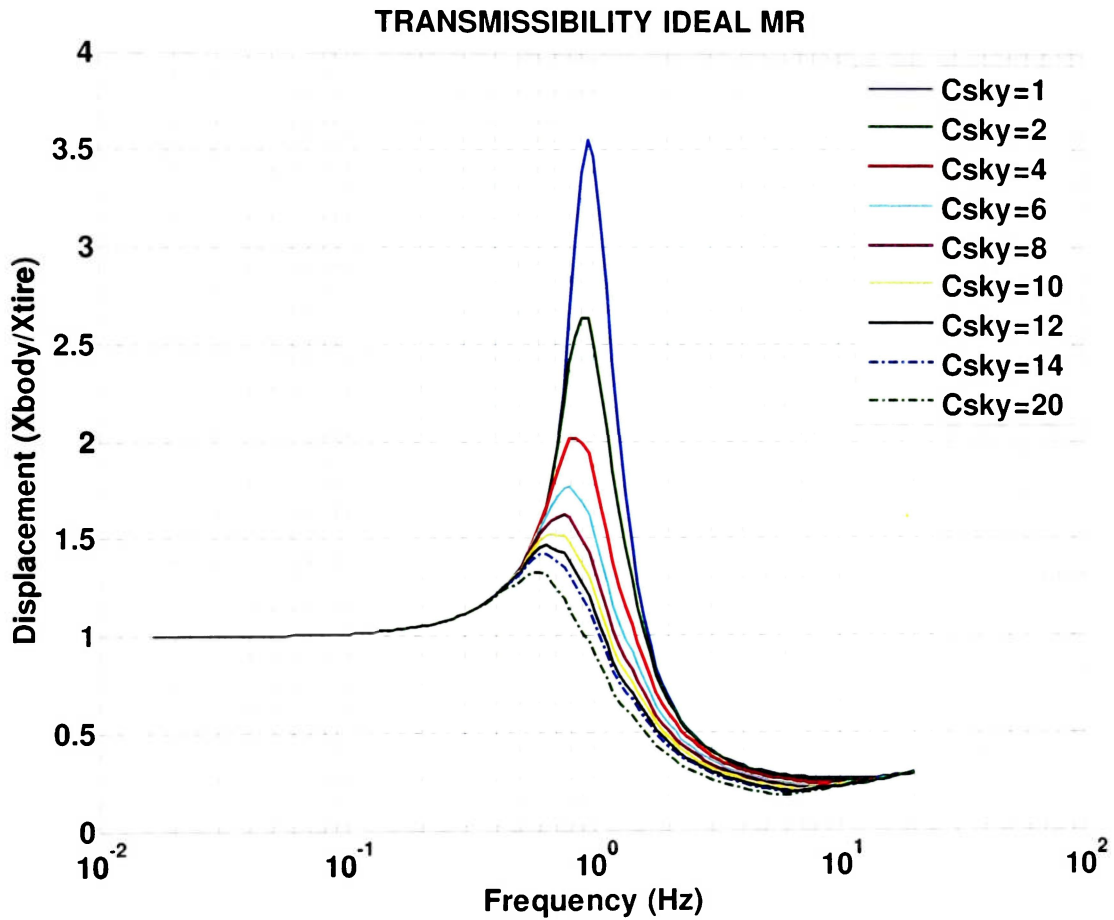
Figure 58: Plot of Ideal MR Transmissibility

This equated to a 58.0 % decrease over the largest amplitude of the stock damper and a slight increase, 20%, over the stock dampers smallest amplitude. However a big difference in the higher frequency range was recorded as well. With an ideal MR damper there is a significant decrease in high frequency isolation. This means that high frequency inputs have little effect on the displacement of the mass. This arrangement is the ideal case with the plot of F_{min} very small and F_{max} very large The actual MR damper designed for this experiment does not have a large range between its soft (F_{min}) and hard (F_{max}). This can be seen in figure [X] of the actual force vs. velocity curves. At first glance with the controllability of the MR damper being very small, results similar to the ideal case were not expected. After running the model, it was surprising to see that the controability of the damper did not have as much as an effect on the transmissibility plots as expected. They were actually very similar concluding that even with a smaller range of controability the MR damper could function almost as well as the ideal case and significantly better than a passive damper.
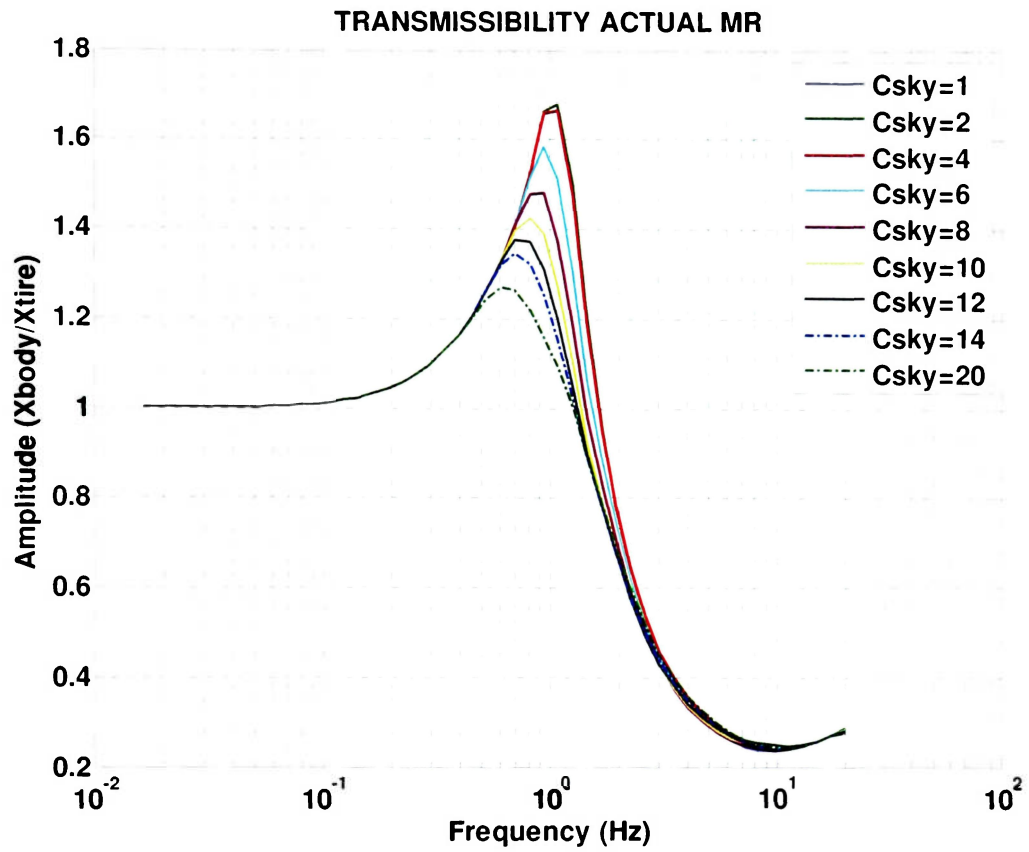
Figure 59. Plot of Actual MR Damper Transmissibility.

Figure 60 compares the best transmissibility plot for each case, which depicts that the MR dampers, both actual and ideal are significantly better at isolating the body at all frequencies.
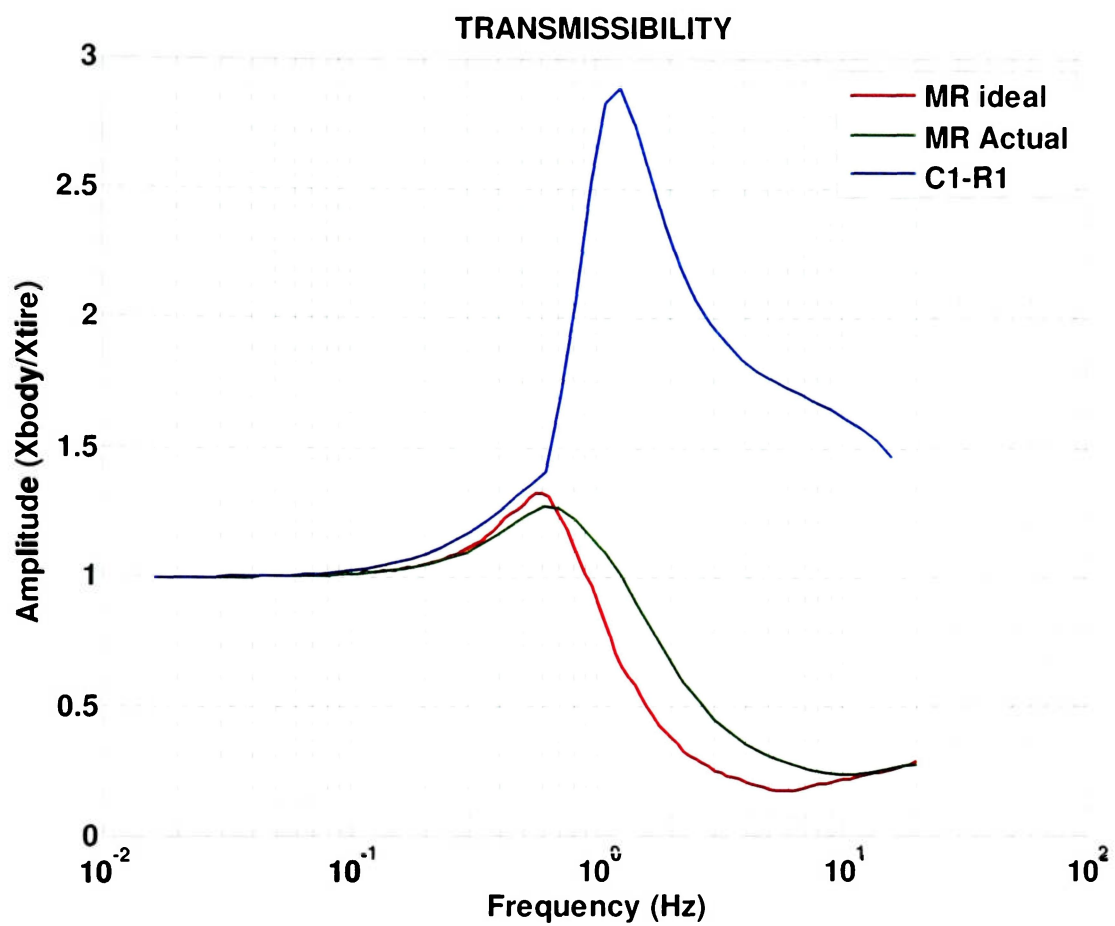
Figure 60. All Three Models Transmissibility Plots.

CHAPTER 4

Chapter 4 deals with the experimental testing of both passive dampers and semi-active dampers on the Baja SAE vehicle. Modifications to the dampers and vehicle are discussed at length along with test set-up and testing equipment required to collect data from the vehicle. Damper dyno results are presented for both passive and semi-active dampers.

VEHICLE / DAMPER HARDWARE

Vehicle testing will be conducted behind the SAE shop on campus. The purpose of testing is to verify results obtained from a SimMechanics model. A basic test including both large and small displacements will be conducted. The experimental data will also be used to validate the SimMechanics model. All data will be recorded in real time with the use of National Instruments hardware and software.

Vehicle set-up and Equipment

Vehicle test were conducted with 4 accelerometers, two on each damper. The accelerometers will measure both the acceleration of the body or sprung mass and the unsprung mass or tire and suspension system components. For this test rugged waterproof accelerometers will be used. Waterproof accelerometers are needed because the university's Baja SAE team will use the dampers at a competition involving water events. Looking at numerous accelerometers; Honeywell's Company Sensotec had the only accelerometer that would meet these requirements. Sensotec recommend their bolt

mounted BG-914 JTFS accelerometer. This accelerometer is a current producing model with an internal amplifier that can be seen in figure 63. Appendix C lists all the specifications on this particular accelerometer. The accelerometers were mounted so they would monitor the acceleration of the body mass, and the unsprung mass of the vehicle. The accelerometers needed to be mounted so that they were parallel to each other. This insured that the measurements taken were of similar type and direction. A mount was designed utilizing the spring mounts on the damper. These two mounts connect the spring to the unsprung mass and the body of the vehicle. The mounts were modeled after the spring retainer perch, with an addition of a platform to house the accelerometer. There design can be seen in figure 61.
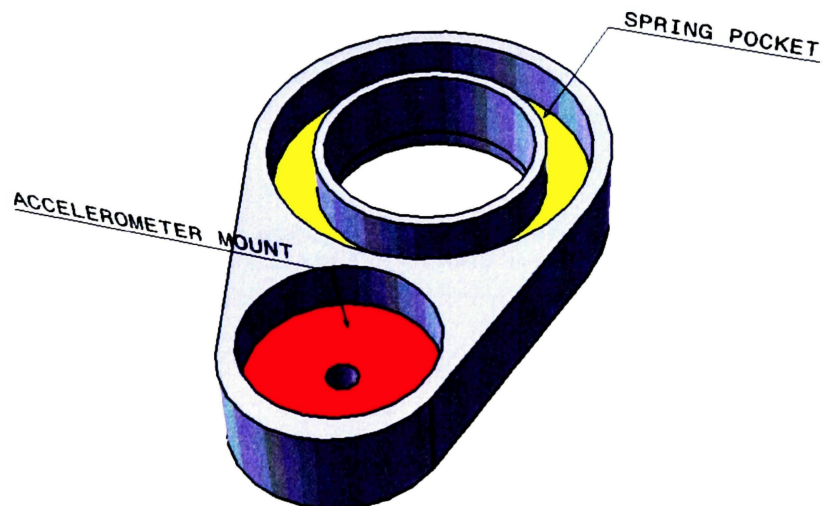
Figure 61. CAD Drawing of Accelerometer Mount.
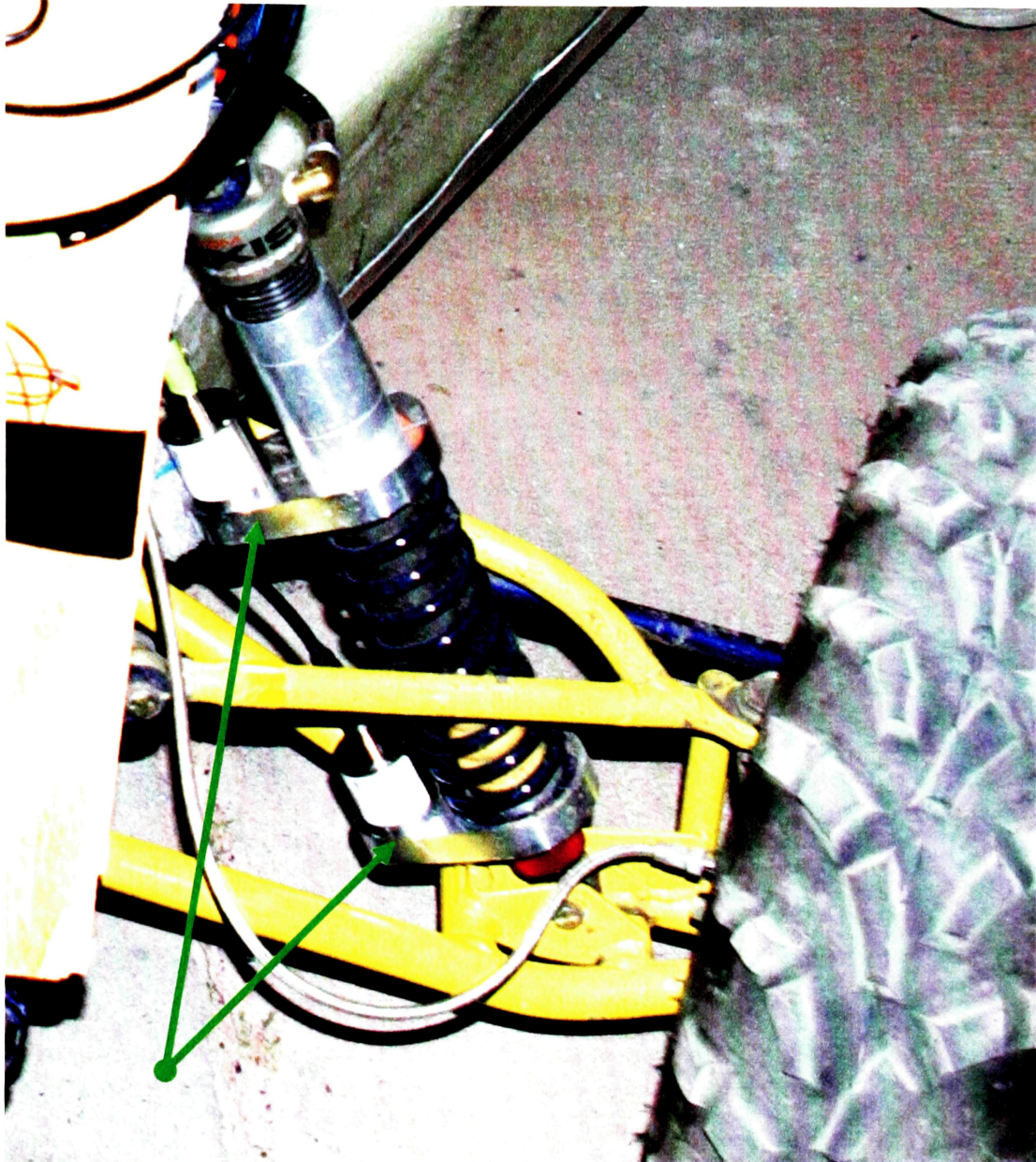
Figure 62. Damper with Accelerometer Mount on Vehicle.

Figure 62 shows the accelerometer mounts on the damper. The top of the damper

is bolted to the frame making the body of the shock move uniformly with the body. The

piston shaft assembly is attached to the lower suspension arm and moves in unity with the

unsprung mass. Since the accelerometer mount is cantilevered from the body of the damper it was robustly designed to prevent flexing of the mount giving false readings. Data acquisition equipment was purchased from National Instruments. Their USB 6210 DAQ model was chosen due to its compact size and simple set-up procedures. The DAQ was set up to measure the voltage change from the accelerometer. Since the accelerometer outputs a varying current with acceleration, resistors were put in-between the accelerometers and the DAQ to convert it to a voltage measurement. The maximum voltage range on the DAQ was -10 volts to +10 volts. The accelerometer puts out a current of -4 mA at -10 g's and 20 mA at +10g's, this required a resistance of 500 ohms to make sure the DAQ was within its specified range of -10 to +10 volts. Since the DAQ is not a standalone system, it required USB power and software to collect data. LabView 8.5 software was used to build a VI used to collect the data. VI stands for Virtual Instrument according to Bishop[5]. The VI can be seen in figure 63.
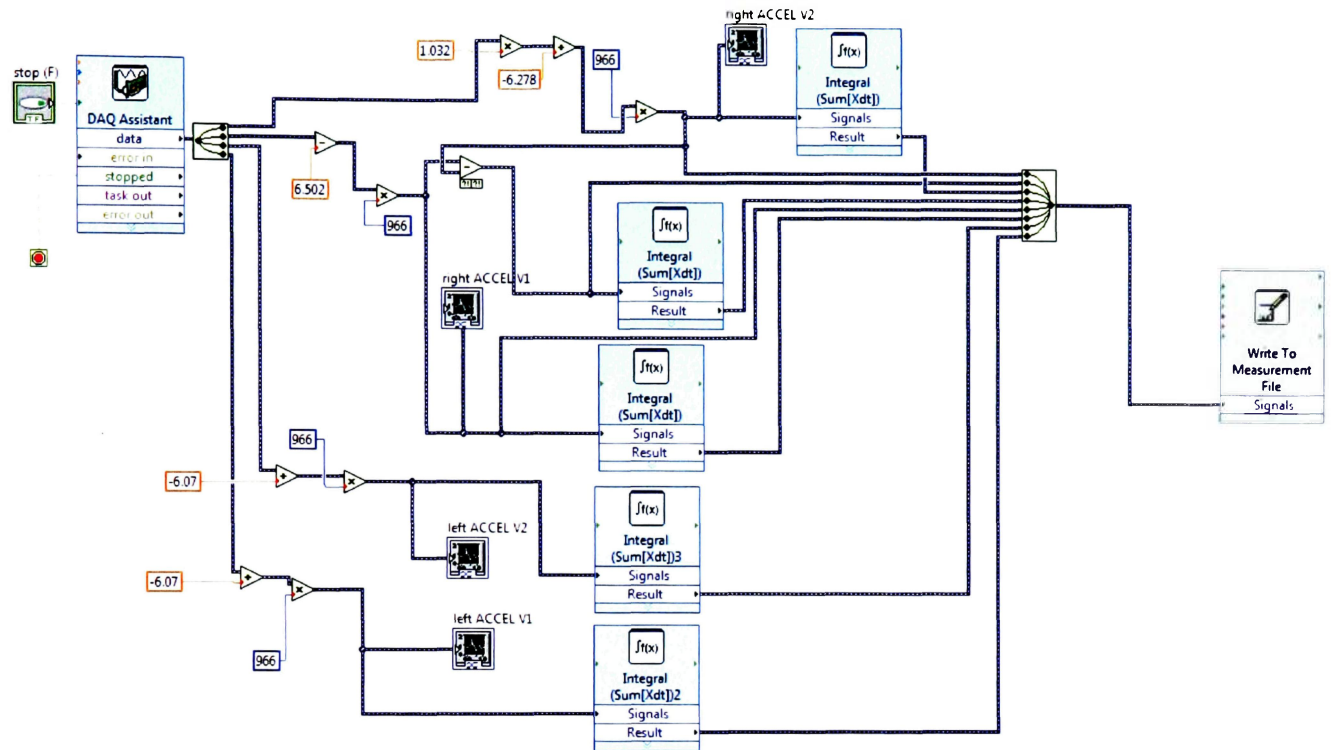
Figure 63. DAQ Model for Collecting Data.

A laptop was used to run this program requiring it to be mounted on the vehicle during testing. The initial laptop mount on the roof of the vehicle encountered many problems. The laptop could not withstand the jolts of the bumps and jump without turning off to protect the hard drive. The addition of polyethylene foam did not help. An alternative box of memory foam was design to mount on the front of the vehicle helping minimize the impacts. This design proved to be effective. Figure 64 shows the box mounted on the vehicle along with all DAQ equipment.

Figure 64. Special Foam Box to Protect Laptop.

Test Set-Up

Outside the SAE shop a small course of two standard parking curbs and a 1 foot ramped jumped were set up. The parking curbs were set-up 14.4 feet apart and the ramp 24 feet from the last parking curb. The test was conducted 9 times changing the rebound and compression rates in a logical pattern. Three different setting were tested for both compression and rebound. Their respective maximum, minimum and intermediate settings were tried.

Passive Test Results

The first test was to determine if the sampling frequency was sufficient to collect all the data. According to efunda[41] in order to sample fast enough to accurately reproduce the signal the sampling frequency f_S must be at least two times greater than the maximum frequency expected. A graphical example in figure 65 shows what would happen if the sampling frequency is slower than the original signal's frequency. As you can see the original signal is not accurately represented leaving out data. This would result in a failed experiment. The Nyquist frequency is defined as half the sampling frequency[4], which is important because this will help avoid aliasing. Aliasing is where based on a sampling rate two different frequency wave forms could fit the data. If this occurs there is no way to distinguish between the two different signals.
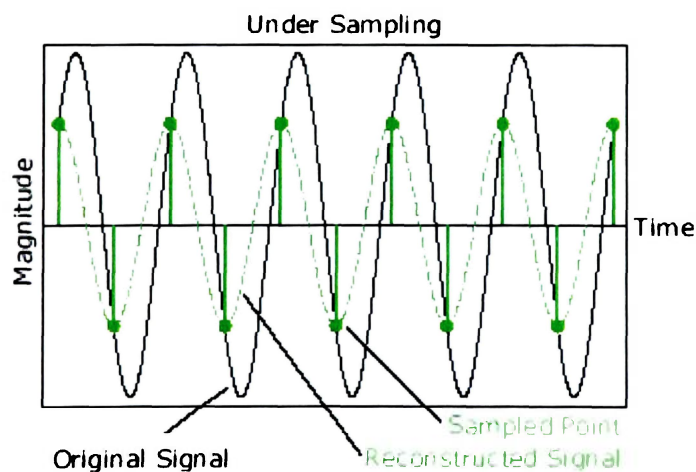
Figure 65. Under Sampling Visual[3].
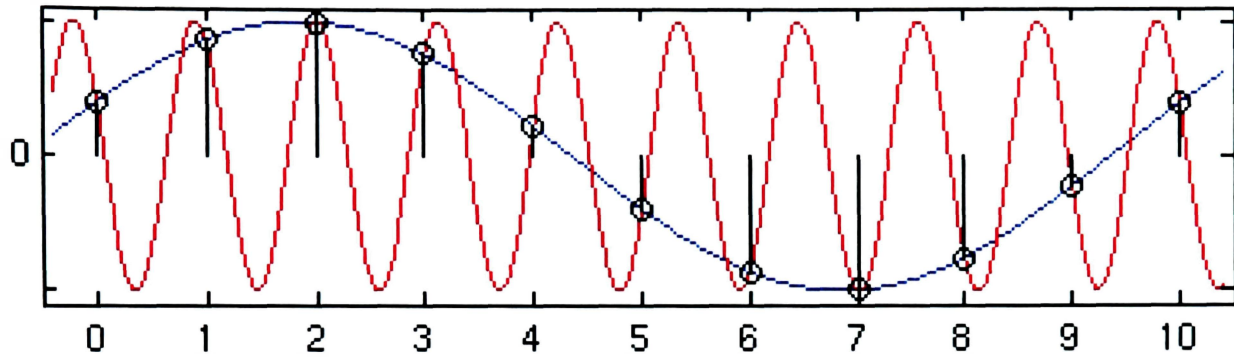
Figure 66. Aliasing Example.

A test using the two different sampling frequencies of 500 and 1000 Hz was conducted. Each set of data was imported into Matlab and power spectral density test was conducted. Figure 67 and 68 show the raw data taken from the two frequency runs.
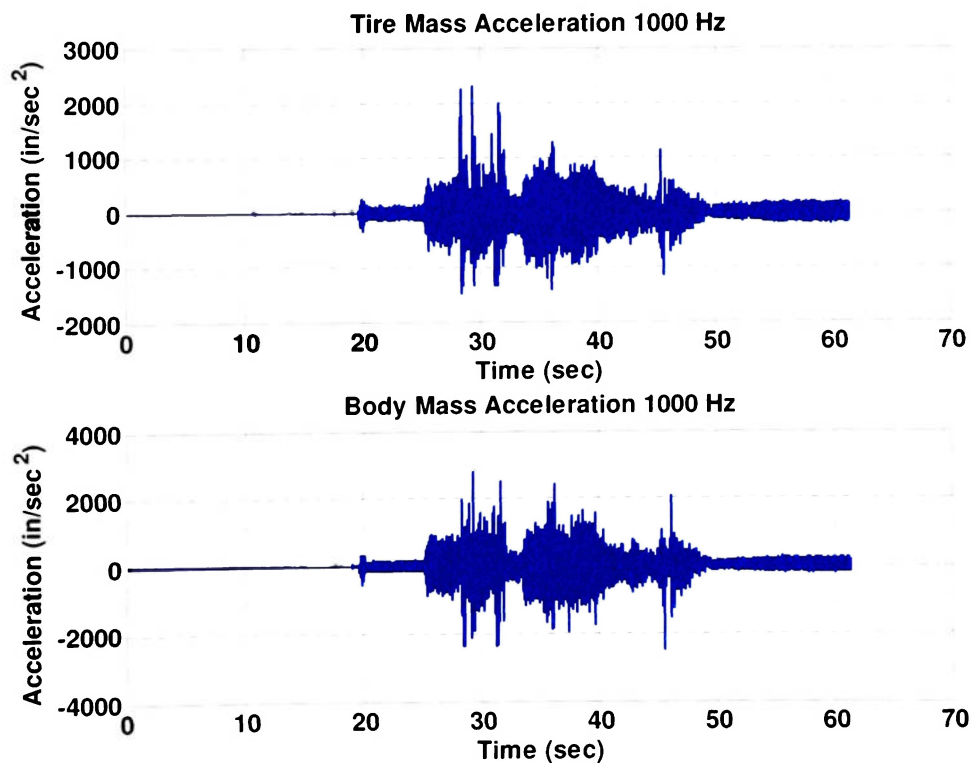
Figure 67. Raw Acceleration Wave Forms Sampled at 1000 Hz.
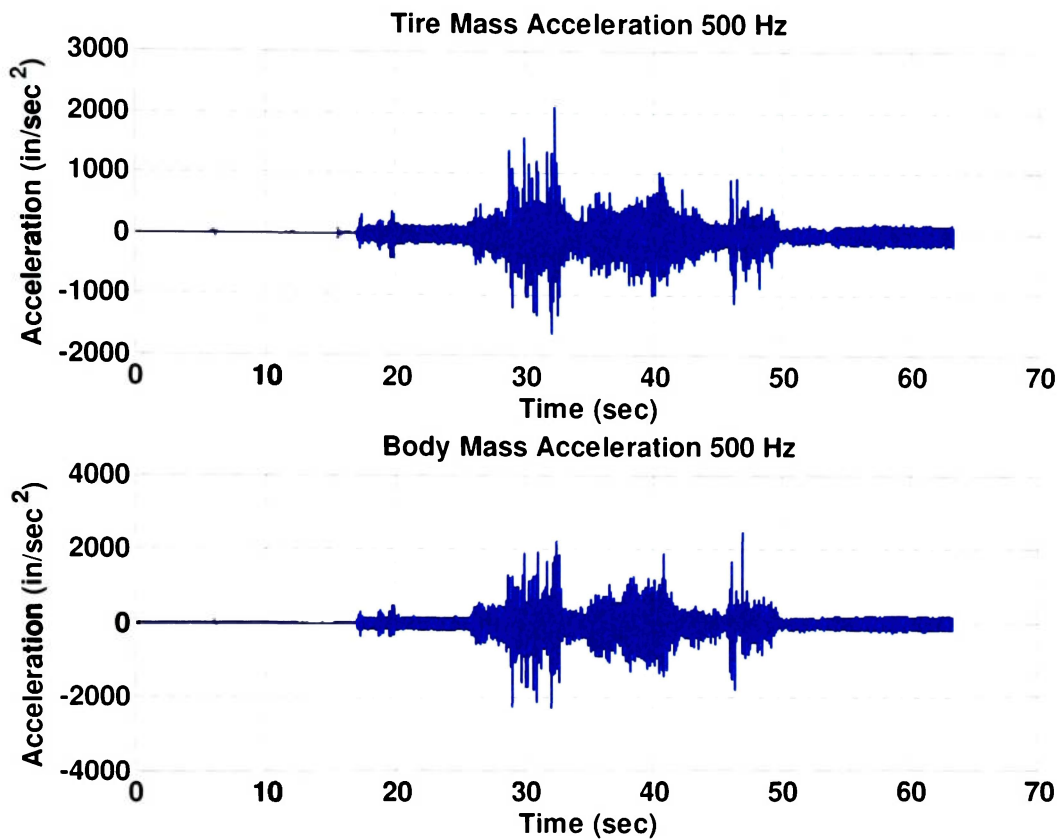
Figure 68. Raw Acceleration Wave forms sampled at 500 Hz.

In these plots you notice three distinct areas of increased acceleration. These areas coincide with the three obstacles on the track.   Figures 69 and 70 are plots of the power spectral density or PSD. PSD is a plot of power in decibels vs. frequency in Hz. This shows the power or occurrence of each type of frequency found in the data. The PSD plot was performed to verify that the sampling rate of 500 times a second was sufficient. From the plots, both body and unsprung mass show similar spikes for different sampling rates at the same frequencies. This verifies that a sampling rate of 500 times a sec is more than adequate to collect all the waveforms from testing and accurately reconstruct them. Having a smaller sampling rate is very helpful when it comes to data

storage. For example; collecting 10 seconds of data at 500 times a sec yields 5000 data points and collecting at 1000 times a sec yields 10,000 data points. This cuts the amount of data storage in half. For much larger systems that collect data for hours makes selecting a sampling rate extremely important.
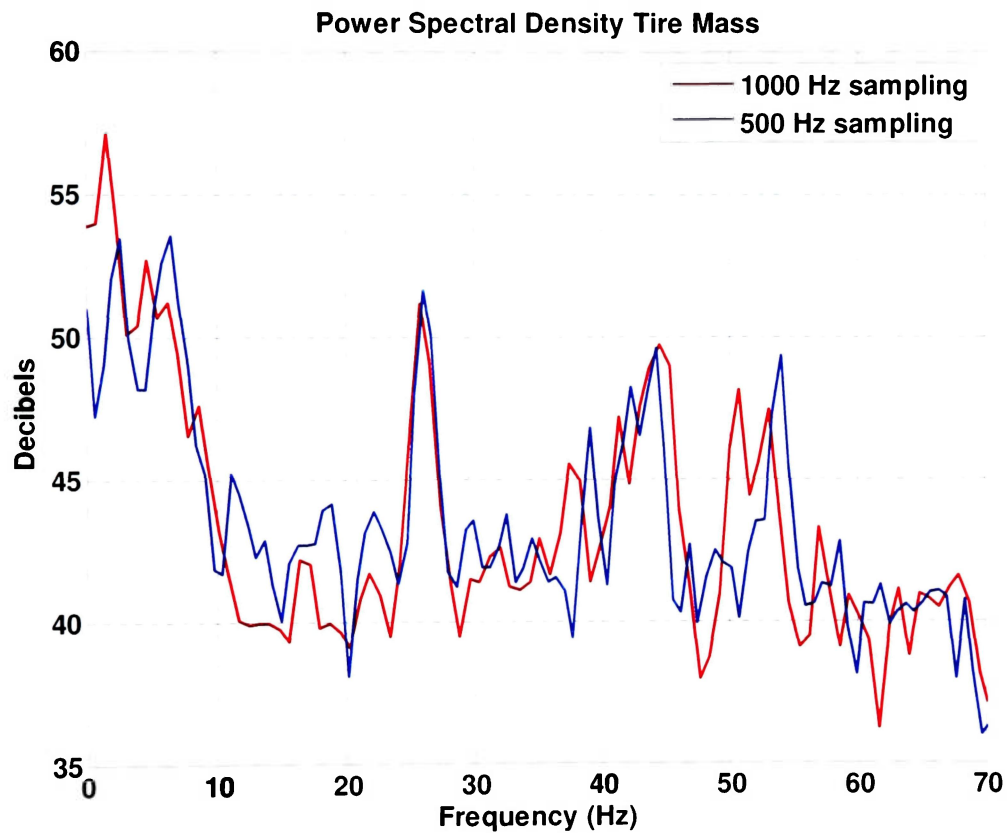
Figure 69. PSD Plot of Tire Mass Sampling Rates.
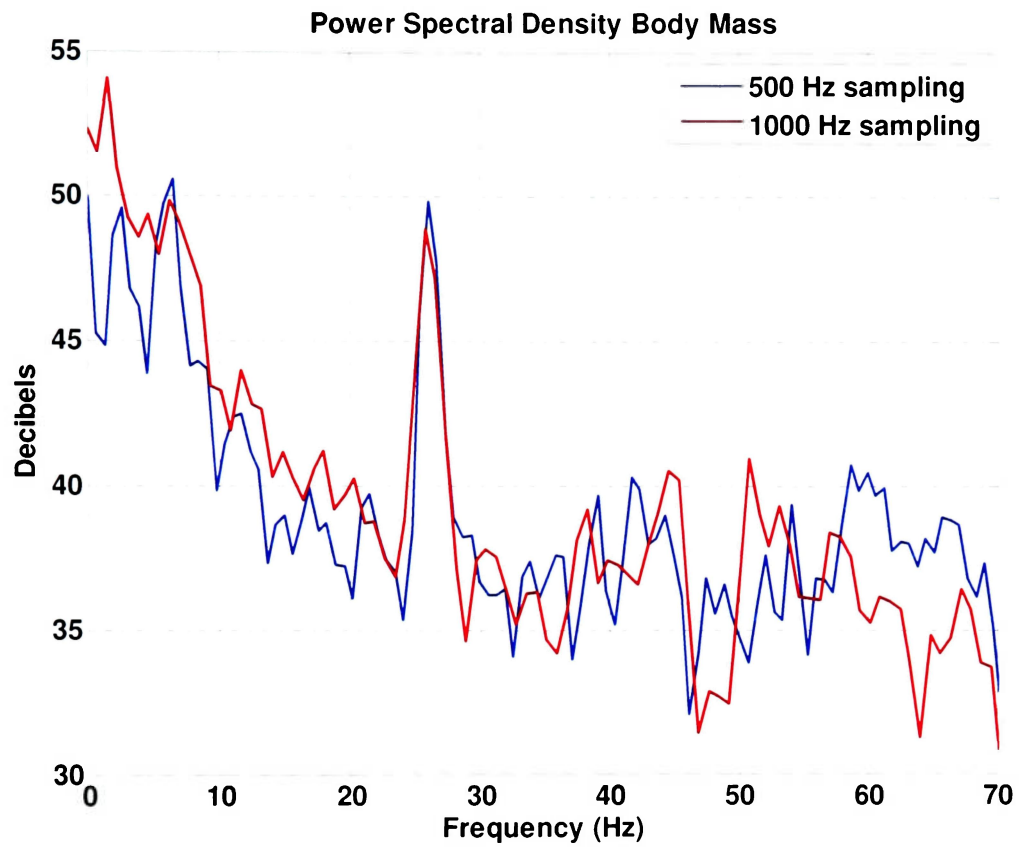
Figure 70. PSD Plot of Body Mass Sampling Rate.

Passive Damper Dyno Results

Passive Damper dyno testing was conducted off site at a local chassis set-up shop. A 2VS Roehrig damper dyno was used to generate all the force vs. velocity plots for each damper. For the passive test the damper has 19 different settings for compression damping and 30 for rebound damping. The dyno has an IR temperature sensor that monitors damper temperature. Before each test the damper was cycled until it reached a temperature of 100 degrees Fahrenheit. The testing procedure started with max compression and was adjusted by two increments for each test until minimum compression damping was reached. Next the rebound damping was set to the maximum and then adjusted 3 clicks each time until minimum rebound damping was reached. During this test the damper fluid remained at the same temperature of 100 degrees plus or minus 3 degrees.
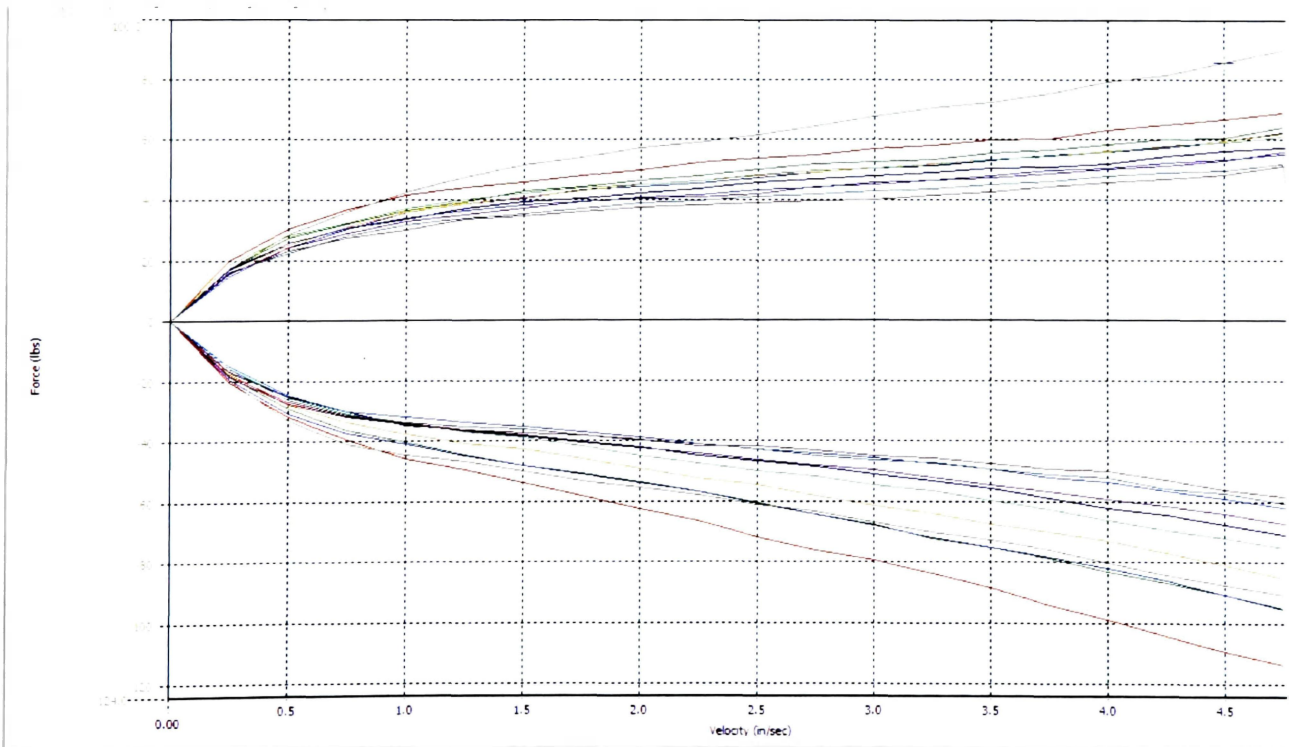
Figure 71. Stock Damper Dyno Resutls.

This is important because temperature can have a dramatic effect on the viscosity of the oil changing its performance characteristics. Figure 71 is a force vs. velocity plot of the compression and rebound characteristics of the damper. Compression curves are the positive force values and rebound force values are negative.

Semi-Active MR Dyno Results

The MR damper was tested on the same dyno as the stock oil filled damper. Figure 72 shows the results of this test. From the graph it is obvious that the controllability of the shock is very limited. The range for compression varies only 10 lbs @ 4.5 in/sec and the rebound varies 12 lbs @ 4.5 in/sec, from an off current setting to max current setting.
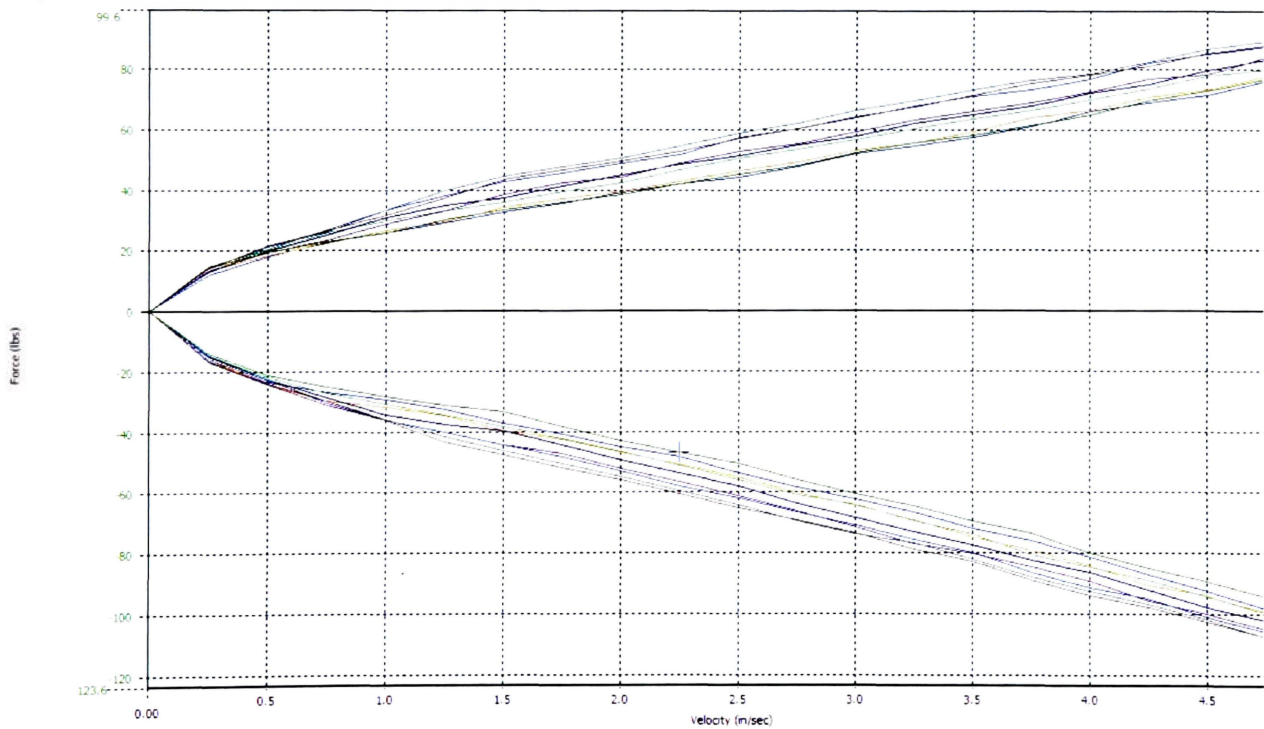
Figure 72. MR Damper Dyno Results.
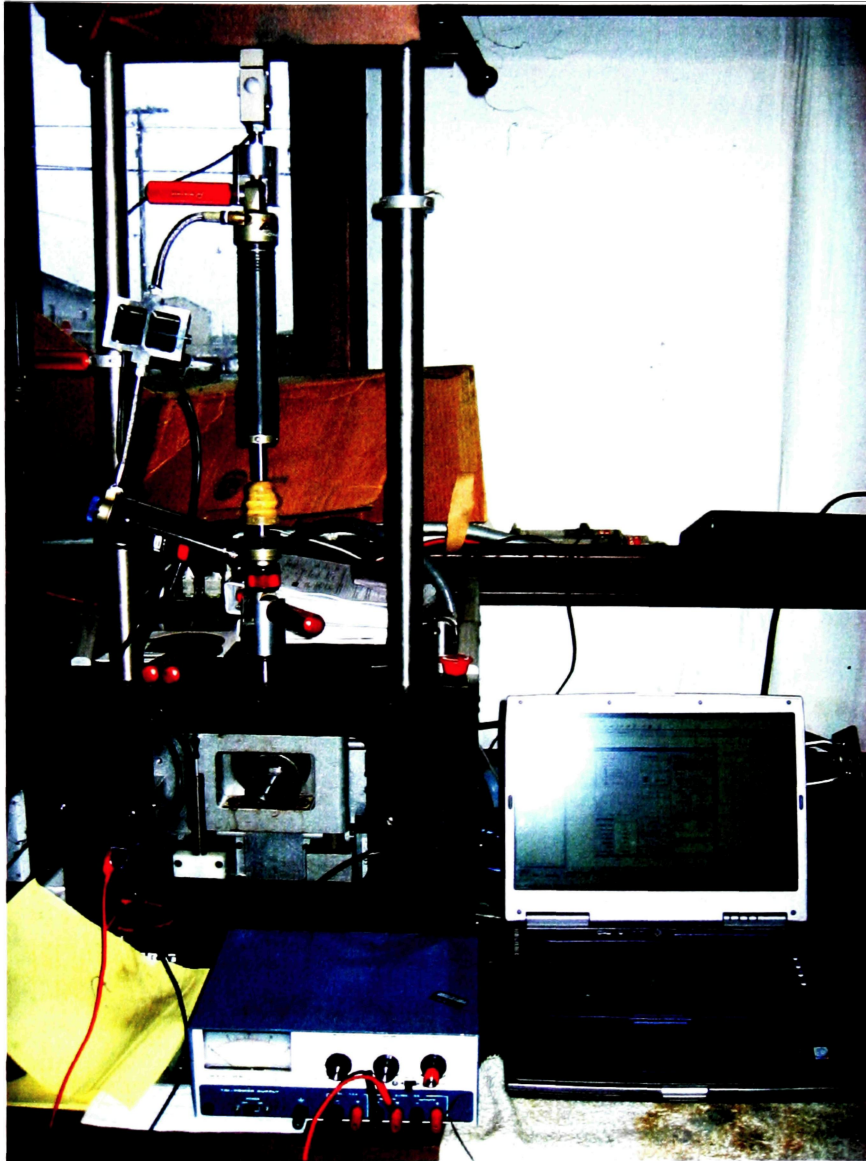
Figure 73. Dyno Set-up.

Figure 73 depicts the test set-up apparatus of the Roehrig damper dyno. The dyno itself is a machine that oscillates the base of the shock back and forth to simulate force acting on the damper. The machine records this force and velocity with the help of Roehrig software and a laptop. Data is stored as graphs shown above. To test the MR

damper a power source, shown in figure 75, capable of supplying current the coils was

used and tested at a range of currents dictated by the specifications of the electromagnets.

Figure 74. Power Source.

CHAPTER 5

EXPERIMENTAL DATA / MODEL VALIDATION

The SimMechanics model was compared the vehicle experimental test data. This comparison was used to verify that the models are accurate and can be used to simulate aircraft landings for future studies. For this comparison PSD plots of the passive experimental data will be plotted on top of a PSD analysis of the simulation. The experimental test setup was modeled as a displacement input disturbance over time. The vehicles speed was averaged from the experimental data, to model the input disturbance accurately.

Passive Results

The average velocity of the SAE Baja car running the course was estimated at 36 in/sec. This was used along with measurements and spacing of the parking curbs and ramp. Assuming the vehicle was at a constant speed throughout the test an input of displacement vs. time was modeled as seen in figure 75. The wave form was calculated using cams equations from mechanisms and dynamics of machinery[26]. This new disturbance replaced the sine wave input seen in previous SimMechanics model figures. Figure 76 depicts the acceleration response of the body mass to this input. Figure 77 depicts the acceleration response of the body mass during the experimental test.
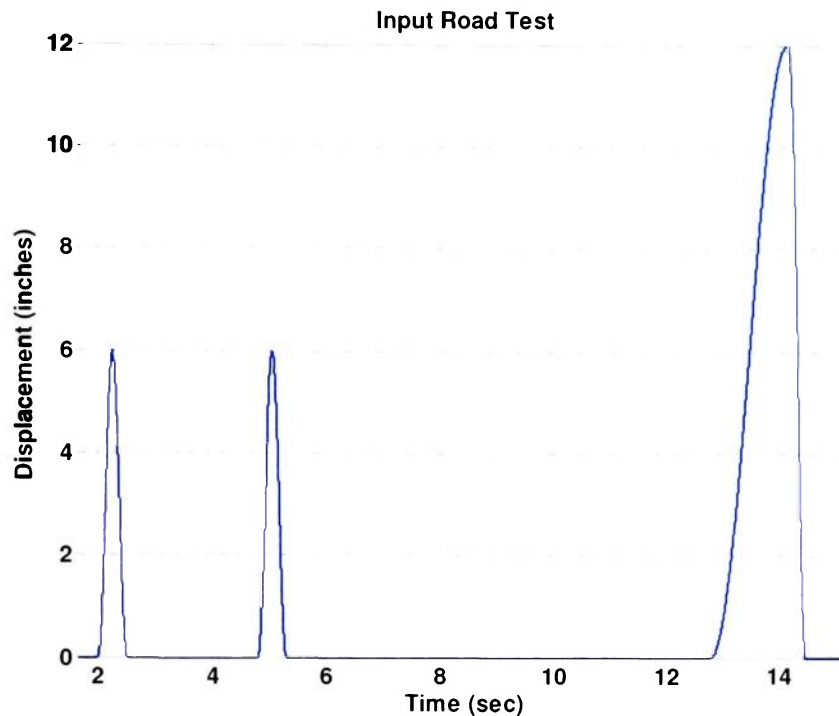
Figure 75. Input Road Disturbance.

Figure 76 was used for comparison with data collected during the passive system road test. Comparing the two figures, 76 and 77, there is a drastic difference at first glance. Both figures do represent the vehicle going over three disturbances, noted by the peaks on each plot. The actual data has other peaks that can be attributed to a number of factors. One being that in the SimMechanics model the wheel of the vehicle is assumed to be in contact with the ground at all times. This means that unlike the model, the experimental testing shows this as large amplitude spikes. The second contributing factor is that the model represents only one quarter of a vehicle, where as in the test there are secondary effects due to the rear suspension.
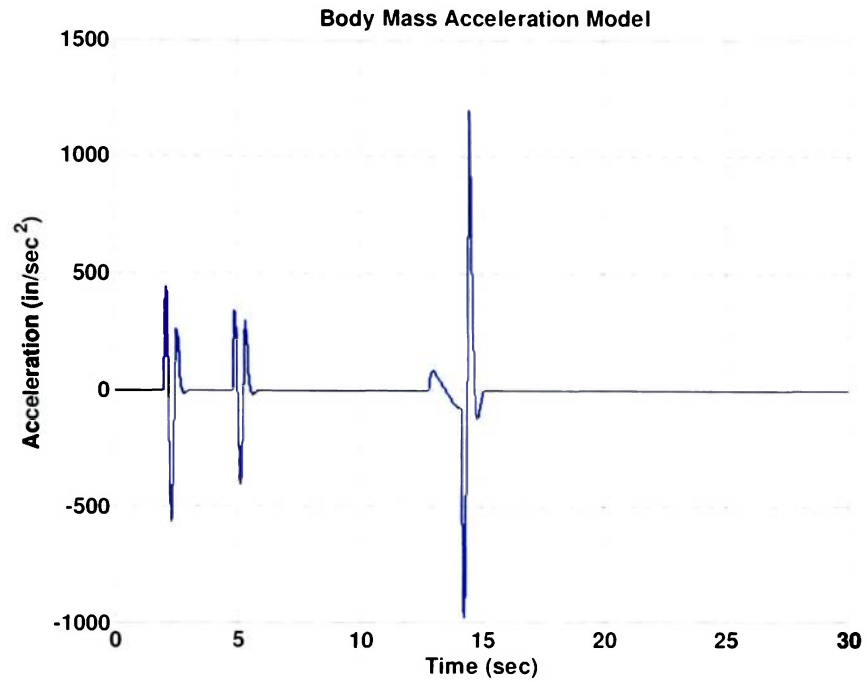
Figure 76: Response of Body Mass to New Input Road Disturbance.
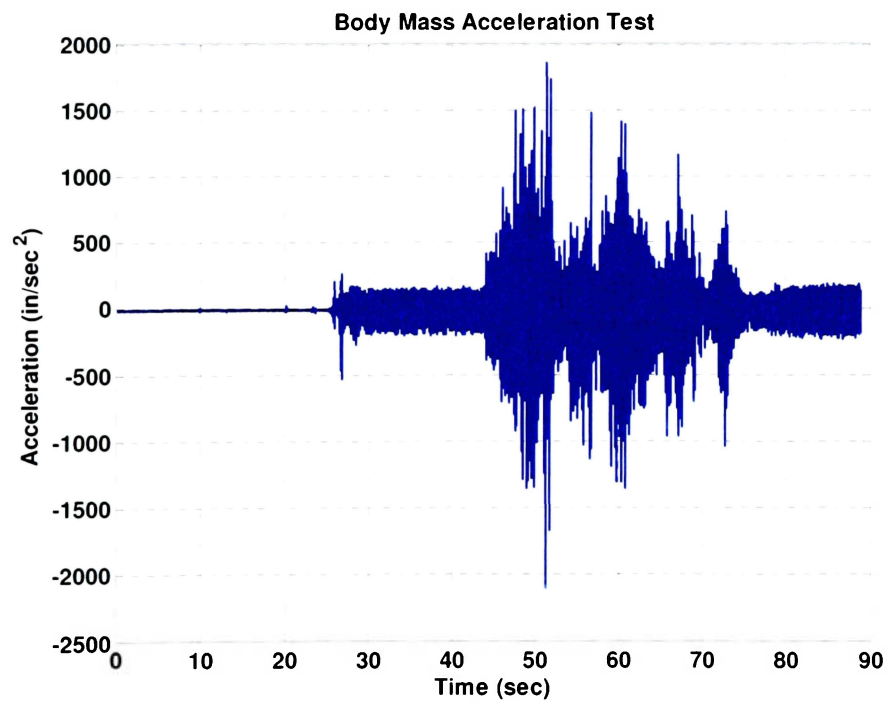
Figure 77: Response of Body Mass to New Input Road Disturbance.

Figure 77 also contains vibrations from the single cylinder engine. Engine RPM varies from idle of 25 Hz. All the way up to 63 Hz. Much of the noise in the signal is due to the engine vibrations being transmitting to the accelerometers through the frame. The PSD plot in figure 78 depicts both model and experimental data. It is known that a vehicles suspension system at low frequencies typically below 10 Hz. For comparison of the model this is the region we will look at. As shown there are two spikes in both model and experimental data in the same region of low frequencies. This validates the simulink model proving it is an accurate representation of a 2DOF base excitation problem. Spikes in the experimental data represent engine frequencies. The large spike around 27 Hz would be linked to the idling speed of the engine. Its large amplitude is accounted for by the amount of time the engine was idling during the test.

PSD Body Mass
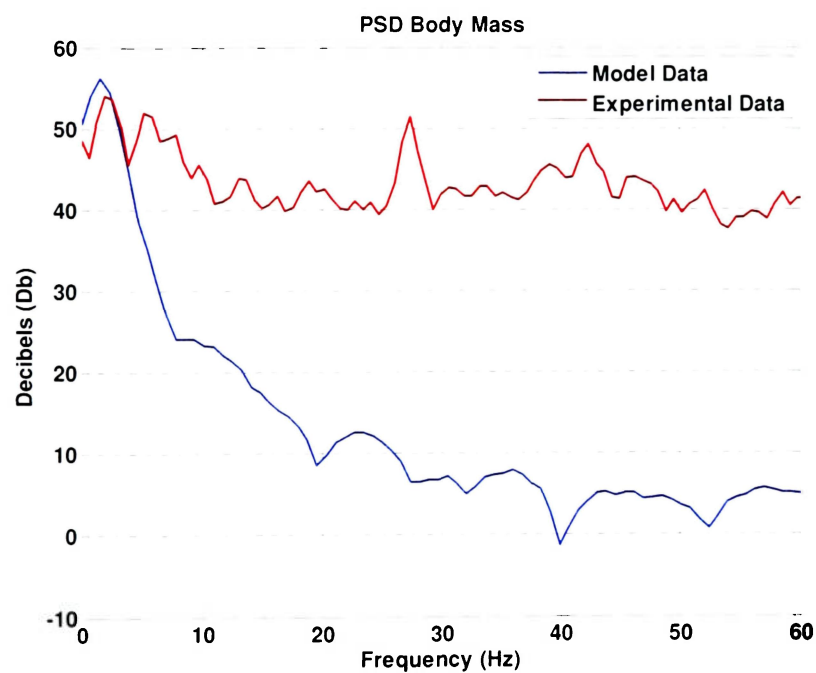
Figure 78. PSD Plot of Model and Experimental Data.

Conclusion

PSD plots of experimental testing, and theoretical modeling of a suspension system proved that a 2DOF system could accurately represent testing results. Shown in figure 79, both systems were able to capture suspension dynamics of a passive damper. Validating the model proved to be a critical step to see the benefits of a semi-active system. With the SimMechanics model, a semi-active "no jerk"[2] skyhook control policy can be optimized for vehicles and aircraft landing gear before experimental testing occurs.

CHAPTER 6 CONCLUSIONS

Summary

Numerous types of controllable suspensions have many distinct advantages over passive ones. Controllable suspension offer a superior vibration isolation system compared to a passive system. Controllable suspensions can come in three different types; active, semi-active, and adaptive. Active types use force generators that have the ability to absorb energy and input energy back into the system in real time, although very effective, their bulky size and high cost have limited there use in suspension systems. Adaptive suspensions adjust damping coefficients periodically when the system is in static equilibrium. This type of system offers some vibration control over the passive system but not as good as the active system. Active systems can become unstable and cause potential failures; this led the way to the development of semi-active systems. Semi-active systems have the ability to adjust damping coefficients in real time to offer a great vibration isolation system. Typical semi-active systems mechanically control the orifice size in a damper which affects damping coefficients. Although extremely effective, mechanical controls have limitations of being bulky, and have slow response times.

The invention of MR fluid in the 1980's with its controllable viscosity and fast response time, are a perfect fit to semi-active suspensions. MR fluid is a fluid medium such as damper oil mixed with tiny magnetic particles. These particles when in the presence of a magnetic field change the viscosity of the fluid from liquid to semi-solid in

a matter of milliseconds. MR fluids ability to change viscosity and easily replace stock damper oil makes it an ideal canadate for use in semi-active suspensions.

Previous MR damper designs modify internal components to supply the magnetic field required. This project focused on developing a magnetic field outside the damper body but still achieving the same results. An electromagnetic was designed to control the flow of MR fluid from the body of the damper to the reservoir. This setup is a faster and easier install compared to modifying the internals of a damper. These features allow dampers to accept a semi-active control system with little modification.

Both passive and semi-active dampers were dyno tested to obtain accurate force vs. velocity curves for analysis. Using SimMechanics a 2DOF base excitation model was developed to simulate the suspension system on an SAE Baja vehicle. Transmissibility plots were obtained for each system and compared to conclude that semi-active systems using a "no jerk"[2] skyhook control policy are more effective at isolating the body mass from ground input.

To validate the models accuracy data was collected using a National Instruments USB powered DAQ, and four accelerometers measuring both the body mass and tire mass acceleration of the passive system. Knowing the input vibration based on average speed and obstacle dimensions, this road disturbance was used as input to the SimMechanics model. Using a PSD plot, simulated results and experimental results were compared showing that the SimMechanics model is an accurate representation of the system. PSD plots look at the number of occurrences and amplitude of certain frequencies. Both experimental and simulated results have spikes in the lower frequency range where suspensions systems typically vibrate.

Recommendations for future studies

Through out the course of this study several observations were made that would be extremely beneficial to future study of this subject. Making an effective electromagnet proved to be harder than anticipated. Unless you have substantial experience making them, don't make your own. Numerous companies make electromagnets that are superior in quality and functionality. Contact one of them with your application and let them design one for your project.

Second, in dealing with an off-road style vehicle it is advisable not to mount a lap on the car to collect data. This set-up worked but was still very dangerous since sever damage could be done to the lap top not to mention all the data already collected could be lost. Since the DAQ system purchased for this project needed a computer to power it, there was no easy alternative choice. There are two different ways to remedy this problem. The first one would be to use a palm pilot and purchase Labview software that runs on a palm pilot operating system. A palm pilot is a lot lighter and smaller allowing it to sit in the operators lap. The second option would be purchasing a standalone DAQ from National Instruments. NI's CompactRio sytem is ideal for this type testing. This system is extremely rugged withstanding large shock impacts. This system uses typical DC power input, which is easily attainable for most applications.

Another observation is when making a control device for the MR fluid surface area seems to be a key component along with orifice diameter. In other studies the internal piston was modified allowing a ring of fluid to be controlled as shown in figure 21. My suggestion would be to use a multi passage design increasing the surface are of the fluid in contact with the magnetic field. Another alternative and probably the

better of the two would be to design a new remote reservoir would house a circular electromagnet that the fluid must pass around. This design would make the system even more compact and allow for maximum surface area to be effected. Although requiring significant modification, this design is still far simpler to manufacture than modifying or making new internal components of the damper. The next step in the project would be to build or buy a micro-controller to run the 'no jerk'[2] skyhook control policy for each damper. Data would be collected using the same test set-up that way results could be compared to the passive tests already performed. Assuming successful test results the next study would obtain a landing gear assembly, and drop testing it in both passive and semi-active MR configurations similar to Ghiringhelli's[13] study Perhaps an alternative to this would be to modify the landing gear on a small UAV and perform landings while recording data. This would be the ultimate goal of the project, a prototype MR landing gear for aircraft.

Figure 79: Internal Piston Modifications[23]

REFERENCES

1. "Active Suspension." 5 November 2008. Wikipedia the free Encyclopedia. 1 November 2008 <http://en.wikipedia.org/wiki/Active_suspension>.

2. Ahmadian, Mehdi. "The Challenge of Designing a Semiactive Damper for Heavy Truck Seat Suspension." SAE Technical Paper Series. 2005:

3. "Aliasing." 18 November 2008. Wikipedia the Free Encyclopedia. 24 August 2008. <http://en.wikipedia.org/wiki/Aliasing>.

4. Beckwith, Thomas, and Roby Marangoni, and John Lienhard. Mechanical Measurements. 6th ed. New Jersey: Pearson Prentice Hall. 2007.

5. Bishop, Robert H. LabVIEW Student Edition 6i. Saddle River, NJ. Prentice Hall. 2001.

6. Bonsor, Kevin. "How Smart Structures Will Work." 01 February 2001. HowStuffWorks.com. <http://science.howstuffworks.com/smart-structure.htm> 22 July 2008.

7. Choi, Young-Tai, and Norman M Wereley. "Vibration Control of a Landing Gear System Featuring Electro rheological/Mangetorheological Fluids." Journal of Aircraft. Vol 40. No 3. 2003.

8. ----"Semi-Active Vibration Isolation Using Magnetorheological Isolators." Journal of Aircraft. Vol.42 No. 3. 2005:

9. Craig, Roy R. Jr, and Andrew Kurdila. Fundamentals of Structural Dynamics. Hoboken, NJ, John Wiley & Sons, Inc. 2006

10. Crosby, M. J. and R. A. Harwood, and D. Karnopp. "Vibration Control Using Semi-Active Force Generators." Lord Libraries of Technical Articles. LL-7004.

11. "Custom Axis Racing Shocks" Technical Manual 167 &206 Series Shocks. Lodi, CA. 2000.

12. "Delphi MagneRide^{tm}," Delphi Corporation. Troy, Michigan, 2005. <www.delphi.com>.

13. Ghiringhelli, Gian. "Testing of Semiactive Landing Gear Control for a General Aviation Aircraft." Journal of Aircraft. Vol. 37. No 4. 2000:

14. Gavin, Henri, and Jesse Hoagg, and Mark Dobossy. "Optimal Design of MR Dampers. Duke University 2001."

15. Grice, Sarah. MR fluid no magnet. 2008, 10 August 2008. <http://www.flickr.com/photos/sgrice/2511052344/>.

16. Haney, Paul. The Racing & High-Performance Tire. Warrendale: Society of Automotive Engineers, Inc. 2003.

17. Harris, William. "How Car Suspensions Work." 11 May 2005. HowStuffWorks.com. <http://auto.howstuffworks.com/car-suspension.htm> 11 November 2007.

18. Hiemenz, Gregory, and Wei Hu, and Norman Wereley. "Semi-Active Magnetorheological Helicopter Crew Seat Suspension for Vibration Isolation." Journal of Aircraft. Vol. 45, No. 3. 2008:

19. Islam, A. S. M. Shawkatul, and A. K. W. Ahmed. "A Comparative Study of Advanced Suspension Dampers for Vibration and Shock Isolation Performance of Road Vehicle." SAE Technical Paper Series. 2006:

20. Jimenex, Alexander, and Andrea Wray. "Magneto-Rheological Fluid Semiactive Suspension System Performance Testing on a Stryker Vehicle." SAE Technical Paper Series. 2006:

21. Krasnicki, E.J."The Experimental Performance of an Off-Road Vehicle Utilizing a Semi-Active Suspension." Lord Library of Technical Articles. LL7400.

22. Kruger, W. R., and W. Kortum. "Multibody Simulation in the Integrated Design of Semi-Active Landing Gears." American Institute of Aeronautics and Astronautics Inc. 1998:

23. Longhurst, Chris. "The Suspension Bible." 18 November 2008. Carbibles.com. 2 February 2008. <http://www.carbibles.com/suspension_bible.html>.

24. Lord Ask us How. 2008. The Lord Corporation. Magneto-Rheological (MR) Technology. 10 September 2007. <http://www.lord.com/>.

25. Lurie, Karen. "Instant Armor." 4 December 2003. Science Central. 5 May 2008 http://www.sciencentral.com/articles/view.php3?article_id=218392121.

26. Mabie, Hamilton, and Charles Reinholtz. Mechanisms and Dynamics of Machinery. New York: John Wiley & Sons. 1987

27. "Magnetorehological Fluid." 18 November 2008. Wikipedia the free Encylopedia. 11 November 2007. <http://en.wikipedia.org/wiki/Magnetorheological_fluid>.

28. Milliken, Douglas, and William Milliken. Race Car Vehicle Dynamics. Warrendale: Society of Automotive Engineers, Inc. 1995.

29. Motta, Daniel, and Douglas Zampieri, and Allan Pereira. "Optimization of a Vehcile Suspension Using a Semi-Active Damper." SAE Technical Paper Series. 2000:

30. "MRF-132DG Magneto-Theological Fluid." Lord Technical Data. Lord Corporation 2008.

31. Munson, Bruce, Donald Young, and Theodore Okiishi. Fundamentals of Fluid Mechanics. 4th ed. Hoboken, NJ, John Wiley & Sons, Inc. 2002.

32. Pasholok, Yuri. Main Landing Gear Details. 10 September 2005. 22 November 2008. <http://mig3.sovietwarplanes.com/mig3/yuri-rr/landing-gear.htm>.

33. Poynor, James. "Innovative Designs for Magneto-Rheological Dampers." MS.Virginia Polytechnic Institute and State University. 2001.

34. Propellers and Cavitation. 20 August 2008. <http://www.hsva.de/index.html>.

35. Rao, Singiresu. Mechanical Vibrations. 4th ed. New Jersey: Pearson Prentice Hall. 2004.

36. Raymer, Daniel P. Aircraft Design: A Conceptual Approach. 3rd ed. Reston, Virginia, American Institute of Aeronautics and Astronautics, Inc. 1999.

37. Serway, Raymond, Robert Beichner. Physics for Scientists and Engineers 5th ed. Philadelphia, Pennsylvania. Saunders College Publishing. 2000.

38. Simon, David E. An Investigation of the Effectiveness of Skyhook Suspensions for Controlling Roll Dynamics of Sport Utility Vehicles Using Magneto-Rheological Dampers. Diss. Virginia Polytechnic Institute and State University. 2001.

39. Singla, U. L., and S. P. Singh. "Semi-active Control of Automotive Vehicle Suspension System Using Magnetorheological Damper- A Review." SAE International. 2004:

40. "Tech Support Technical Training Shock Absorbers." Monroe Shocks and Struts. 2008. 10 August 2008. <http://www.monroe.com/support/tec_shockabsorbers.asp>.

41. Under Sampling. Efunda Engineering Fundamentals. 2008 15 August 2008 <http://www.efunda.com/designstandards/sensors/methods/DSP_Aliasing.cfm#aliasing>.

42. Unsal, Memet. Semi-Active Vibration Control of a Parallel Platform Mechanism Using Magnetorheloogical Damping. Diss. University of Florida, 2006

43. Wang, Ximing, and Udo Carl. "Fuzzy Control of Aircraft Semi-Active Landing Gear System." American Institute of Aeronautics and Astronautics Inc. 1999:

44. Wilson, Tracy V. "How Liquid Body Armor Works." 26 February 2007. HowStuffWorks.com. 27 May 2008. <http://science.howstuffworks.com/liquid-body-armor.htm>

APPENDIX A *MATLAB CODE*

Matlab code to run nonlinear passive model.

```
tic
clear all
n=25;
exstart=-1;
exend=2;
exstep=(exend-exstart)/(n-1);
k=.4^2*125;
        for s=1:2;
            s
          if s==1;
              comp=1;
              reb=1;
                  damp=1*.4;

              elseif s==2;
                  comp=1;
                  reb=10;
                      damp=2*.4;

              elseif s==3;
                      comp=1;
                      reb=20;
                          damp=4*.4;

              elseif s==4;
                      comp =10;
                      reb=1;
                          damp=6*.4;

               elseif s==5;
                       comp=10;
                       reb=10;
                        damp=8;

               elseif s==6;
                           comp=10;
                           reb=20;
                           damp=10;

               elseif s==7
                               comp=20;
                               reb=1;
                                   damp =12;

                elseif s==8;
                               comp=20;
                               reb=10;
                               damp=14;

                    else   s==9;
```

```
                                            comp=20;
                                            reb=20;
                                                damp=16;
            end

for  i = 1:n;
i
                    ex = exstart:exstep:exend;

                    w = 10^ex(i);
                    Hz(i)= w/(2*3.1415);
                    if Hz(i)<.333;
                    tfinal=ceil(1/Hz(i)*10);
                    else
                        tfinal=30;
                    end
                    sim('passivel_linear', [0 tfinal]);

                    body=bodypos(round(500*tfinal*.7):floor(tfinal*500),3);
                    bodyrange(i)=range(body);
                    tire=tirepos(round(500*tfinal*.7):floor(tfinal*500),3);
                    %tire=[-w^2  w^2],
                    tirerange(i)=range(tire);
                end




trans(:,s)=bodyrange./tirerange;
%semilogx(Hz, trans,'c');
        end
        semilogx(Hz,trans)
toc
```

Matlab code used to obtain PSD plots.

```
function [freq,dbs] = dave_psd(t,data)

%Find Sampling and Nyquist Frequencies
Fs = 1/mean(diff(t));
Fny = Fs/2;
if Fs > 200
    N = round(Fs/200);
    data = decimate(data,N);
    Fny = Fny/N;
end


    dbs = psd(data);

dbs = psd(data);
dbs = 10*log10(dbs);
freqt = [1:length(dbs)]-1;
freq = freqt/max(freqt)*Fny;
```

Matlab code to run linear 1DOF model.

```
tic
clear all
n=15;
exstart=-1;
exend=2;
exstep=(exend-exstart)/(n-1);
k=.4^2*125;
      for s=1:2;
          s
        if s==1;
%               comp=1;
%               reb=1;
                damp=1*.4;

                elseif s==2;
%                   comp=1;
%                   reb=10;
                    damp=2*.4;

                elseif s==3;
%                       comp=1;
%                       reb=10;
                        damp=4*.4;

                elseif s==4;
%                       comp =10;
%                       reb=1;
                        damp=6*.4;

                    elseif s==5;
%                           comp=10;
```

```
%                                          reb=10;
                                           damp=8;

                          elseif  s==6;
%                                                 comp=10;
%                                                   reb=20;
                                             damp=10;

                          elseif  s==7
%                                                 comp=20;
%                                                 reb=1;
                                               damp =12;

                      elseif  s==8;
%                                                    comp=20;
%                                                    reb=10;
                                             damp=14;

                          else   s==9;
%                                                    comp=20;
%                                                    reb=20;
                                                damp=16;

            end

for  i = 1:n;
i
                    ex = exstart:exstep:exend;

                    w = 10^ex(i);
                    Hz(i)= w/(2*3.1415);
                    if Hz(i)<.333;
                    tfinal=ceil(1/Hz(i)*10);
                    else
                         tfinal=30;
                    end
                    sim('passivel_linear', [0 tfinal]);

                    body=bodypos(round(500*tfinal*.7):floor(tfinal*500),3);
                    bodyrange(i)=range(body);
                    tire=tirepos(round(500*tfinal*.7):floor(tfinal*500),3);
                    %tire=[-w 2 w _];
                    tirerange(i)=range(tire);
                end




trans(:,s)=bodyrange./tirerange;
%semilog (Hz, trans,'c');
      end
      semilogx(Hz,trans)
toc
```

Matlab code to run semi-active MR damper model.

```
tic
clear all
n=125;
exstart=-1;
exend=2.1;
exstep=(exend-exstart)/(n-1);
for s=1:9;
    s
        if s==1;
            Csky=1;

        elseif s==2;
                Csky=2;

        elseif s==3;
                    Csky=4;

        elseif s==4;
                        Csky=6;

        elseif s==5;
                            Csky=8;

        elseif s==6;
                                Csky=10;

        elseif s==7
                                    Csky=12;

        elseif s==8;
                                        Csky=14;

                                else   s==9;
                                            Csky=20;

        end

for  i = 1:n;
i
                ex = exstart:exstep:exend;

                w = 10^ex(i);
                Hz(i)= w/(2*3.1415);
                if Hz(i)<.333;
                tfinal=ceil(1/Hz(i)*10);
                else
                    tfinal=30;
                end
                sim('MR_ideal', [0 tfinal]);
```

```
body=bodypos(round(length(bodypos)*.7):floor(length(bodypos)),3);


tire=tirepos(round(length(tirepos)*.7):floor(length(tirepos)),3);

                trans(1) =
max((abs(fft(tire)).*abs(fft(body))))./max((abs(fft(tire)).*abs(fft(tir
e))));

end
trans2(:,s)=trans;
end

figure
        semilogx(Hz,trans2)
    toc
```

APPENDIX B *DRAWINGS AND SPECIFICATIONS*

1-888-282-9891

Submersible Accelerometer
Model JTFS

SUBMERSIBLE

LOW IMPEDANCE

EASY CALIBRATION

Amplified

SENSOTEC's Model JTFS Submersible Accelerometers provide underwater measurement over full scale ranges of 5 to 500g. An all-welded, stainless steel construction and special cable permit immersion for indefinite periods. Units will operate at external pressures to 500 psi. Additional features include low impedance and simple calibration.

MODEL JTFS
Amplified
(±5 VDC) Order Code BG913
(4-20mA) Order Code BG914

PERFORMANCE

Ranges (in Peak g)	±5 to 500
Non-linearity and Hysteresis	±1% F.S.
Output....................................	±5 volts or 12 ± 8 mA
Frequency Response (%)	±10%
Transverse Sensitivity................	5% max
Damping Ratio (nominal)	.7 C @ 70° F
Resolution	Infinite

ENVIRONMENTAL

Temperature, Operating	0° F to 200° F
Temperature, Compensated	70° F to 200° F
Temperature Effect	
- Zero (max)...........................	.015% F.S./° F
- Sensitivity (max)...................	±10%

ELECTRICAL

Excitation/supply	26-32VDC (BG913)
	22-32VDC (BG914)
Bridge Resistance	4000 ohms
Wiring Code (std)	±5 VDC #10 (See Pg. AP-8)
	4-20mA Consult factory
Electrical Termination (std)	Submersible cable (10 ft.)

MECHANICAL

Overload, Safe	5 X F.S.
Weight	10 oz.
Case Material	316 Stainless

NOTE: Amplified 4-20mA units swing ±8mA centered on 12mA. Zero vibration is 12mA output.

Available Ranges (Peak g)	Usable Frequency Range (Hz)	Mounted Resonant Frequency (Hz)
±5	0-200	300
±10	N/A	N/A
±50	0-600	1000
±100	0-800	1500
±500	0-200	3000

Dimensions

2.0" SENSITIVE AXIS

1/4 28 UNF
1/4 DP

1.3"
DIA.
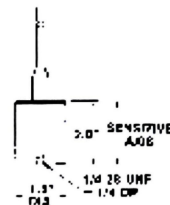
Order Code BG913 (±5VDC output)
Order Code BG914 (4-20mA output)

ACCELERATION SUBMERSIBLE

AC-5

FUCHS

Silkolene

Race Technical Data

Pro RSF

Racing Suspension Fluids

Pro RSF Racing Suspension Fluids are designed for the latest competition suspension systems. Extensive use by factory teams and suspension specialists in road racing and rallying competition has proved that Pro RSF provides the answer to any situation regardless of climate or terrain.

Pro RSF fluids are used by factory teams using for example Penske, Proflex, Ohlins, White Power and Showa.

Unique fluid engineering techniques integrate low-friction synthetics with anti-foam and wear-resistant additives to ensure predictable suspension performance, long seal life and silky smooth action.

High viscosity index (VI) eliminates the 'fade' experienced when shocks are required to operate at high temperatures.

Pro RSF fluids are thermally stable and provide exceptional performance in air, nitrogen and argon filled systems. The various grades may be individually blended to give fine-tuned suspension response.

With the available grades: 2.5wt, 5wt, 7.5wt, 10wt, 15wt, it is possible to cover all applications in any climate or racing conditions.

Typical Technical Data	PRO RSF				
	2.5wt	5wt	7.5wt	10wt	15wt
Kinematic Viscosity @ 100°C ... cSt	5.93	9.45	11.55	13.69	19.5
Kinematic Viscosity @ 40°C ... cSt	13.6	26.70	37.19	47.36	92.95
Viscosity Index (VI)	464	372	322	303	235
Specific Gravity @ 20°C	0.815	0.847	0.841	0.868	0.871
Pourpoint ... °C	-37	-45	-30	-39	-39
SAE Rating	0W-20	5W-30	5W-30	5W-40	5W-50
Flash Point (Closed) ... °C	75	120	132	140	185
ISO Viscosity Rating	15	22/32	32	46	100
Colour	Yellow	Blue	Purple	Red (Fluorescent)	Amber